

1 **Indicators of Global Climate Change 2023: annual update of key** 2 **indicators of the state of the climate system and human influence**

3
4 Piers M. Forster¹, Chris Smith^{1,2,3}, Tristram Walsh⁴, William F. Lamb^{5,1}, Robin Lamboll⁶, Bradley
5 Hall²³, Mathias Hauser⁷, Aurélien Ribes⁸, Debbie Rosen¹, Nathan P. Gillett⁹, Matthew D.
6 Palmer^{3,10}, Joeri Rogelj⁶, Karina von Schuckmann¹¹, Blair Trewin¹², Myles Allen⁴, Robbie
7 Andrew¹³, Richard A. Betts^{3,18}, Alex Borger⁴³, Tim Boyer¹⁵, Jiddu A. Broersma⁴³, Carlo
8 Buontempo¹⁴, Samantha Burgess¹⁴, Chiara Cagnazzo¹⁴, Lijing Cheng¹⁶, Pierre Friedlingstein^{18,19},
9 Andrew Gettelman³⁸, Johannes Gütschow²⁰, Masayoshi Ishii²², Stuart Jenkins⁴, Xin Lan^{21,35}, Colin
10 Morice³, Jens Mühle⁴², Christopher Kadow²³, John Kennedy²⁴, Rachel E. Killick³, Paul B.
11 Krummel⁴¹, Jan C. Minx^{5,1}, Gunnar Myhre¹³, Vaishali Naik¹⁷, Glen P. Peters¹³, Anna Pirani²⁵, Julia
12 Pongratz^{26,34}, Carl-Friedrich Schleussner²⁷, Sonia I. Seneviratne⁷, Sophie Szopa²⁸, Peter Thorne²⁹,
13 Mahesh V. M. Kovilakam³⁸, Elisa Majamäki³⁹, Jukka-Pekka Jalkanen³⁹, Margreet van Marle⁴⁰,
14 Rachel M. Hoesly³⁷, Robert Rohde³⁰, Dominik Schumacher⁷, Guido van der Werf³⁶, Russell
15 Vose³¹, Kirsten Zickfeld³², Xuebin Zhang⁹, Valerie Masson-Delmotte²⁸, Panmao Zhai³³

16
17 ¹Priestley Centre, University of Leeds, Leeds, LS2 9JT, UK

18 ²International Institute for Applied Systems Analysis (IIASA), Austria

19 ³Met Office Hadley Centre, Exeter, UK

20 ⁴Environmental Change Institute, University of Oxford, UK

21 ⁵Mercator Research Institute on Global Commons and Climate Change (MCC), Berlin, Germany

22 ⁶Centre for Environmental Policy, Imperial College London, UK

23 ⁷Institute for Atmospheric and Climate Science, Department of Environmental Systems Science, ETH Zurich, Zurich,
24 Switzerland

25 ⁸Université de Toulouse, Météo France, CNRS, France

26 ⁹Environment and Climate Change Canada, Canada

27 ¹⁰School of Earth Sciences, University of Bristol, UK

28 ¹¹Mercator Ocean international, Toulouse, France

29 ¹²Bureau of Meteorology, Melbourne, Australia

30 ¹³CICERO Center for International Climate Research, Oslo, Norway

31 ¹⁴ECWMF, Bonn, Germany

32 ¹⁵NOAA's National Centers for Environmental Information (NCEI), Silver Spring, MD, USA

33 ¹⁶Institute of Atmospheric Physics, Chinese Academy of Sciences, Beijing, China

34 ¹⁷NOAA Geophysical Fluid Dynamics Laboratory, Princeton, NJ, USA

35 ¹⁸Faculty of Environment, Science and Economy, University of Exeter, UK

36 ¹⁹Laboratoire de Météorologie Dynamique/Institut Pierre-Simon Laplace, CNRS, Ecole Normale
37 Supérieure/Université PSL, Paris, France

38 ²⁰Climate Resource, Australia/Germany
39 ²¹NOAA Global Monitoring Laboratory, Boulder, CO, USA
40 ²²Meteorological Research Institute, Tsukuba, Japan
41 ²³German Climate Computing Center, Hamburg, Germany (DKRZ)
42 ²⁴No affiliation, Verdun, France.
43 ²⁵Euro-Mediterranean Center on Climate Change (CMCC), Venice, Italy; Università Cà Foscari, Venice, Italy
44 ²⁶Ludwig-Maximilians-Universität München, Germany
45 ²⁷Climate Analytics, Berlin, Germany and Geography Department and IRI THESys, Humboldt-Universität zu Berlin,
46 Berlin, Germany
47 ²⁸Institut Pierre Simon Laplace, Laboratoire des sciences du climat et de l'environnement, UMR8212 CNRS-CEA-
48 UVSQ, Université Paris-Saclay, 91191, Gif-sur-Yvette, France
49 ²⁹ICARUS Climate Research Centre, Maynooth University, Maynooth, Ireland
50 ³⁰Berkeley Earth, Berkeley, CA, USA
51 ³¹NOAA's National Centers for Environmental Information (NCEI), Asheville, NC, USA
52 ³²Simon Fraser University, Vancouver, Canada
53 ³³Chinese Academy of Meteorological Sciences, Beijing, China
54 ³⁴Max Planck Institute for Meteorology, Hamburg, Germany
55 ³⁵CIRES, University of Colorado Boulder, Boulder, CO, USA
56 ³⁶Wageningen University and Research, Wageningen, The Netherlands
57 ³⁷Pacific Northwest National Laboratory, Richland, WA, USA
58 ³⁸LARC, NASA, USA
59 ³⁹Finnish Meteorological Institute, Helsinki, Finland
60 ⁴⁰Deltras, Delft, The Netherlands
61 ⁴¹Global Systems Institute, University of Exeter, UK
62 ⁴²Scripps Institution of Oceanography, University of California San Diego, La Jolla, CA, USA
63 ⁴³Climate Change Tracker, Data for Action Foundation, Amsterdam, Netherlands
64 *Correspondence to:* Piers. M. Forster (p.m.forster@leeds.ac.uk)

65

66 **Abstract.**

67 Intergovernmental Panel on Climate Change (IPCC) assessments are the trusted source of scientific evidence for
68 climate negotiations taking place under the United Nations Framework Convention on Climate Change (UNFCCC).
69 Evidence-based decision-making needs to be informed by up-to-date and timely information on key indicators of the
70 state of the climate system and of the human influence on the global climate system. However, successive IPCC
71 reports are published at intervals of 5–10 years, creating potential for an information gap between report cycles.

72

73 We follow methods as close as possible to those used in the IPCC Sixth Assessment Report (AR6) Working Group
74 One (WGI) report. We compile monitoring datasets to produce estimates for key climate indicators related to forcing
75 of the climate system: emissions of greenhouse gases and short-lived climate forcers, greenhouse gas concentrations,
76 radiative forcing, the Earth's energy imbalance, surface temperature changes, warming attributed to human activities,
77 the remaining carbon budget, and estimates of global temperature extremes. The purpose of this effort, grounded in
78 an open data, open science approach, is to make annually updated reliable global climate indicators available in the

79 public domain (<https://doi.org/10.5281/zenodo.11388387> Smith et al., 2024a). As they are traceable to IPCC report
80 methods, they can be trusted by all parties involved in UNFCCC negotiations and help convey wider understanding
81 of the latest knowledge of the climate system and its direction of travel.

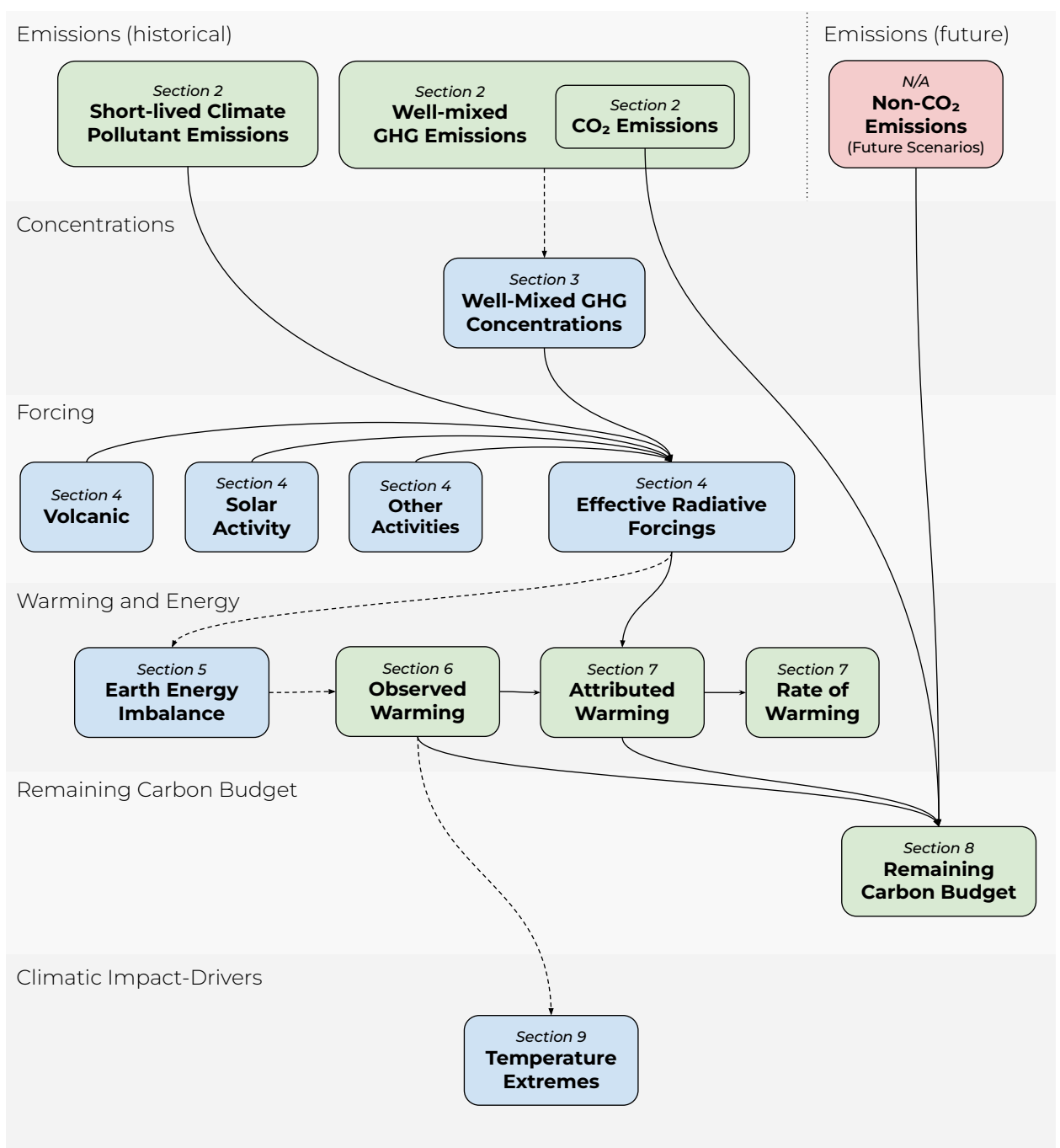
82
83 The indicators show that, for the 2014–2023 decade average, observed warming was 1.19 [1.06 to 1.30] °C, of which
84 1.19 [1.0 to 1.4] °C was human-induced. For the single year average, human-induced warming reached 1.31 [1.1 to
85 1.7] °C in 2023 relative to 1850-1900. The best estimate is below the 2023 observed warming record of 1.43 [1.32 to
86 1.53] °C, indicating a substantial contribution of internal variability in the 2023 record. Human-induced warming has
87 been increasing at a rate that is unprecedented in the instrumental record, reaching 0.26 [0.2 - 0.4] °C per decade over
88 2014-2023. This high rate of warming is caused by a combination of greenhouse gas emissions being at an all-time
89 high of 53 ± 5.4 GtCO₂e per year over the last decade, as well as reductions in the strength of aerosol cooling. Despite
90 this, there is evidence that the rate of increase in CO₂ emissions over the last decade has slowed compared to the
91 2000s, and depending on societal choices, a continued series of these annual updates over the critical 2020s decade
92 could track a change of direction for some of the indicators presented here.

93 **1 Introduction**

94 The IPCC AR6 has provided an assessment of human influence on key indicators of the state of climate grounded in
95 data up to year 2019 (IPCC WGI 2021, Supplement Sect. S1). The next IPCC AR7 assessment report is due towards
96 the end of the decade. Given the speed of recent change, and the need for updated climate knowledge to inform
97 evidence-based decision-making, the Indicators of Global Climate Change (IGCC) was initiated to provide
98 policymakers with annual updates of the latest scientific understanding on the state of selected critical indicators of
99 the climate system and of human influence.

100
101 This second annual update follows broadly the format of last year (Forster et al., 2023), focussing on indicators related
102 to heating of the climate system, building from greenhouse gas emissions towards estimates of human-induced
103 warming and the remaining carbon budget. Fig. 1 presents an overview of the aspects assessed and their interlinkages
104 from cause (emissions) through effect (changes in physical indicators) to Climatic Impact-Drivers. It also provides a
105 visual roadmap as to the structure of remaining sections in this paper to guide the reader.

106



Key

IGCC Section # Indicator Name
 Available in both Dashboard & Data Repository
 Available in Data Repository
 Available in neither

- A** —————> **B** Indicator B calculation depends on results from Indicator A
- A** - - - - -> **B** Indicator B calculation does not depend on results from Indicator A, but there is still a physical causal link between the two Indicators

110 **Figure 1 The flow chart of data production from emissions to human induced warming and the remaining carbon budget,**
111 **illustrating both the rationale and workflow within the paper production.**

112 The update is based on methodologies assessed by the IPCC Sixth Assessment Report (AR6) of the physical science
113 basis of climate change (Working Group One (WGI) report; IPCC, 2021a) as well as Chap. 2 of the WGIII report
114 (Dhakal et al., 2022) and is aligned with the efforts initiated in AR6 to implement FAIR (Findable, Accessible,
115 Interoperable, Reusable) principles for reproducibility and reusability (Pirani et al., 2022; Iturbide et al., 2022). IPCC
116 reports make a much wider assessment of the science and methodologies – we do not attempt to reproduce the
117 comprehensive nature of these IPCC assessments here. As such, we do not consider adopting fundamentally different
118 approaches to AR6. Rather, our aim is to rigorously track both climate system change and evolving methodological
119 improvements between IPCC report cycles, thereby transparency and consistency in between successive reports.

120

121 The update is organised as follows: emissions (Sect. 2) and greenhouse gas (GHG) concentrations (Sect. 3) are used
122 to develop updated estimates of effective radiative forcing (Sect. 4). Earth's energy imbalance (Sect. 5) and
123 observations of global surface temperature change (Sect. 6) are key global indicators of a warming world. The
124 contributions to global surface temperature change from human and natural influences are formally attributed in Sect.
125 7, which tracks the level and rate of human-induced warming. Sect. 8 updates the remaining carbon budget to policy-
126 relevant temperature thresholds. Sect. 9 gives an example of global-scale indicators associated with climate extremes
127 of maximum land surface temperatures. An important purpose of the exercise is to make these indicators widely
128 available and understood. Code and data availability are given in Sect. 10, and conclusions are presented in Sect. 11.
129 Data are available at <https://doi.org/10.5281/zenodo.11388387> (Smith et al., 2024a).

130

131 **2 Emissions**

132 Historic emissions from human activity were assessed in both AR6 WGI and WGIII. Chapter 5 of WGI assessed CO₂
133 and CH₄ emissions in the context of the carbon cycle (Canadell et al., 2021). Chapter 6 of WGI assessed emissions in
134 the context of understanding the climate and air quality impacts of short-lived climate forcers (Szopa et al., 2021).
135 Chapter 2 of WGIII, published one year later (Dhakal et al., 2022), assessed the sectoral sources of emissions and
136 gave the most up-to-date understanding of the current level of emissions. This section bases its methods and data on
137 those employed in this WGIII chapter.

138 **2.1 Methods of estimating greenhouse gas emissions changes**

139 Like in AR6 WGIII, net GHG emissions in this paper refer to releases of GHGs from anthropogenic sources minus
140 removals by anthropogenic sinks, for greenhouse gases reported under the common reporting format of the UNFCCC.
141 This includes CO₂ emissions from fossil fuels and industry (CO₂-FFI); net CO₂ emissions from land use, land-use
142 change and forestry (CO₂-LULUCF); CH₄; N₂O; and fluorinated gas (F-gas) emissions. CO₂-FFI mainly comprises
143 fossil-fuel combustion emissions, as well as emissions from industrial processes such as cement production. This

144 excludes biomass and biofuel use. CO₂-LULUCF is mainly driven by deforestation but also includes anthropogenic
145 removals on land from afforestation and reforestation, emissions from logging and forest degradation, and emissions
146 and removals in shifting cultivation cycles, as well as emissions and removals from other land-use change and land
147 management activities, including peat burning and drainage. The non-CO₂ GHGs – CH₄, N₂O and F-gas emissions –
148 are linked to the fossil-fuel extraction, agriculture, industry and waste sectors.

149
150 Global regulatory conventions have led to a twofold categorisation of F-gas emissions (also known as halogenated
151 gases). Under UNFCCC accounting, countries record emissions of hydrofluorocarbons (HFCs), perfluorocarbons
152 (PFCs), sulfur hexafluoride (SF₆) and nitrogen trifluoride (NF₃) – hereinafter “UNFCCC F-gases”. However, national
153 inventories tend to exclude halons, chlorofluorocarbons (CFCs) and hydrochlorofluorocarbons (HCFCs) – hereinafter
154 “ODS (ozone-depleting substance) F-gases” – as they have been initially regulated under the Montreal Protocol and
155 its amendments. In line with the WGIII assessment, ODS F-gases and other substances, are not included in our GHG
156 emissions reporting but are included in subsequent assessments of concentration change (including compounds formed
157 in the atmosphere as ozone), effective radiative forcing, human-induced warming, carbon budgets and climate impacts
158 in line with the WGI assessment.

159
160 There are also varying conventions used to quantify CO₂-LULUCF fluxes. These include the use of bookkeeping
161 models, dynamic global vegetation models (DGVMs) and aggregated national inventory reporting (Pongratz et al.,
162 2021). Each differs in terms of their applied system boundaries and definitions and they are not directly comparable.
163 However, efforts to “translate” between bookkeeping estimates and national inventories using DGVMs have
164 demonstrated a degree of consistency between the varying approaches (Friedlingstein et al., 2022; Grassi et al., 2023).

165
166 Each category of GHG emissions included here is covered by varying primary sources and datasets. Although many
167 datasets cover individual categories, few extend across multiple categories, and only a minority have frequent and
168 timely update schedules. The Global Carbon Budget (GCB; Friedlingstein et al., 2023) covers CO₂-FFI and CO₂-
169 LULUCF. The Emissions Database for Global Atmospheric Research (EDGAR; Crippa et al., 2023) and the Potsdam
170 Real-time Integrated Model for probabilistic Assessment of emissions Paths (PRIMAP-hist; Gütschow et al., 2016;
171 Gütschow et al., 2024) cover CO₂-FFI, CH₄, N₂O and UNFCCC F-gases. The Community Emissions Data System
172 (CEDS; Hoesly et al. 2018; Hoesly and Smith, 2024) covers CO₂-FFI, CH₄, and N₂O. The Global Fire Emissions
173 Database (GFED; van der Werf et al., 2017) version 4.1s covers CO₂, CH₄, and N₂O. As detailed below, for various
174 reasons not all these datasets were employed in this update.

175
176 In AR6 WGIII, total net GHG emissions were calculated as the sum of CO₂-FFI, CH₄, N₂O and UNFCCC F-gases
177 from EDGAR, and net CO₂-LULUCF emissions from the GCB. Net CO₂-LULUCF emissions followed the GCB
178 convention and were derived from the average of three bookkeeping models (Hansis et al., 2015; Houghton and
179 Nassikas, 2017; Gasser et al., 2020). Version 6 of EDGAR was used (with a fast-track methodology applied for the
180 final year of data – 2019), alongside the 2020 version of the GCB (Friedlingstein et al., 2020). CO₂-equivalent

181 emissions were calculated using global warming potentials with a 100-year time horizon (GWP100 henceforth) from
182 AR6 WGI Chap. 7 (Forster et al., 2021). Uncertainty ranges were based on a comparative assessment of available data
183 and expert judgment, corresponding to a 90 % confidence interval (Minx et al., 2021): ± 8 % for CO₂-FFI, ± 70 % for
184 CO₂-LULUCF, ± 30 % for CH₄ and F-gases, and ± 60 % for N₂O (note that the GCB assesses 1 standard deviation
185 uncertainty for CO₂-FFI as ± 5 % and for CO₂-LULUCF as ± 2.6 GtCO₂; Friedlingstein et al., 2022). The total
186 uncertainty was summed in quadrature, assuming independence of estimates per species/source. Reflecting these
187 uncertainties, AR6 WGIII reported emissions to two significant figures only. Uncertainties in GWP100 metrics of
188 roughly ± 10 % were not applied (Minx et al., 2021).

189
190 This analysis tracks the same compilation of GHGs as in AR6 WGIII. We follow the same approach for estimating
191 uncertainties and CO₂-equivalent emissions. We also use the same type of data sources but make important changes
192 to the specific selection of data sources to further improve the quality of the data, as suggested in the knowledge gap
193 discussion of the WGIII report (Dhakal et al., 2022). Instead of using EDGAR data (which are now available as version
194 8), we use GCB data for CO₂-FFI, PRIMAP-hist “CR” data for CH₄ and N₂O, and atmospheric concentrations with
195 best-estimate lifetimes for UNFCCC F-gas emissions (Hodnebrog et al., 2020). As in AR6 WGIII we use GCB for
196 net CO₂-LULUCF emissions, taking the average of three bookkeeping models (BLUE by Hansis et al., 2015; H&C
197 by Houghton and Castanho, 2023; OSCAR by Gasser et al., 2020). The GCB methodology includes CO₂ emissions
198 from deforestation and forest degradation fires, but excludes wildfires, which are assumed to be natural even if climate
199 change affects their intensity and frequency. Bunker emissions are included but military emissions excluded (e.g. Bun
200 et al. 2024). For more completeness, this year we also include estimates of N₂O and CH₄ emissions from global
201 biomass fires, sourced from GFED4.1s.

202 There are three reasons for these specific data choices. First, national greenhouse gas emissions inventories tend to
203 use improved, higher-tier methods for estimating emissions fluxes than global inventories such as EDGAR (Dhakal
204 et al., 2022; Minx et al., 2021). As GCB and PRIMAP-hist “CR” integrate the most recent national inventory
205 submissions to the UNFCCC, selecting these databases makes best use of country-level improvements in data-
206 gathering infrastructures. It is important to acknowledge, however, that national inventories differ substantially with
207 respect to reporting intervals, applied methodologies and emissions factors (Minx et al. 2021). Notably, the PRIMAP-
208 hist “CR” dataset has significantly lower total CH₄ emissions relative to both the other datasets reported here, and the
209 global atmospheric inversion estimates evaluated in this paper. A substantive body of literature has evaluated national
210 level CH₄ inversions versus inventories, finding a tendency for the former to exceed the latter (Deng et al. 2022;
211 Tibrewal et al. 2024; Janardanan et al. 2024; Scarpelli et al. 2022). Compared to the median of reported inversion
212 models from Deng et al. 2022, PRIMAP-Hist CR reports lower CH₄ emissions for India, the EU27+UK, Brazil, Russia
213 and Indonesia, but not in the case of China and the United States (see Supplement Fig 1).

214
215 Second, comprehensive reporting of F-gas emissions has remained challenging in national inventories and may
216 exclude some military applications (see Minx et al., 2021; Dhakal et al., 2022). However, F-gases are entirely

217 anthropogenic substances, and their concentrations can be measured effectively and reliably in the atmosphere. We
218 therefore follow the AR6 WGI approach in making use of direct atmospheric observations.

219
220 Third, the choice of GCB data for CO₂-FFI means we can integrate its projection of that year's CO₂ emissions at the
221 time of publication (i.e. for 2023). No other dataset except GCB provides projections of CO₂ emissions on this time
222 frame. At this point in the publication cycle (mid-year), the other chosen sources provide data points with a 2-year
223 time lag (i.e. for 2022). While these data choices inform our overall assessment of GHG emissions, we provide a
224 comparison across datasets for each emissions category, as well as between our estimates and an estimate derived
225 from AR6 WGIII-like databases (i.e. EDGAR for CO₂-FFI and non-CO₂ GHG emissions, GCB for CO₂-LULUCF).

226 **2.2 Updated greenhouse gas emissions**

227 Updated GHG emission estimates are presented in Fig. 2 and Table 1. Total global GHG emissions were
228 55 ± 5.3 GtCO₂e in 2022, the same as previous high levels in 2019 and 2021. Of this total, CO₂-FFI contributed
229 36.4 ± 2.9 GtCO₂, CO₂-LULUCF contributed 4.3 ± 3 GtCO₂, CH₄ contributed 9 ± 2.7 GtCO₂e, N₂O contributed
230 3.1 ± 1.9 GtCO₂e and F-gas emissions contributed 1.8 ± 0.54 GtCO₂e. Initial projections indicate that total CO₂
231 emissions remained similar in 2023, with emissions from fossil fuel and industry at 36.8 ± 3 and from land-use change
232 at 4.1 ± 2.9 GtCO₂ (Friedlingstein et al., 2023; see also Liu et al., 2024; IEA, 2023). Note that ODS F-gases such as
233 chlorofluorocarbons and hydrochlorofluorocarbons are excluded from national GHG emissions inventories. For
234 consistency with AR6, they are also excluded here. Including them here would increase total global GHG emissions
235 by 1.5 GtCO₂e in 2022.

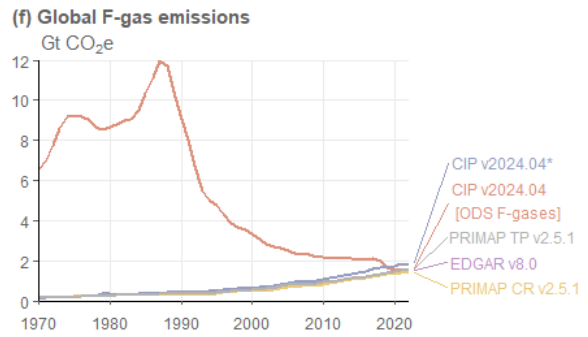
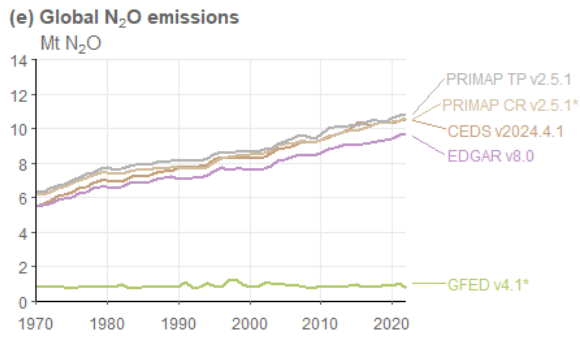
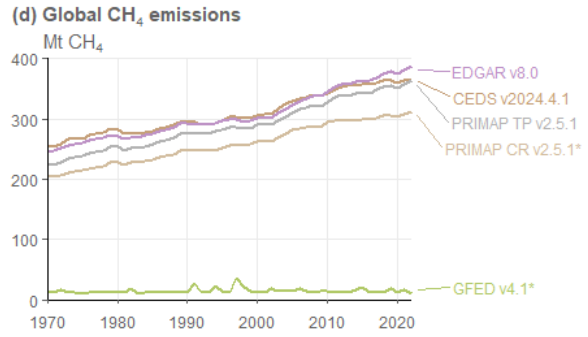
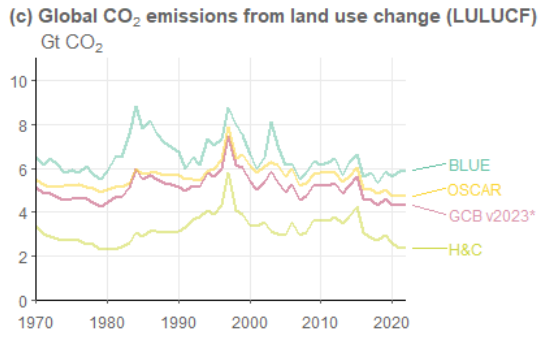
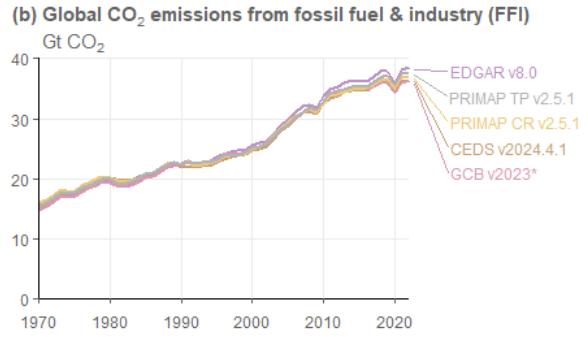
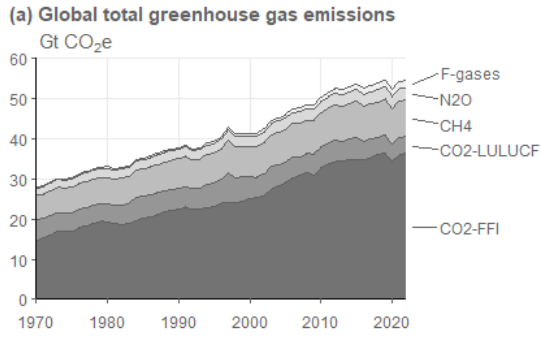
236
237 Average annual GHG emissions for the decade 2013–2022 were 53 ± 5.4 GtCO₂e, which is the same as the estimate
238 from last year for 2012–2021. Average decadal GHG emissions have increased steadily since the 1970s across all
239 major groups of GHGs, driven primarily by increasing CO₂ emissions from fossil fuel and industry but also rising
240 emissions of CH₄ and N₂O. Stratospheric ozone-depleting F-gases are regulated under the Montreal Protocol and its
241 amendments and their emissions have declined substantially since the 1990s, whereas emissions of other F-gases,
242 regulated under the UNFCCC, have grown more rapidly than other greenhouse gas emissions, but from low levels.
243 Both the magnitude and trend of CO₂ emissions from land-use change remain highly uncertain, with the latest data
244 indicating an average net flux between $4\text{--}5$ GtCO₂ yr⁻¹ for the past few decades.

245
246 AR6 WGIII reported total net anthropogenic emissions of 59 ± 6.6 GtCO₂e in 2019 and decadal average annual
247 emissions of 56 ± 6.0 GtCO₂e from 2010–2019. By comparison, our estimates here for the AR6 period sum to
248 55 ± 5.5 GtCO₂e in 2019 and an annual average of 53 ± 5.5 GtCO₂e for the same decade (2010–2019). The difference
249 between these figures, including the reduced relative uncertainty range, is partly driven by the substantial revision in
250 GCB CO₂-LULUCF estimates between the 2020 version (used in AR6 WGIII) of 6.6 GtCO₂ and the 2022 version
251 (used here) of 4.6 GtCO₂. The main reason for this downward revision comes from updated estimates of agricultural
252 areas by the FAO, which uses multi-annual land-cover maps from satellite remote sensing, leading to lower emissions

253 from cropland expansion, particularly in the tropical regions. It is important to note that this change is not a reflection
254 of changed and improved methodology per se but an update of the resulting estimation due to updates in the available
255 input data. Second, there are relatively small changes resulting from improvements in datasets since AR6, including
256 the new addition of global biomass burning (landscape fire) emissions. Datasets impacts are largest for CH₄, where
257 the emission estimate has reduced by 1.6 GtCO₂e in 2019. This is related to the switch from EDGAR in AR6 to
258 PRIMAP-hist CR in this study. EDGAR estimates considerably higher CH₄ emissions – from fugitive fossil sources,
259 as well as the livestock, rice cultivation and waste sectors – compared to country-reported data using higher tier
260 methods, as compiled in PRIMAP-hist CR (see Sect 2.1). The estimate for CO₂-FFI is also 1.6 GtCO₂e lower in 2019
261 in this study due to the switch from EDGAR to GCB, as the latter includes a cement carbonation sink not considered
262 in EDGAR. Differences in the remaining gases for 2019 are relatively small in magnitude (increases in N₂O
263 (+0.42 GtCO₂e) and UNFCCC-F-gases (+0.35 GtCO₂e).

264
265 The fossil fuel share of global greenhouse gas emissions was approximately 70% in 2022 (GWP100 weighted), based
266 on the EDGAR v8 dataset (Crippa et al. 2023) and net land use CO₂ emissions from the Global Carbon Budget
267 (Friedlingstein et al. 2023). Non fossil fuel emissions are mostly from land-use change, agriculture, cement production,
268 waste and F-gas emissions.

269
270 New literature not available at the time of the AR6 suggests that increases in atmospheric CH₄ concentrations are also
271 driven by methane emissions from wetland changes resulting from climate change (e.g. Basu et al., 2022; Peng et al.,
272 2022; Nisbet et al., 2023; Zhang et al., 2023). There is also a possible effect from CO₂ fertilisation (Feron et al., 2024;
273 Hu et al., 2023). Such carbon cycle feedbacks are not considered here as they are not a direct emission from human
274 activity, yet they will contribute to greenhouse gas concentration rise, forcing and energy budget changes discussed
275 in the next sections. They will become more important to properly account for in future years.



277 **Figure 2 Annual global anthropogenic greenhouse gas emissions by source, 1970–2022. Refer to Sect. 2.1 for a list of**
 278 **datasets. Datasets with an asterisk (*) indicate the sources used to compile global total greenhouse gas emissions in (a). CO₂-**
 279 **equivalent emissions in (a) and (f) are calculated using GWP100 from the AR6 WGI Chap. 7 (Forster et al., 2021). F-gas**
 280 **emissions in (a) comprise only UNFCCC F-gas emissions (see Sect. 2.1 for a list of species). F-gas emissions in (f) refer to**
 281 **UNFCCC F-gases, except for “CIP v2024.04 [ODS F-gases]”. GFED refers to CH₄ and N₂O emissions from global biomass**
 282 **fires only. The GCB v2023 dataset in (b) includes the cement carbonation sink, so is slightly lower than other estimates.**

283 **Table 1 Global anthropogenic greenhouse gas emissions by source and decade. All numbers refer to decadal averages,**
 284 **except for annual estimates in 2022 and 2023. CO₂-equivalent emissions are calculated using GWP100 from AR6 WGI**
 285 **Chap. 7 (Forster et al., 2021). Projections of non-CO₂ GHG emissions in 2023 remain unavailable at the time of publication.**
 286 **Uncertainties are ±8 % for CO₂-FFI, ±70 % for CO₂-LULUCF, ±30 % for CH₄ and F-gases, and ±60 % for N₂O,**
 287 **corresponding to a 90 % confidence interval. ODS F-gases are excluded, as noted in Sect. 2.1. CO₂-FFI includes the cement**
 288 **carbonation sink calculated in Friedlingstein et al. (2023).**

Units: GtCO ₂ e	1970- 1979	1980- 1989	1990- 1999	2000- 2009	2010- 2019	2013- 2022	2022	2023 (projectio n)
GHG	30±4.2	35±4.7	40±5.2	45±5.2	53±5.5	53±5.4	55±5.3	
CO ₂ - FFI	17.2±1.4	20.1±1.6	23.3±1.9	28.5±2.3	34.8±2.8	35.3±2.8	36.4±2.9	36.8±3
CO ₂ - LULUCF	4.6±3.3	5.2±3.7	5.8±4	5.2±3.6	5.2±3.5	4.7±3.3	4.3±3	4.1±2.9
CH ₄	6.3±1.9	6.9±2.1	7.5±2.3	8.1±2.4	8.8±2.6	8.8±2.7	9±2.7	
N ₂ O	2.1±1.2	2.3±1.4	2.5±1.5	2.7±1.6	2.9±1.8	3±1.8	3.1±1.9	
UNFCCC F-gases	0.21±0.06 4	0.37±0.11	0.52±0.15	0.84±0.25	1.4±0.42	1.6±0.48	1.8±0.54	

289

290 **2.3 Non-methane short-lived climate forcers**

291 In addition to GHG emissions, we provide an update of anthropogenic emissions of non-methane short-lived climate
 292 forcers (SLCFs) (SO₂, black carbon (BC), organic carbon (OC), NO_x, volatile organic compounds (VOCs), CO and
 293 NH₃). Data is presented in Table 2. HFCs are considered in Sect. 2.2.

294

295 Sectoral emissions of SLCFs are derived from two sources. For fossil fuel, industrial, waste and agricultural sectors,
 296 we use the CEDS dataset. CEDS provides global emissions totals from 1750 to 2022 in its most recent version
 297 (v_2024_04_01) (Hoesly et al., 2018; Hoesly & Smith, 2024). No CEDS emissions data are currently available for
 298 2023. The estimate for 2023 was derived by assuming a scaled return to an underlying SSP2-4.5 emissions scenario,
 299 used for inputs to COVID-MIP (Forster et al., 2020, Lamboll et al. 2021). We find that the 2020-2022 emissions trends
 300 comparing CEDS and the COVID-MIP extrapolation are not substantially different (Supplement Fig. S2), so the

301 COVID-MIP extension to 2023 is justifiable. In Forster et al. (2023), the CEDS dataset was only available to 2019,
302 so the COVID-MIP extension was used to 2022. Therefore, emissions from 2020 have been revised in this year's
303 paper with 2020-2022 data now arising from CEDS.

304
305 Overall, the net SO₂ emissions were similar (within 2 TgSO₂, see Supplement Sect. S2) over the 2020-22 period in
306 the CEDS dataset than our estimate in Forster et al. (2023). The CEDS dataset accounts for the introduction of strict
307 fuel sulphur controls brought in by the International Maritime Organization on 1 January 2020. Total SO₂ emissions
308 in 2019 were 84.2 TgSO₂ (Table 2). The SO₂ emissions from international shipping declined by 7.4 TgSO₂ from 10.4
309 TgSO₂ in 2019 to 3.0 TgSO₂ in 2020, which is close to the expected 8.5 TgSO₂ reduction estimated by the International
310 Maritime Organization, approximately -80% from the 2019 number, accounting for a 3-month phase in period and
311 COVID-19 changes. Non-shipping SO₂ emissions were impacted slightly by COVID-19, but had rebounded to close
312 to 2019 levels by 2022 in CEDS.

313
314 For biomass burning SLCF emissions, we follow AR6 WGIII (Dhakal et al., 2022) and use GFED (van der Werf et
315 al., 2017) version 4 with small fires (GFED4.1s) for 1997 to 2023, with the dataset extended back to 1750 for CMIP6
316 (van Marle et al., 2017). Estimates from 2017 to 2023 are provisional. As demonstrated with the update to CEDS
317 emissions, the potential for both sources of emissions data to be updated in future versions exists, for example with a
318 planned introduction of GFED5 in preparation for CMIP7.

319
320 Using our combined estimate of GFED and CEDS with a 2023 extrapolation, emissions of all SLCFs were reduced in
321 2022 relative to 2019, but rebounded again in 2023 (Table 2). The primary driver of the increase in 2023 is an
322 anomalous biomass burning year, mostly related to the unprecedented 2023 Canadian fire season (Barnes et al. 2023),
323 with a smaller contribution from a continued recovery from COVID-19. Under these assumptions, 2023 was a record
324 year for emissions of organic carbon (driven again by a very active biomass burning season) and ammonia (driven by
325 a steady background increase in agricultural sources, plus a contribution from biomass burning). Causes of the
326 enhanced burning are not distinguished in the GFED data. Whether human-caused burning, a feedback due to the
327 extreme heat or naturally occurring, we choose to include them in our tracking, as historical biomass burning emissions
328 inventories have previously been consistently treated as an anthropogenic forcing (for example in CMIP6), though
329 this assumption may need to be revisited in the future. This differs from the treatment of accounting for CO₂ and CH₄
330 emissions at present (Sect. 2.2), where we do not include natural emissions in the inventories. As described in Sect.
331 4, the treatment of all biomass burning emissions as a forcing has implications for several categories of anthropogenic
332 radiative forcing. Trends in SLCFs emissions are spatially heterogeneous (Szopa et al., 2021), with strong shifts in the
333 locations of reductions and increases over the 2010–2019 decade (Hodnebrog et al. 2024).

334 **Table 2 Emissions of the major SLCFs in 1750, 2019, 2022 and 2023 from a combination of CEDS and GFED. Emissions of**
335 **SO₂+SO₄ use SO₂ molecular weights. Emissions of NO_x use NO₂ molecular weights. VOCs are for the total mass.**

Compound	1750 emissions (Tg yr ⁻¹)	2019 emissions (Tg yr ⁻¹)	2022 emissions (Tg yr ⁻¹)	2023 emissions (Tg yr ⁻¹)
----------	---------------------------------------	---------------------------------------	---------------------------------------	---------------------------------------

Sulfur dioxide (SO ₂) + sulfate (SO ₄ ²⁻)	2.8	84.2	75.3	79.1
Black carbon (BC)	2.1	7.5	6.8	7.3
Organic carbon (OC)	15.5	34.2	25.8	40.7
Ammonia (NH ₃)	6.6	67.6	67.3	71.1
Oxides of nitrogen (NO _x)	19.4	141.7	130.4	139.4
Volatile organic compounds (VOCs)	60.9	217.3	183.9	228.1
Carbon monoxide (CO)	348.4	853.8	686.4	917.5

336
337 Uncertainties associated with these emission estimates are difficult to quantify. From the non-biomass-burning sectors
338 they are estimated to be smallest for SO₂ ($\pm 14\%$), largest for black carbon (BC) (a factor of 2) and intermediate for
339 other species (Smith et al., 2011; Bond et al., 2013; Hoesly et al., 2018). Uncertainties are also likely to increase both
340 backwards in time (Hoesly et al., 2018) and again in the most recent years. The estimates of non-biomass-burning
341 emissions for 2023, especially SO₂ are highly uncertain, owing to the use of proxy activity data used with a SSP2-4.5
342 scenario extension (see above). Future updates of CEDS are expected to include uncertainties (Hoesly et al., 2018).
343 Even though trends over recent years are uncertain, the general decline in some SLCF emissions derived from
344 inventories punctuated by temporary anomalous years with high biomass burning emissions including 2023 is
345 supported by MODIS Terra and Aqua aerosol optical depth measurements (e.g. Quaas et al., 2022, Hodnebrog et al
346 2024).

347 **3 Well-mixed greenhouse gas concentrations**

348 As in Forster et al. (2023), we report best-estimate global mean concentrations for 52 well-mixed greenhouse gases.
349 These concentrations are updated to 2023.

350
351 As in AR6 and Forster et al. (2023), CO₂ mixing ratios were taken from the NOAA Global Monitoring Laboratory
352 (GML) and are updated here through 2023 (Lan et al., 2024a). As in Forster et al. (2023), CO₂ is reported on the
353 WMO-CO₂-X2019 scale, which differs from the WMO-CO₂-X2007 scale used in AR6. Prior to the use of NOAA
354 GML data from 1980 onwards, a conversion is applied to the AR6 CO₂ time series to take into account the scale
355 change using $X_{2019} = 1.00079 * X_{2007} - 0.142$ ppm. Other LLGHG records were compiled from NOAA and AGAGE
356 global networks or extrapolated from literature. An average of NOAA and AGAGE data were used for N₂O, CH₄,
357 CFC-11, CFC-12, CFC-113, CCl₄, HCFC-22, HFC-134a, and HFC-125 (Lan et al., 2024b; Dutton et al., 2024; Prinn
358 et al., 2018), which, along with CO₂, account for over 98% of the ERF from well-mixed greenhouse gases. In cases

359 where no updated information is available, global estimates were extrapolated from Vimont et al. (2022), Western et
360 al. (2023), or other literature and scaled to be consistent with those reported in AR6. Some extrapolations are based
361 on data from the mid-2010s (Droste et al., 2020; Laube et al., 2014; Simmonds et al., 2017; Vollmer et al., 2018), but
362 have an imperceptible effect on the total ERF assessed in Sect. 4, and are included to maintain consistency with AR6.
363 Mixing ratio uncertainties for 2023 are assumed to be similar to 2019, and we adopt the same uncertainties as assessed
364 in AR6 WGI.

365
366 The global surface mean concentrations of CO₂, CH₄ and N₂O in 2023 were 419.3 [±0.4] parts per million (ppm),
367 1922.5 [±3.3] parts per billion (ppb) and 336.9 [±0.4] ppb, respectively. Concentrations of all three major GHGs have
368 increased since 2019, with CO₂ increasing by 9.2 ppm, CH₄ by 56 ppb, and N₂O by 4.8 ppb. Increases since 2019 are
369 consistent with those from the CSIRO network (Francey et al., 1999), which are 9.3 ppm, 55 ppb, and 5.0 ppb for
370 CO₂, CH₄, and N₂O, respectively. With few exceptions, concentrations of ozone-depleting substances, such as CFC-
371 11 and CFC-12, continue to decline, while those of replacement compounds (HFCs) have increased. HFC-134a, for
372 example, has increased 20% since 2019 to 129.5 parts per trillion (ppt). Aggregated across all gases, PFCs have
373 increased from 109.7 to an estimated 115 ppt CF₄-eq from 2019 to 2023, HFCs from 237 to 301 ppt HFC-134a-eq,
374 while Montreal gases have declined from 1032 to 1004 ppt CFC-12-eq. Mixing ratio equivalents are determined by
375 the radiative efficiencies of each greenhouse gas from Hodnebrog et al. (2020).

376
377 Ozone is an important greenhouse gas with strong regional variation both in the stratosphere and troposphere (Szopa
378 et al., 2021). Its ERF arising from its regional distribution is assessed in Sect. 4 but following AR6 convention is not
379 included with the GHGs discussed here. Other non-methane SLCFs are heterogeneously distributed in the atmosphere
380 and are also not typically reported in terms of a globally averaged concentration. Globally averaged concentrations
381 for these are normally model-derived, supplemented by local monitoring networks and satellite data (Szopa et al.,
382 2021).

383
384 In this update we employ AR6-derived uncertainty estimates and do not perform a new assessment. Table S2 in
385 Supplement Sect. S3 shows specific updated concentrations for all the GHGs considered.

386 **4 Effective radiative forcing (ERF)**

387 ERFs were principally assessed in Chap. 7 of AR6 WGI (Forster et al., 2021), which focussed on assessing ERF from
388 changes in atmospheric concentrations; it also supported estimates of ERF in Chap. 6 that attributed forcing to specific
389 precursor emissions (Szopa et al., 2021) and also generated the time history of ERF shown in AR6 WGI Fig. 2.10 and
390 discussed in Chap. 2 (Gulev et al., 2021). Only the concentration-based estimates are updated herein.

391
392 The ERF calculation follows the methodology used in AR6 WGI (Smith et al., 2021) as updated by Forster et al.
393 (2023). For each category of forcing, a 100 000-member probabilistic Monte Carlo ensemble is sampled to span the

394 assessed uncertainty range in each forcing. All uncertainties are reported as 5 %–95 % ranges and provided in square
 395 brackets. The methods are all detailed in the Supplement, Sect. S4.

396
 397 The summary results for the anthropogenic constituents of ERF and solar irradiance in 2023 relative to 1750 are shown
 398 in Fig. 3a. In Table 3 these are summarised alongside the equivalent ERFs from AR6 (1750–2019) and last year’s
 399 Climate Indicators update (1750–2022). Fig. 3b shows the time evolution of ERF from 1750 to 2023.

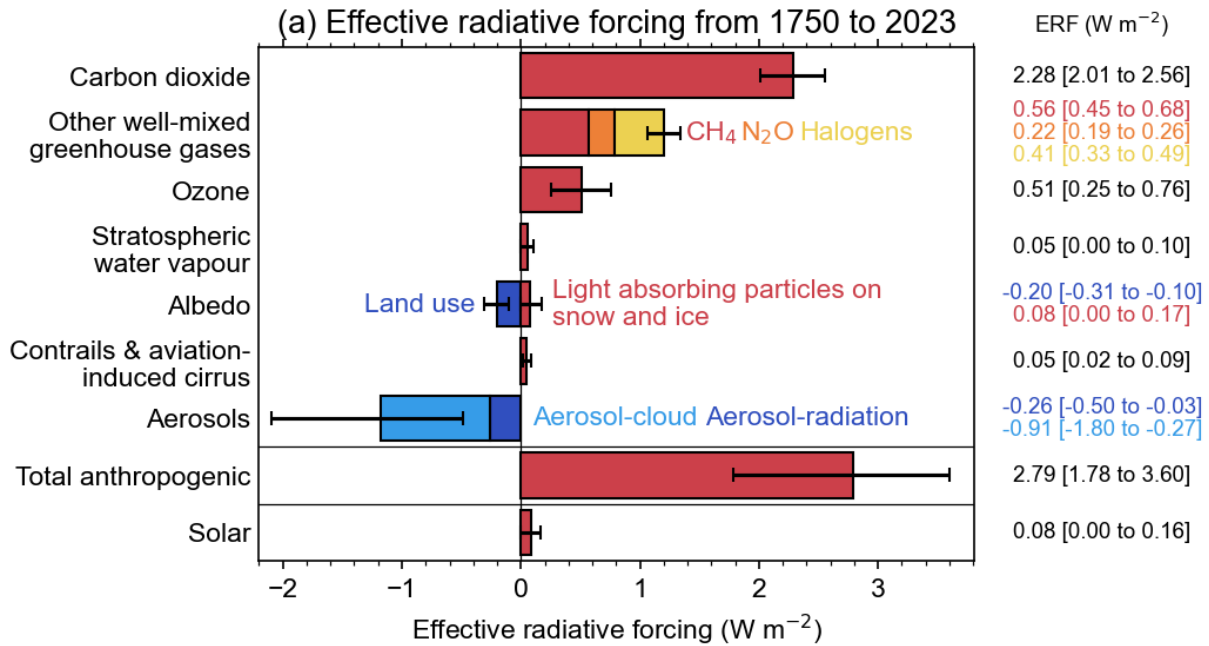
401 **Table 3 Contributions to anthropogenic effective radiative forcing (ERF) for 1750–2023 assessed in this section. Data is for**
 402 **single year estimates unless specified. All values are in watts per square metre (W m^{-2}), and 5 %–95 % ranges are in square**
 403 **brackets. As a comparison, the equivalent assessments from AR6 (1750–2019) and last year’s Climate Indicators (1750–**
 404 **2022) are shown. Solar ERF is included and unchanged from AR6, based on the most recent solar cycle (2009–2019), thus**
 405 **differing from the single-year estimate in Fig. 3a. Volcanic ERF is excluded due to the sporadic nature of eruptions.**

Forcer	1750-2019 [W m^{-2}] (AR6)	1750-2022 [W m^{-2}] (Forster et al., 2023)	1750-2023 [W m^{-2}]	Reason for change since last year
CO ₂	2.16 [1.90 to 2.41]	2.25 [1.98 to 2.52]	2.28 [2.01 to 2.56]	Increases in GHG concentrations resulting from increases in emissions
CH ₄	0.54 [0.43 to 0.65]	0.56 [0.45 to 0.67]	0.56 [0.45 to 0.68]	
N ₂ O	0.21 [0.18 to 0.24]	0.22 [0.19 to 0.25]	0.22 [0.19 to 0.26]	
Halogenated GHGs	0.41 [0.33 to 0.49]	0.41 [0.33 to 0.49]	0.41 [0.33 to 0.49]	
Ozone	0.47 [0.24 to 0.71]	0.48 [0.24 to 0.72]	0.51 [0.25 to 0.76]	Increase in precursors (CO, VOC, CH ₄)
Stratospheric water vapour	0.05 [0.00 to 0.10]	0.05 [0.00 to 0.10]	0.05 [0.00 to 0.10]	
Aerosol-radiation interactions	-0.22 [-0.47 to +0.04]	-0.21 [-0.42 to 0.00]	-0.26 [-0.50 to -0.03]	Large increases in biomass burning aerosol in 2023; continued recovery from COVID-19; drop in sulphur from shipping
Aerosol-cloud interactions	-0.84 [-1.45 to -0.25]	-0.77 [-1.33 to -0.13]	-0.91 [-1.80 to -0.27]	
Land use (surface albedo changes and effects of irrigation)	-0.20 [-0.30 to -0.10]	-0.20 [-0.30 to -0.10]	-0.20 [-0.31 to -0.10]	
Light-absorbing	0.08 [0.00 to 0.18]	0.06 [0.00 to 0.14]	0.08 [0.00 to 0.17]	Rebound in BC

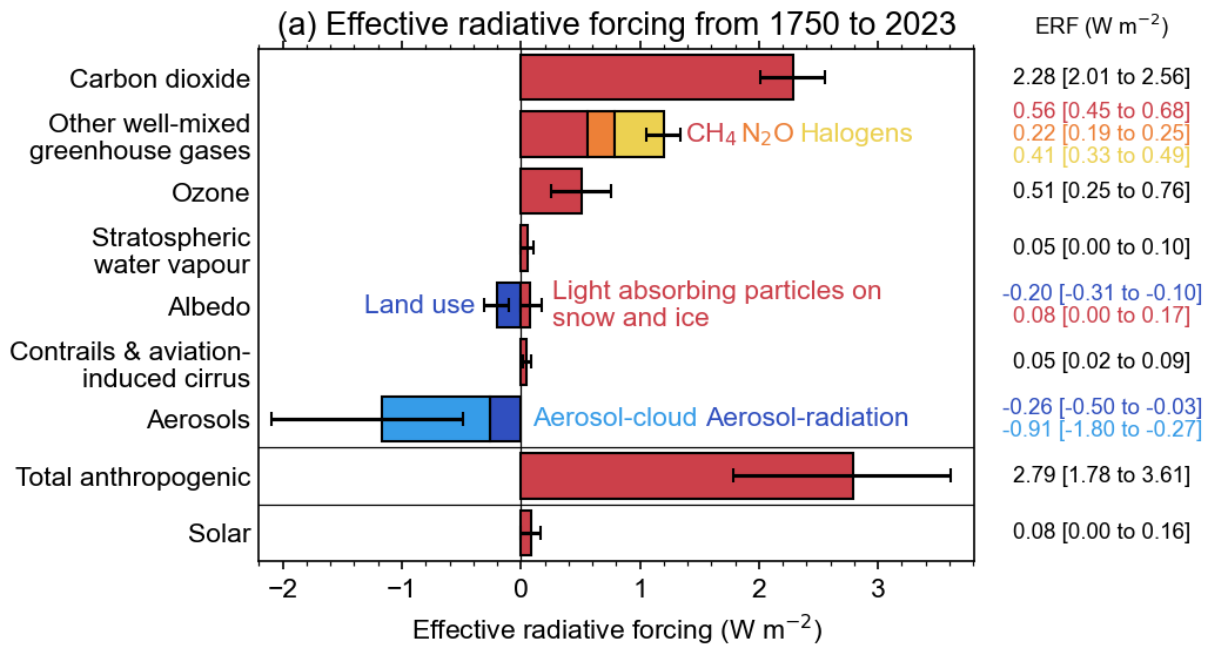
particles on snow and ice				emissions from biomass burning
Contrails and contrail-induced cirrus	0.06 [0.02 to 0.10]	0.05 [0.02 to 0.09]	0.05 [0.02 to 0.09]	Estimates of aviation activity are rebounding since the pandemic but still below 2019 levels in 2023
Total anthropogenic	2.72 [1.96 to 3.48]	2.91 [2.19 to 3.63]	2.79 [1.78 to 3.61]	Possible strong aerosol forcing in 2023 partly offset by increases in GHG and ozone forcing
Solar irradiance	0.01 [-0.06 to 0.08]	0.01 [-0.06 to 0.08]	0.01 [-0.06 to 0.08]	

406

407

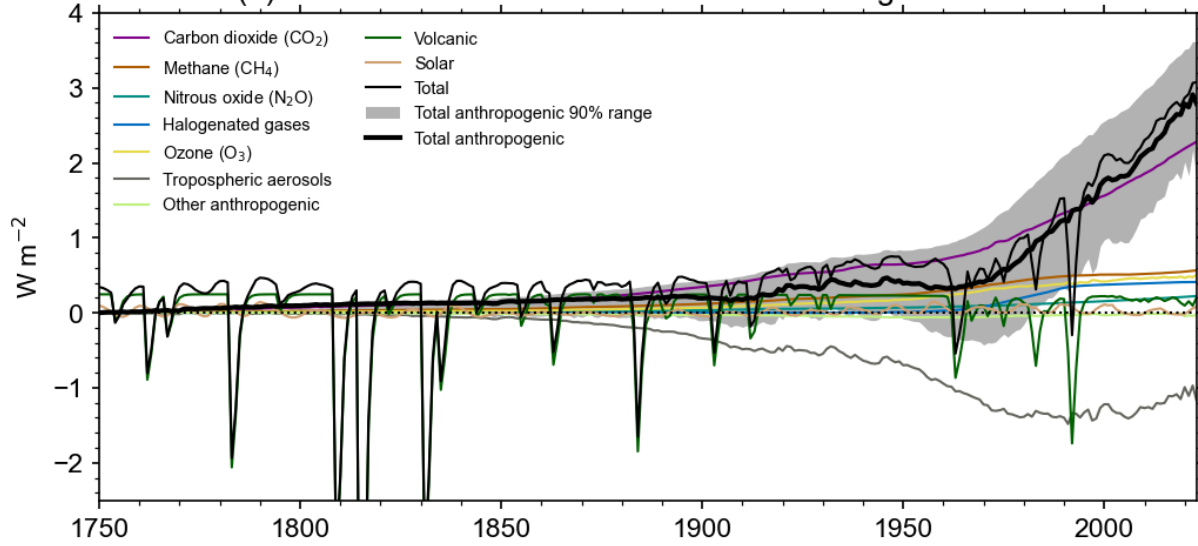


408



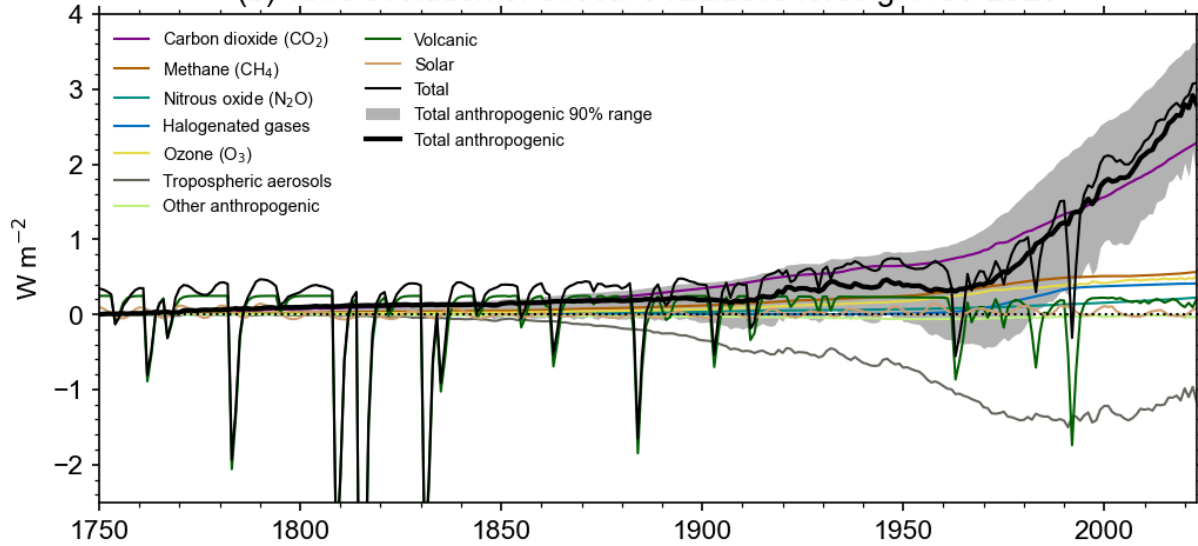
409

(b) Time evolution of effective radiative forcing 1750-2023



410

(b) Time evolution of effective radiative forcing 1750-2023



411

412 **Figure 3 Effective radiative forcing from 1750–2023. (a) 1750–2023 change in ERF, showing best estimates (bars) and 5%–**
413 **95 % uncertainty ranges (lines) from major anthropogenic components to ERF, total anthropogenic ERF and solar forcing.**
414 **Note that solar forcing in 2023 is a single-year estimate. (b) Time evolution of ERF from 1750 to 2023. Best estimates from**
415 **major anthropogenic categories are shown along with solar and volcanic forcing (thin coloured lines), total (thin black line),**
416 **and anthropogenic total (thick black line). The 5%–95 % uncertainty in the anthropogenic forcing is shown by grey**
417 **shading.**

418 Total anthropogenic ERF has increased to 2.79 [1.78 to 3.61] W m^{-2} in 2023 relative to 1750, compared to 2.72 [1.96
419 to 3.48] W m^{-2} for 2019 relative to 1750 in AR6. The estimate of ERF for 2023 is lower than the 2.91 [2.19 to 3.63]
420 W m^{-2} in 2022 evaluated in last year's Indicators. The main reason for the decline in 2023 relative to 2022 is a very
421 strong contribution from biomass burning aerosol in 2023, particularly organic carbon emissions which strengthened

422 the negative aerosol ERF (see also Sect. 2.3). Sulphur emissions from shipping have declined since 2020, weakening
423 the aerosol ERF and adding around $+0.1 \text{ W m}^{-2}$ over 2020 to 2023 (Gettelman et al., 2024; see Supplement Sect.
424 S4.2.2). However, the strengthened negative ERF from increased biomass burning likely dominated the effect of
425 reduced shipping emissions. As discussed in Sect. 2, it is not easy to determine how much of the biomass burning
426 contribution is from natural wildfires in response to 2023's anomalously warm year, which would be a climate
427 feedback rather than a forcing. We follow the convention of CMIP and count all biomass burning emissions as
428 anthropogenic, though this assumption may need revision in future. The approach of including all biomass burning
429 aerosols is consistent with reporting ERF based on concentration increase of GHGs independent of whether CO_2 and
430 CH_4 are caused by anthropogenic emissions or a smaller part is caused by any feedbacks such as from biomass burning
431 fires or wetlands. However, changes in mineral dust and sea salt are not included in ERF of aerosols and any changes
432 are interpreted as yearly variations or related to feedbacks.

433
434 The relative uncertainty in the total ERF was at the lowest reported in 2022, see Table 3, but with the strengthening
435 of the aerosol ERF due to biomass additional burning, the relative uncertainty in total ERF for 2023 is higher than in
436 2019 reported in AR6 (Forster et al., 2021). Despite the strong aerosol forcing in 2023, decadal trends in anthropogenic
437 ERF remain high, and are over 0.6 W m^{-2} per decade. These are discussed further in Sect. 7.3.

438
439 The ERF from well-mixed GHGs is $3.48 [3.18 \text{ to } 3.79] \text{ W m}^{-2}$ for 1750–2023, of which 2.28 W m^{-2} is from CO_2 ,
440 0.56 W m^{-2} from CH_4 , 0.22 W m^{-2} from N_2O and 0.41 W m^{-2} from halogenated gases (contributions do not sum to
441 total due to rounding). This is an increase from $3.32 [3.03 \text{ to } 3.61] \text{ W m}^{-2}$ for 1750–2019 in AR6. ERFs from CO_2 ,
442 CH_4 and N_2O have all increased since the AR6 WG1 assessment for 1750–2019, owing to increases in atmospheric
443 concentrations.

444
445 The total aerosol ERF (sum of the ERF from aerosol–radiation interactions (ERF_{ari}) and aerosol–cloud interactions
446 (ERF_{aci})) for 1750–2023 is $-1.18 [-2.10 \text{ to } -0.49] \text{ W m}^{-2}$ compared to $-0.98 [-1.58 \text{ to } -0.40] \text{ W m}^{-2}$ in Forster et
447 al. (2023) and $-1.06 [-1.71 \text{ to } -0.41] \text{ W m}^{-2}$ assessed for 1750–2019 in AR6 WG1. This counters a recent trend of
448 reductions in aerosol forcing, and is related in most part to 2023 being an extremely active biomass burning season.
449 Most of this reduction is from ERF_{aci}, which is determined to be $-0.91 [-1.80 \text{ to } -0.27] \text{ W m}^{-2}$ in 2023 compared to
450 $-0.77 [-1.33 \text{ to } -0.23] \text{ W m}^{-2}$ for 1750–2022 (Forster et al. 2023) and $-0.84 [-1.45 \text{ to } -0.25] \text{ W m}^{-2}$ in AR6 for 1750–
451 2019. ERF_{ari} for 1750–2023 is $-0.26 [-0.50 \text{ to } -0.03] \text{ W m}^{-2}$, stronger than the $-0.21 [-0.42 \text{ to } 0.00] \text{ W m}^{-2}$ for 1750–
452 2022 and the $-0.22 [-0.47 \text{ to } 0.04] \text{ W m}^{-2}$ assessed for 1750–2019 in AR6 WG1 (Forster et al., 2021). The largest
453 contributions to ERF_{ari} are from SO_2 (primary source of sulfate aerosol; -0.24 W m^{-2}), BC ($+0.16 \text{ W m}^{-2}$), OC
454 (-0.11 W m^{-2}) and NH_3 (primary source of nitrate aerosol; -0.04 W m^{-2}). ERF_{ari} also includes terms from CH_4 , N_2O ,
455 VOCs and NO_x which are small.

456
457 Ozone ERF is determined to be $0.51 [0.25 \text{ to } 0.76] \text{ W m}^{-2}$ for 1750–2023, slightly higher than the AR6 assessment of
458 $0.47 [0.24 \text{ to } 0.71] \text{ W m}^{-2}$ for 1750–2019. This is due to the increase in emissions of some of its precursors (CO , VOC ,
459 CH_4), but this result is highly uncertain since the preliminary OMI/MLS satellite data indicate tropospheric ozone

460 burden is stable from 2020 to 2023 (meaning that the 2023 level does not reach the 2019 level) which could be partly
461 due to the 2020-2023 levels of tropospheric NO₂ being lower than the pre-COVID levels (OMI data from Krotkov et
462 al. 2019). Land-use forcing and stratospheric water vapour from methane oxidation are unchanged (to two decimal
463 places) since AR6. BC emissions have increased between 2022 and 2023, and were similar to 2019 levels in 2023
464 resulting in ERF from light-absorbing particles on snow and ice being 0.08 [0.00 to 0.17] W m⁻² for 1750–2023,
465 similar to AR6. We determine from provisional data that aviation activity in 2023 had not yet returned to pre-COVID
466 levels (IATA, 2024). Therefore, ERF from contrails and contrail-induced cirrus remains lower than AR6, at 0.05 [0.02
467 to 0.09] W m⁻² in 2023 compared to 0.06 [0.02 to 0.10] W m⁻² in 2019.

468
469 The headline assessment of solar ERF is unchanged, at 0.01 [–0.06 to +0.08] W m⁻² from pre-industrial to the 2009–
470 2019 solar cycle mean. Separate to the assessment of solar forcing over complete solar cycles, we provide a single-
471 year solar ERF for 2023 of 0.08 [0.00 to +0.16] W m⁻². This is higher than the single-year estimate of solar ERF for
472 2019 (a solar minimum) of –0.02 [–0.08 to 0.06] W m⁻².

473
474 Volcanic ERF is included in the overall time series (Fig. 3b) but following IPCC convention we do not provide a
475 single-year estimate for 2023 given the sporadic nature of volcanoes. Alongside the time series of stratospheric aerosol
476 optical depth derived from proxies and satellite products, for 2022 and 2023 we include the stratospheric water vapour
477 contribution from the Hunga Tonga-Hunga Ha’apai (HTHH) eruption derived from Microwave Limb Sounder (MLS)
478 data.

479
480 Stratospheric water vapour forcing is estimated to be +0.14 W m⁻² in 2022 and +0.18 W m⁻² in 2023, and in 2023
481 almost totally offsets the negative forcing from stratospheric aerosol.

482

483 **5 Earth energy imbalance**

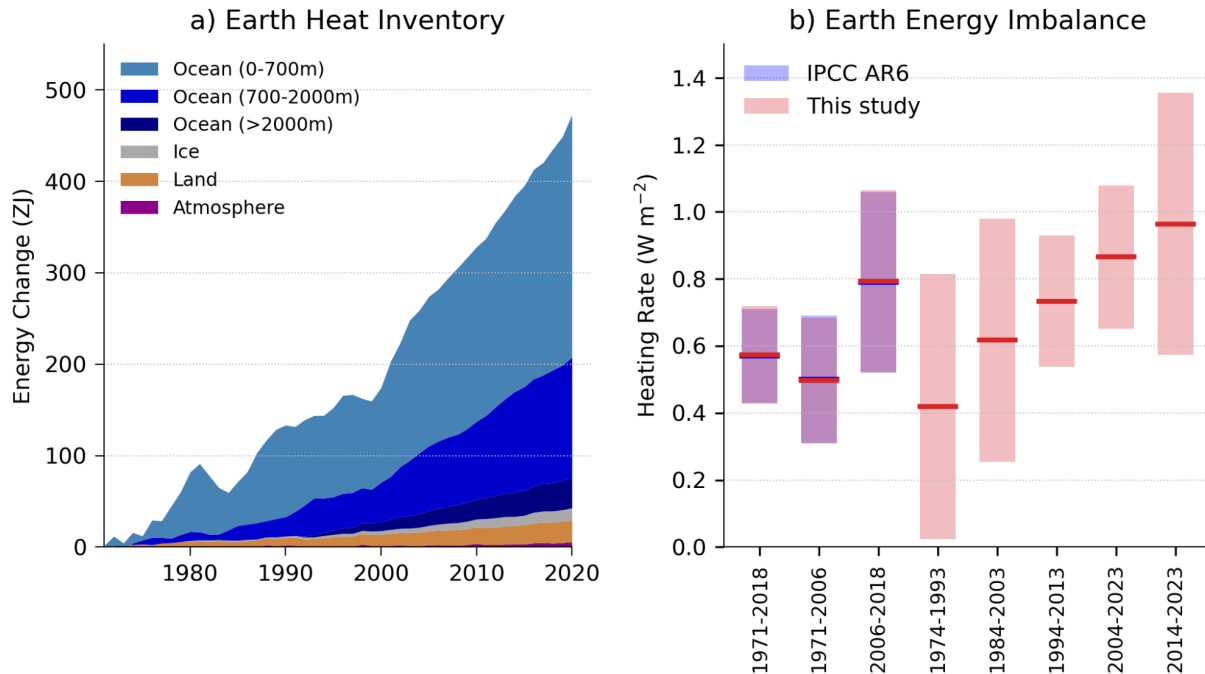
484 The Earth energy imbalance (EEI), assessed in Chap. 7 of AR6 WGI (Forster et al., 2021), provides a measure of
485 accumulated surplus energy (heating) in the climate system, and is hence an essential indicator to monitor the current
486 and future status of global warming. It represents the difference between the radiative forcing acting to warm the
487 climate and Earth’s radiative response, which acts to oppose this warming. On annual and longer timescales, the global
488 Earth heat inventory changes associated with EEI are dominated by the changes in global ocean heat content (OHC),
489 which accounts for about 90 % of global heating since the 1970s (Forster et al., 2021). This planetary heating results
490 in changes in all components of the Earth system such as sea level rise, ocean warming, ice loss, rise in temperature
491 and water vapor in the atmosphere, changes in ocean and atmospheric circulation, ice loss and permafrost thawing
492 (e.g. Cheng et al., 2022; von Schuckmann et al., 2023a), with adverse impacts for ecosystems and human systems
493 (Douville et al., 2021; IPCC, 2022).

494

495 On decadal timescales, changes in global surface temperatures (Sect. 5) can become decoupled from EEI by ocean
496 heat rearrangement processes (e.g. Palmer and McNeall, 2014; Allison et al., 2020). Therefore, the increase in the
497 Earth heat inventory provides a robust indicator of the rate of global change on interannual-to-decadal timescales
498 (Cheng et al., 2019; Forster et al., 2021; von Schuckmann et al., 2023a). AR6 WGI found increased confidence in the
499 assessment of change in the Earth heat inventory compared to previous IPCC reports due to observational advances
500 and closure of the energy and global sea level budgets (Forster et al., 2021; Fox-Kemper et al., 2021).

501
502 AR6 estimated that EEI increased from 0.50 [0.32–0.69] W m^{-2} during the period 1971–2006 to 0.79 [0.52–
503 1.06] W m^{-2} during the period 2006–2018 (Forster et al., 2021). The contributions to increases in the Earth heat
504 inventory throughout 1971–2018 remained stable: 91 % for the full-depth ocean, 5 % for the land, 3 % for the
505 cryosphere and about 1 % for the atmosphere (Forster et al., 2021). Two recent studies demonstrated independently
506 and consistently that since 1960, the warming of the world ocean has accelerated at a relatively consistent pace
507 of $0.15 \pm 0.05 \text{ W m}^{-2}$ per decade (Minière et al., 2023; Storto and Yang, 2024), while the land, cryosphere, and
508 atmosphere have been warming at a pace of $0.013 \pm 0.003 \text{ W m}^{-2}$ per decade (Minière et al., 2023). The increase
509 in EEI over the most recent quarter of a decade (Fig. 4) has also been reported by Cheng et al. (2019), von Schuckmann
510 et al. (2020, 2023a), Loeb et al. (2021), Hakuba et al. (2021), Kramer et al. (2021) Raghuraman et al. (2021) and
511 Minère et al. (2023). Drivers for the observed increase over the most recent period (i.e. past 2 decades) are discussed
512 to be linked to rising concentrations of well-mixed greenhouse gases and recent reductions in aerosol emissions
513 (Raghuraman et al., 2021; Kramer et al., 2021; Hansen et al., 2023), and to an increase in absorbed solar radiation
514 associated with decreased reflection by clouds and sea-ice and a decrease in outgoing longwave radiation (OLR) due
515 to increases in trace gases and water vapor (Loeb et al., 2021) . The degree of contribution from the different drivers
516 is uncertain and still under active investigation.

517
518
519 We carry out an update to the AR6 estimate of changes in the Earth heat inventory based on updated observational
520 time series for the period 1971–2020 (Table 4 and Fig. 4). Time series of heating associated with loss of ice and
521 warming of the atmosphere and continental land surface are obtained from the recent Global Climate Observing
522 System (GCOS) initiative (von Schuckmann et al., 2023b; Adusumilli et al., 2022; Cuesta-Valero et al., 2023;
523 Vanderkelen and Thiery, 2022; Nitzbon et al., 2022; Kirchengast et al., 2022). We use the original AR6 time series
524 ensemble OHC time series for the period 1971–2018 and then an updated five-member ensemble for the period 2019–
525 2023. We “splice” the two sets of time series by adding an offset as needed to ensure that the 2018 values are identical.
526 The AR6 heating rates and uncertainties for the ocean below 2000 m are assumed to be constant throughout the period.
527 The time evolution of the Earth heat inventory is determined as a simple summation of time series of atmospheric
528 heating; continental land heating; heating of the cryosphere; and heating of the ocean over three depth layers: 0–700,
529 700–2000 and below 2000 m (Fig. 4a). While von Schuckmann et al. (2023a) have also quantified heating of
530 permafrost and inland lakes and reservoirs, these additional terms are very small and are omitted here for consistency
531 with AR6 (Forster et al., 2021).



533
 534 **Figure 4 (a) Observed changes in the Earth heat inventory for the period 1971–2020, with component contributions as**
 535 **indicated in the figure legend. (b) Estimates of the Earth energy imbalance for the IPCC AR6 assessment periods, for**
 536 **consecutive 20-year periods and the most recent decade. Shaded regions indicate the *very likely* range (90 % to 100 %**
 537 **probability). Data use and approach are based on the AR6 methods and further described in the Supplement Sect. 5**
 538 **Materials. For the IPCC AR6 periods our assessment closely matches that in AR6. Note the periods in our assessment**
 539 **overlap with different IPCC AR6 periods.**

540 In our updated analysis, we find successive increases in EEI for each 20-year period since 1974, with an estimated
 541 value of 0.42 [0.02 to 0.81] $W m^{-2}$ during 1974–1993 that more than doubled to 0.87 [0.65 to 1.08] $W m^{-2}$ during
 542 2004–2023 (Fig. 4b). In addition, there is some evidence that the warming signal is propagating into the deeper ocean
 543 over time, as seen by a robust increase of deep (700–2000 m) ocean warming since the 1990s (von Schuckmann et al.,
 544 2020; 2023; Cheng et al., 2019, 2022). The model simulations qualitatively agree with the observational evidence (e.g.
 545 Gleckler et al., 2016; Cheng et al., 2019), further suggesting that more than half of the OHC increase since the late
 546 1800s occurs after the 1990s.

547

548 The update of the AR6 assessment periods to end in 2023 results in systematic increases of EEI: 0.65 $W m^{-2}$ during
 549 1976–2023 compared to 0.57 $W m^{-2}$ during 1971–2018; and 0.96 $W m^{-2}$ during 2011–2023 compared to 0.79 $W m^{-2}$
 550 2006–2018 (Table 4). The trend and interannual variability of EEI can largely be explained by a combination of
 551 surface temperature changes and radiative forcing (Hodnebrog et al., 2024), although there was a jump in 2023 which
 552 is still being investigated (Hansen et al., 2023).

553

554 **Table 4 Estimates of the Earth energy imbalance (EEI) for AR6 and the present study.**

Time Period	Earth energy imbalance (W m^{-2}). Square brackets [show 90% confidence intervals].	
	IPCC AR6	This Study
1971-2018	0.57 [0.43 to 0.72]	0.57 [0.43 to 0.72]
1971-2006	0.50 [0.32 to 0.69]	0.50 [0.31 to 0.68]
2006-2018	0.79 [0.52 to 1.06]	0.79 [0.52 to 1.07]
1976-2023	-	0.65 [0.48 to 0.82]
2011-2023	-	0.96 [0.67 to 1.26]

555

556 **6 Global surface temperatures**

557 AR6 WGI Chap. 2 assessed the 2001–2020 globally averaged surface temperature change above an 1850–1900
558 baseline to be 0.99 [0.84 to 1.10] °C and 1.09 [0.95 to 1.20] °C for 2011–2020 (Gulev et al., 2021). Updated estimates
559 to 2022 of 1.15 [1.00–1.25] °C were given in AR6 SYR (Lee et al., 2023), matching the estimate in Forster et al.
560 (2023).

561

562 There are choices around the methods used to aggregate surface temperatures into a global average, how to correct for
563 systematic errors in measurements, methods of infilling missing data, and whether surface measurements or
564 atmospheric temperatures just above the surface are used. These choices, and others, affect temperature change
565 estimates and contribute to uncertainty (IPCC AR6 WGI Chap. 2, Cross Chap. Box 2.3, Gulev et al., 2021). The
566 methods chosen here closely follow AR6 WGI and are presented in the Supplement, Sect. S6. Confidence intervals
567 are taken from AR6 as only one of the employed datasets regularly updates ensembles (see Supplement, Sect. S6).

568

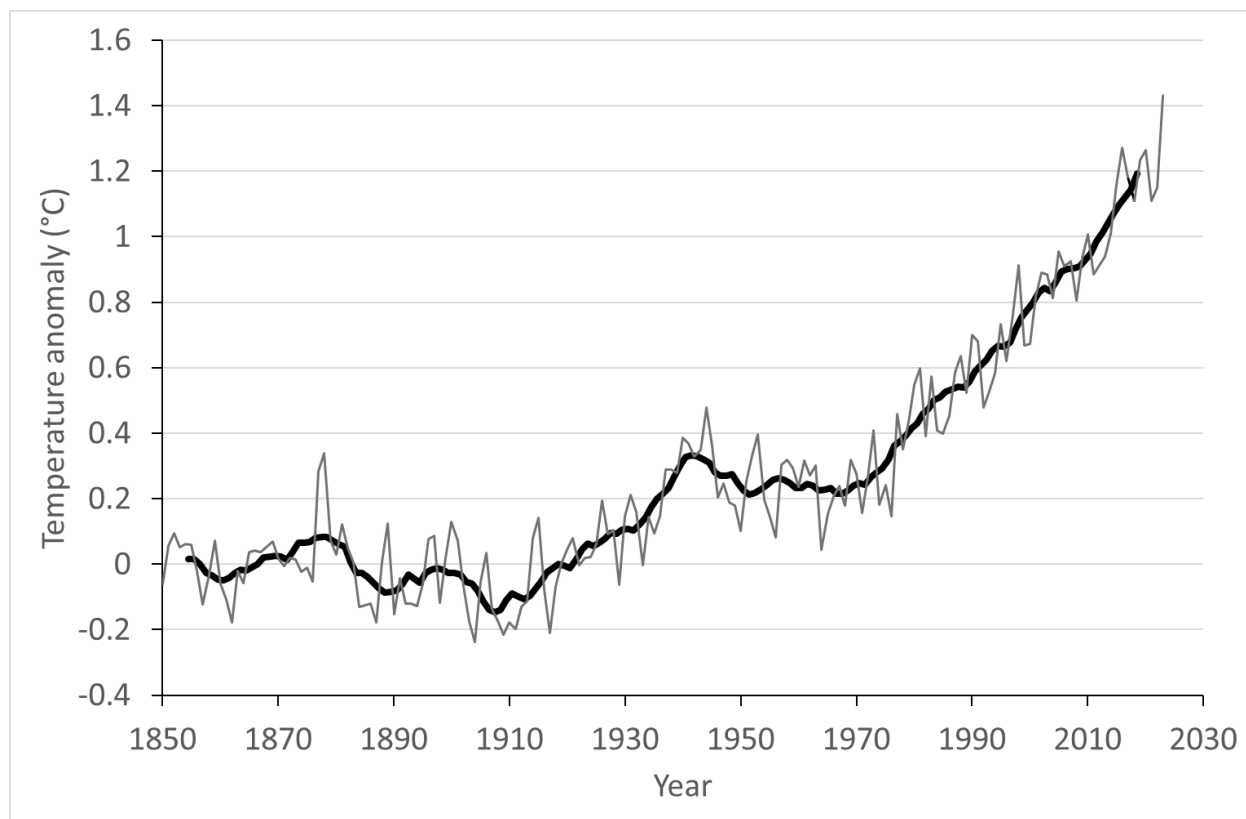
569 Based on the updates available as of March 2024, the change in global surface temperature from 1850–1900 to 2014–
570 2023 is presented in Fig. 5. These data, using the same underlying datasets and methodology as AR6, give 1.19 [1.06–
571 1.30] °C, an increase of 0.10 °C within three years from the 2011–2020 value reported in AR6 WGI (Table 5) and
572 0.09 °C from the 2011–2020 value in the most recent dataset versions. The change from 1850–1900 to 2004–2023
573 was 1.05 [0.90–1.16] °C, 0.07 °C higher than the value reported in AR6 WGI from three years earlier. These changes,
574 although amplified somewhat by the exceptionally warm 2023, are broadly consistent with typical warming rates over
575 the last few decades, which were assessed in AR6 as 0.76 °C over the 1980–2020 period (using ordinary-least-square
576 linear trends) or 0.019 °C per year (Gulev et al., 2021). They are also broadly consistent with projected warming rates

577 from 2001–2020 to 2021–2040 reported in AR6, which are in the order of 0.025 °C per year under most scenarios
 578 (Lee et al., 2021). See Sect. 7.4 for further discussion of trends.

579
 580 **Table 5 Estimates of global surface temperature change from 1850–1900 [very likely (90 %–100 % probability) ranges] for**
 581 **IPCC AR6 and the present study.**

Time period	Temperature change from 1850-1900 (°C)	
	IPCC AR6	This study
Global, most recent 10 years	1.09 [0.95 to 1.20] (to 2011-2020)	1.19 [1.06 to 1.30] (to 2014-2023)
Global, most recent 20 years	0.99 [0.84 to 1.10] (to 2001-2020)	1.05 [0.90 to 1.16] (to 2004-2023)
Land, most recent 10 years	1.59 [1.34 to 1.83] (to 2011-2020)	1.71 [1.41 to 1.94] (to 2014-2023)
Ocean, most recent 10 years	0.88 [0.68 to 1.01] (to 2011-2020)	0.97 [0.77 to 1.09] (to 2014-2023)

582



583

584

585 **Figure 5 Annual (thin line) and decadal (thick line) means of global surface temperature (expressed as a change from the**
586 **1850–1900 reference period).**

587
588 The global surface temperature in 2023 was 1.43 [1.32 to 1.53] °C above the 1850-1900 average in the multi-data set
589 mean used here. This is similar to the combined estimate from six datasets quoted in the 2023 WMO State of the
590 Climate report 1.45 [1.33 to 1.57] °C (WMO, 2024). As seen in Fig. 5 and discussed in Sect. 7.3, this is considerably
591 above the human induced warming estimate, indicating a significant role for internal variability.

592 **7 Human-induced global warming**

593 Human-induced warming, also known as anthropogenic warming, refers to the component of observed global surface
594 temperature increase attributable to both the direct and indirect effects of human activities, which are typically grouped
595 as follows: well-mixed greenhouse gases (consisting of CO₂, CH₄, N₂O and F-gases) and other human forcings
596 (consisting of aerosol–radiation interaction, aerosol–cloud interaction, black carbon on snow, contrails, ozone,
597 stratospheric H₂O and land use) (Eyring et al., 2021). The remaining contributors to total warming are natural:
598 consisting of both natural forcings (such as solar and volcanic activity) and internal variability of the climate system
599 (such as variability related to El Niño/La Nina events).

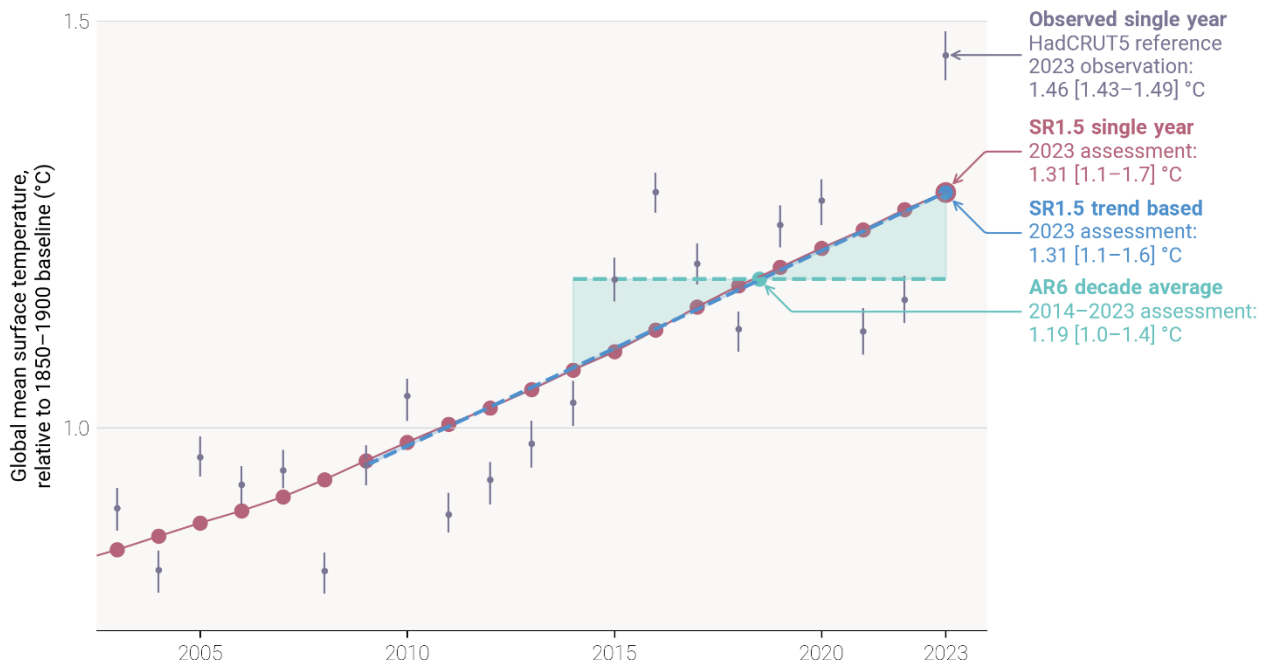
600
601 An assessment of human-induced warming was provided in two reports within the IPCC's 6th assessment cycle: first
602 in SR1.5 in 2018 [Chap. 1 Sect. 1.2.1.3 and Fig. 1.2 (Allen et al., 2018), summarised in the Summary for Policymakers
603 (SPM) Sect. A.1 and Fig. SPM.1 (IPCC, 2018)] and second in AR6 in 2021 [WGI Chap. 3 Sect. 3.3.1.1.2 and Fig. 3.8
604 (Eyring et al., 2021), summarised in the WGI Summary for Policymakers (SPM) Sect. A.1.3 and Fig. SPM.2 (IPCC,
605 2021b), and quoted again without any updates in SYR Sect. 2.1.1 and Fig. 2.1 (IPCC,2023a) and SYR Summary for
606 Policymakers (SPM) Sect. A.1.2. (IPCC 2023b).

607 **7.1 Warming period definitions in the IPCC Sixth Assessment cycle**

608 Temperature increases are defined relative to a baseline; IPCC assessments typically use the 1850–1900 average
609 temperature, as a proxy for the climate in pre-industrial times, referred to as the period before 1750 (see AR6 WGI
610 Cross Chapter Box 1.2).

611
612 Tracking progress towards the long-term global goal to limit warming, in line with the Paris Agreement, requires the
613 assessment of both what the current level of global surface temperatures are and whether a level of global warming,
614 such as 1.5°C, is being reached. Definitions for these were not specified in the Paris Agreement, and several ways of
615 tracking levels of global warming are in use (Betts et al. 2023); here we focus on those adopted within the IPCC's
616 AR6 (Fig. 6). When determining whether warming thresholds have been passed, both AR6 and SR1.5 adopted
617 definitions that depend on future warming; in practice, levels of current warming were therefore reported in AR6 and
618 SR.15 using additional definitions that circumvented the need to wait for observations of the future climate. AR6

619 defined crossing-time for a level of global warming as the midpoint of the first 20-year period during which the average
 620 *observed* warming for that period, in GSAT, exceeds that level of warming (see AR6 WGI Chapter 2 Box 2.3). It then
 621 reported current levels of both *observed* and *human-induced* warming as their averages over the most recent decade
 622 (see AR6 WGI Chapter 3 Sect. 3.3.1.1.2). This still effectively gives the warming level with a crossing time 5 years
 623 in the past, so would need to be combined with a projection of temperature change over the next decade to give a 20-
 624 year mean with crossing time at the current year (Betts et al., 2023); we do not focus on this here due to the need for
 625 further examination of methods and implications. SR1.5 defined the current level of warming as the average *human-*
 626 *induced* warming, in GMST, of a 30-year period centred on the current year, extrapolating any multidecadal trend into
 627 the future if necessary (see SR1.5 Chapter 1 Sect. 1.2.1). If the multidecadal trend is interpreted as being linear, this
 628 definition of current warming is equivalent to the end-point of the trend line through the most recent 15 years of
 629 human-induced warming, and therefore depends only on historical warming. This interpretation produces results that
 630 are almost all identical to the present-day single-year value of human-induced warming (see Fig. 6, results in Sect.
 631 7.3, and Supplement Sect. S7.3), so in practice the attribution assessment in SR1.5 was based on the single-year
 632 attributed warming calculated using the Global Warming Index, not the trend-based definition.



633

634 **Figure 6 Anthropogenic warming period definitions adopted in the IPCC Sixth assessment cycle. A single sampled**
635 **timeseries of anthropogenic warming is shown in red (in this case from the GWI method - see Supplement Sect. S7). Single-**
636 **year warming is given by the annual values of this timeseries. The AR6 decade average warming is given by the average of**
637 **the 10 most-recent single year anthropogenic warming values; this is depicted by the green dashed line with shading between**
638 **this and the red single year values; the decade-average value for 2014-2023 is given by the green dot. SR1.5 trend-based**
639 **warming is given by the end-point of the linear trend line through the 15 most-recent single year anthropogenic warming**
640 **values; this is depicted by the blue dashed line with shading between this and the red single-year values; the trend-based**
641 **value for 2023 is given by the blue dot. Reference observations of GMST are provided from HadCRUT5, with 5-95%**
642 **uncertainty range. The single-year, trend-based, and decade-average calculations are applied at the level of the individual**
643 **ensemble members for each attribution method; percentiles of those ensemble results provide central estimates and**
644 **uncertainty ranges for each method, and the multi-method assessment combines those into the final assessment results with**
645 **uncertainty (as described in Supplement Sect. S7.4); for reference, the assessment results for 2023 provided in Sect. 7.3 are**
646 **annotated in the figure (though the data in the figure does not correspond to the final assessment results).**

647 **7.2 Updated assessment approach of human-induced warming to date**

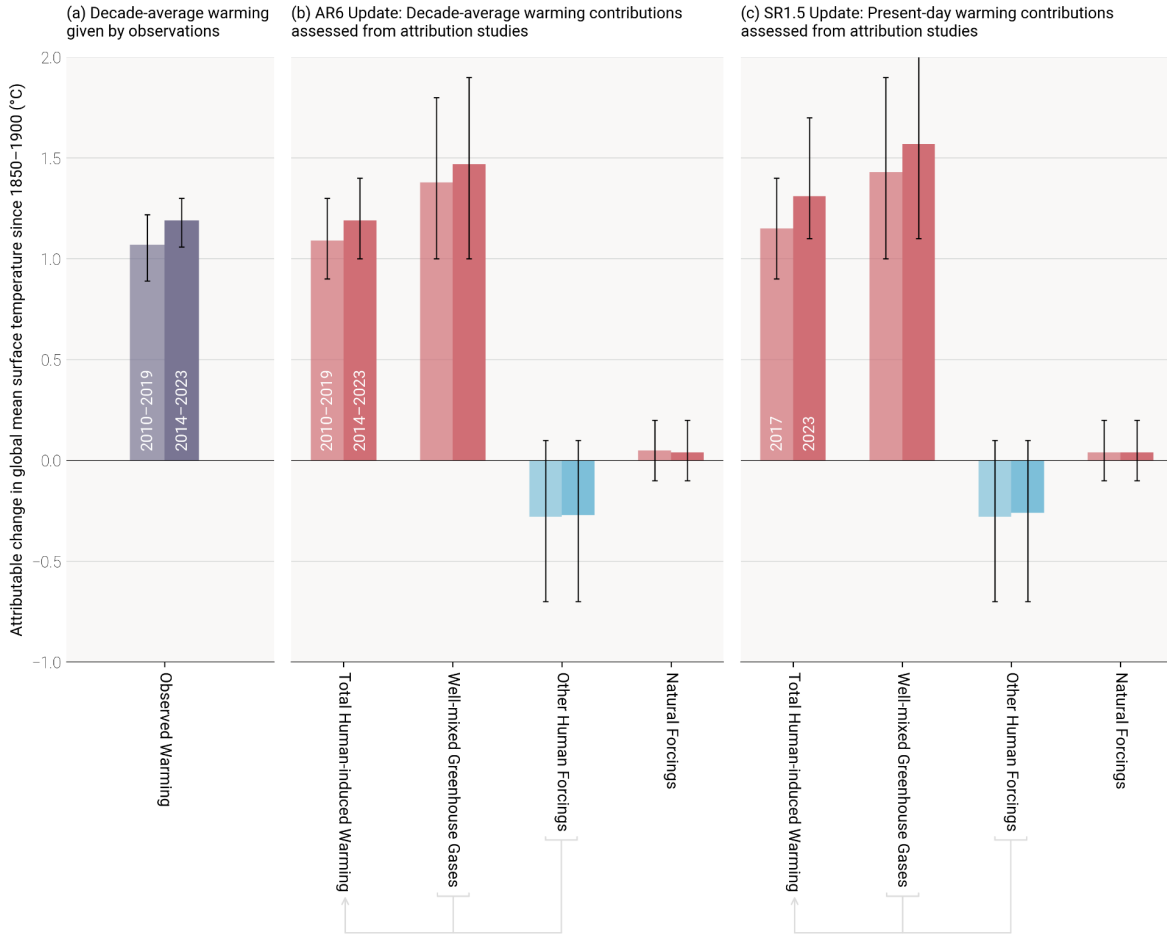
648 This paper provides an update of the AR6 WGI and SR1.5 human-induced warming assessments, including for
649 completeness all three definitions (AR6 decade-average, SR1.5 trend-based, and SR1.5 single-year). The 2023 updates
650 in this paper follow the same methods and process as the 2022 updates provided in Forster et al. (2023). Global mean
651 surface temperature is adopted as the definition of global surface temperature (see Supplement Sect. S7.1). The three
652 attribution methods used in AR6 are retained: the Global Warming Index (GWI) (building on Haustein et al., 2017),
653 regularised optimal fingerprinting (ROF) (as in Gillett et al., 2021) and kriging for climate change (KCC) (Ribes et
654 al., 2021). Details of each method, their different uses in SR1.5 and AR6, and any methodological changes, are
655 provided in Supplement Sect. S7.2; method-specific results are also provided in Supplement Sect. S7.3. The overall
656 estimate of attributed global warming for each definition (decade-average, trend-based, and single-year), is based on
657 a multi-method assessment of the three attribution methods (GWI, KCC, ROF); the best estimate is given as the
658 0.01°C-precision mean of the 50th percentiles from each method, and the *likely* range is given as the smallest 0.1°C-
659 precision range that envelops the 5th to 95th percentile ranges of each method. This assessment approach is identical
660 to last year's update (Forster et al. (2023)); it is directly traceable to and fully consistent with the assessment approach
661 in AR6, though it has been extended in ways that are explained in Supplement Sect. S7.4.

663 **7.3 Results**

664 Results are summarised in Table 6 and Figs. 6 and 7. Method-specific contributions to the assessment results, along
665 with time series, are given in the Supplement, Sect. S7.3. Where results reported in GSAT differ from those reported
666 in GMST (see Supplement Sect. S7.1), the additional GSAT results are given in Supplement Sect. S7.3.




Observed Warming

Contributions to observed warming expressed in terms of two IPCC warming definitions



668 Figure 7 Updated assessed contributions to observed warming relative to 1850–1900; see AR6 WGI SPM.2. Results for all
 669 time periods in this figure are calculated using updated datasets and methods. To show how these updates have affected the
 670 previous assessments, the 2010–2019 *decade-average* assessed results repeat the AR6 2010–2019 assessment, and the 2017
 671 *single-year* assessed results repeat the SR1.5 2017 assessment. The 2014–2023 *decade-average* and 2023 *single-year* results
 672 are this year’s updated assessments for AR6 and SR1.5, respectively. For each double bar, the lighter and darker shading
 673 refers to the earlier and later period, respectively. Panel (a) shows updated observed global warming from Sect. 6, expressed
 674 as total global mean surface temperature (GMST), due to both anthropogenic and natural influences. Whiskers give the
 675 “very likely” range. Panels (b) and (c) show updated assessed contributions to warming, expressed as global mean surface
 676 temperature (GMST), from natural forcings and total human-induced forcings, which in turn consist of contributions from
 677 well-mixed greenhouse gases and other human forcings. Whiskers give the “likely” range.

678 Table 6 Updates to assessments in the IPCC 6th assessment cycle of warming attributable to multiple influences. Estimates
 679 of warming attributable to multiple influences, in °C, relative to the 1850–1900 baseline period. Results are given as best
 680 estimates, with the *likely* range in brackets, and reported as global mean surface temperature (GMST). Results from the
 681 IPCC 6th assessment cycle, for both AR6 and SR1.5, are quoted in columns labelled (i) and are compared with repeat
 682 calculations in columns labelled (ii) for the same period using the updated methods and datasets in order to see how
 683 methodological and dataset updates alone would change previous assessments. Assessments for the updated periods are
 684 reported in columns labelled (iii). * Updated GMST observations, quoted from Sect. 6 of this update, are marked with an
 685 asterisk, with “very likely” ranges given in brackets. ** In AR6 WGI, best-estimate values were not provided for warming
 686 attributable to well-mixed greenhouse gases, other human forcings and natural forcings (though they did receive a “likely”
 687 range); for comparison, best estimates (marked with two asterisks) have been retrospectively calculated in an identical way
 688 to the best estimate that AR6 provided for anthropogenic warming (see discussion in Supplement Sect. S7.4.1). *** The
 689 SR1.5 assessment drew only on GWI rounded to 0.1°C precision, whereas the repeat and updated calculations use the
 690 updated multi-method assessment approach.

Estimates of warming attributable to multiple influences, in °C, relative to the 1850–1900 baseline period						
Results are given as best estimates, with the <i>likely</i> range in brackets, and reported as Global Mean Surface Temperature (GMST).						
Definition 	(a) IPCC AR6 Attributable Warming Update <i>Average value for previous 10-year period</i>			(b) IPCC SR1.5 Attributable Warming Update <i>Value for single-year period</i>		
Period 	(i) 2010-2019 <i>Quoted from AR6 Chapter 3 Sect. 3.3.1.1.2 Table 3.1</i>	(ii) 2010-2019 <i>Repeat calculation using the updated methods and datasets</i>	(iii) 2014-2023 <i>Updated value using updated methods and datasets</i>	(i) 2017 <i>Quoted from SR1.5 Chapter 1 Sect. 1.2.1.3</i>	(ii) 2017 <i>Repeat calculation using the updated methods and datasets</i>	(iii) 2023 <i>Updated value using updated methods and datasets</i>
Component 						
Observed	1.06 [0.88 to 1.21]	1.07 [0.89 to 1.22] *	1.19 [1.06 to 1.30] *	-	-	1.43 [1.32 to 1.53]
Anthropogenic	1.07 [0.8 to 1.3]	1.09 [0.9 to 1.3]	1.19 [1.0 to 1.4]	1.0 [0.8 to 1.2] ***	1.15 [0.9 to 1.4]	1.31 [1.1 to 1.7]
Well-mixed greenhouse gases	1.40** [1.0 to 2.0]	1.38 [1.0 to 1.8]	1.47 [1.0 to 1.9]	N/A	1.43 [1.0 to 1.9]	1.57 [1.1 to 2.1]
Other human forcings	-0.32** [-0.8 to 0.0]	-0.28 [-0.7 to 0.1]	-0.27 [-0.7 to 0.1]	N/A	-0.28 [-0.7 to 0.1]	-0.26 [-0.7 to 0.1]
Natural forcings	0.03** [-0.1 to 0.1]	0.05 [-0.1 to 0.2]	0.04 [-0.1 to 0.2]	N/A	0.04 [-0.1 to 0.2]	0.04 [-0.1 to 0.2]

691
 692 The repeat calculations for attributable warming in 2010–2019 exhibit good correspondence with the results in AR6
 693 WGI for the same period (see also Supplement, Sect. S7). The repeat calculation for the level of attributable
 694 anthropogenic warming in 2017 is about 0.1 °C larger than the estimate provided in SR1.5 for the same period,

695 resulting from changes in methods and observational data (see AR6 WGI Chapter 2 Box 2.3). The updated results for
696 warming contributions in 2023 are higher than in 2017 due also to 6 additional years of increasing anthropogenic
697 forcing. Note also that the SR1.5 assessment only used the GWI method, whereas these annual updates apply the full
698 AR6 multi-method assessment (see Supplement Sect. S7.4 for details and rationale). A repeat assessment using the
699 SR1.5 trend-based definition (see Sect. 7.1) leads to results that are very similar to the single-year results reported in
700 Table 6b; best estimates across all components for single-year and trend-based definitions are identical to each other
701 for 2023, and identical or well within uncertainty range for 2017 (Supplement, Sect. S7.3 Table S4).

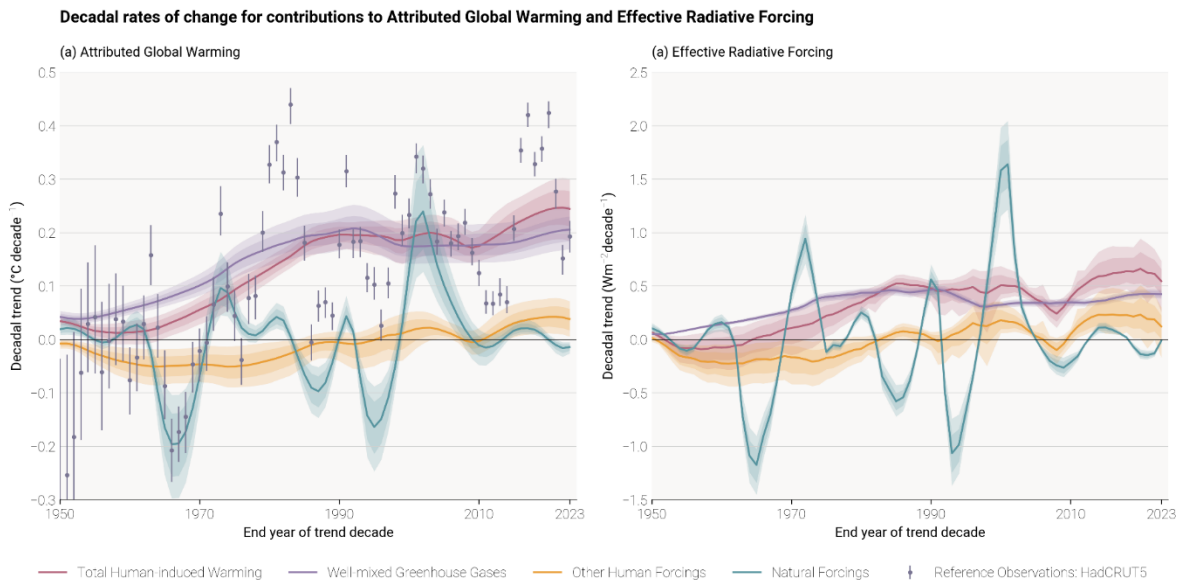
702
703 In this 2024 update, we assess the 2014–2023 decade average human induced-warming at 1.19 [1.0 to 1.4] °C, which
704 is 0.12°C above the AR6 assessment for 2010–2019. The single year average human-induced warming is assessed to
705 be 1.31 [1.1 to 1.7] °C in 2023 relative to 1850–1900. This best-estimate for the current level of human-induced
706 warming reaches the 1.3°C threshold for the first time. The best estimate is below the observed temperature in 2023
707 (1.43 [1.32 to 1.53] °C, see Sect. 6), but note the overlap of uncertainties. These best estimates for decade-average and
708 single-year human-induced warming are both 0.05 °C above the value estimated in the previous update for the year
709 2022 (Forster et al., 2023). The increase of 0.05° C in the single-year anthropogenic warming level since last year’s
710 assessment (Forster et al., 2023) is broken down in the following way: (i) around half of the increase is due to a
711 revision of the historical period due to the additional year of observations (i.e. the 2023 analysis of single-year
712 warming for 2022 is 0.026°C warmer than the 2022 analysis of single-year warming for 2022), and (ii) around half of
713 the increase is due to the additional year itself (i.e. the 2023 analysis of the single-year warming for 2023 is 0.025°C
714 warmer than the 2023 analysis of the single-year warming for 2022); therefore, the variability in human-induced
715 warming from adding one particularly hot year of observations (which 2023 was, see Sect. 6) corresponded to
716 advancing only one additional year at the current warming rate (0.026°C/year, see Sect. 7.4), which is significantly
717 smaller than other sources of uncertainty in the assessment. At the attribution level, this slightly strengthened
718 anthropogenic warming is comprised of a slightly larger greenhouse gas attributable warming, partially offset by a
719 slightly stronger aerosol-induced attributable cooling.

720
721 WGI AR6 found that, averaged for the 2010–2019 period, essentially all observed global surface temperature change
722 was human-induced, with solar and volcanic drivers and internal climate variability making a negligible contribution.
723 This conclusion remains the same for the 2014–2023 period. Generally, whatever methodology is used, on a global
724 scale, the best estimate of the human-induced warming is (within small uncertainties) similar to the observed global
725 surface temperature change (Table 6).

726 727 **7.4 Rate of human-induced global warming**

728 Estimates of the human-induced warming rate refer to the rate of increase in the level of attributed anthropogenic
729 warming over time; this is distinct from the rate of increase in the observed global surface temperature (Sect. 6) which
730 is affected by internal variability such as El Niño and natural forcings such as volcanic activity (Jenkins et al 2023).

731 The rate of anthropogenic warming is driven by the rate of change of anthropogenic ERF, meaning variations in the
732 rate of climate forcing over time correlate with variations in the rate of attributed warming (see Fig. 8).



733
734 **Figure 8 Rates of (a) attributable warming (global mean surface temperature (GMST)) and (b) effective radiative forcing.**
735 **The attributable warming rate time-series are calculated using the Global Warming Index method with full ensemble**
736 **uncertainty. The observed GMST rates included for reference are also calculated with uncertainty from the HadCRUT5**
737 **ensemble, and, for consistency with the attributed warming rates, do not include standard regression error, which, for**
738 **observed warming, would increase the size of the error bars. The effective radiative forcing rates are calculated using a**
739 **representative 1000-member ensemble of the forcings provided in Sect. 4 of this paper.**

740
741 A very simple estimate of the rate of human-induced warming and effective radiative forcing was made last year by
742 Forster et al. 2023, which indicated that warming rates were unprecedented, surpassing 0.2 °C per decade (although
743 no uncertainty range was given). That rate calculation was based on annual changes in decade-average anthropogenic
744 warming levels from the GWI method (see Supplement Sect. S7.2). This year, attributed anthropogenic warming rates
745 are calculated for all attribution methods using linear trends, as used in AR6, with the overall rate estimate updated in
746 a manner that is fully traceable to and consistent with the rate assessment in AR6.

747 748 **7.4.1 SR1.5 and AR6 definitions of warming rate**

749 In recent IPCC assessments the definition of warming rate follows two approaches, both of which rely to some extent
750 on expert judgment. In SR1.5 several studies were considered, each defining the rate of warming in various ways and
751 over various timescales; the assessment concluded that the rate of increase of anthropogenic warming in 2017 was
752 0.2°C per decade with a likely range of 0.1°C to 0.3°C per decade. In AR6 WGI the rate of anthropogenic warming
753 utilised three methods (GWI, KCC, ROF, see Supplement Sect. S7.2) with the rate defined consistently across all
754 three as the linear trend in the preceding decade of attributed anthropogenic warming. While the best estimate trends
755 reported in AR6 were all higher than the SR1.5 assessment, Eyring et al. (2021) concluded that there was insufficient

756 evidence to change the SR1.5 assessed anthropogenic warming trend in the AR6 WGI report, which therefore
757 remained unchanged from SR1.5 at 0.2°C per decade (with a likely range of 0.1°C to 0.3°C per decade). Both the
758 SR1.5 and AR6 assessments were given to 0.1°C per decade precision only.

759

760 **7.4.2 Methods**

761 Following AR6's definition, the rate of warming is defined here as the rolling 10-year linear trend in attributed
762 anthropogenic warming, calculated using ordinary least-squares linear regression. Note that, as with the level of
763 anthropogenic warming, this decadal approach means the rate of warming in a given year is the trend centred on the
764 preceding decade (i.e. it is 5 years out of date). Each of the three attribution methods used to calculate the level of
765 warming are again used here to estimate separate anthropogenic warming rates.

766

767 Note that only the GWI methodology relies on the updated historical forcing timeseries presented in Sect. 4, with the
768 other two methods (ROF and KCC) relying on CMIP6 SSP2-4.5 simulations, which are increasingly out of date (see
769 Supplement Sect. S7.2). Very recent changes in anthropogenic forcing, for example desulphurisation of shipping fuels
770 or the impact of COVID-19, may therefore not be captured fully in the decade-average trend. Further, the
771 anthropogenic forcing record used for attributing warming contains small contributions from biomass burning in the
772 natural environment, because of difficulty separating this in estimates of anthropogenic aerosol emissions. It is not
773 expected that either of these effects substantially bias the globally-averaged rate of warming estimated here.

774 **7.4.3 Results**

775 Estimates from the GWI (based on observed warming and forcing), and KCC (based on CMIP simulations), both
776 report results in terms of GMST and are in close agreement across each time period. Estimates derived with the ROF
777 method (also based on CMIP simulations), are also reported for GMST here and are more strongly influenced by
778 residual internal variability that remains in the anthropogenic warming signal due to the limitations in size of the CMIP
779 ensemble, as reflected in their broader uncertainty ranges. Given that the ROF results are in this sense outlying, the
780 standard approach of taking the median result for the overall multi-method assessment is adopted.

781

782 Results for human-induced warming rate are summarised in Table 7 and Fig 8. For the purpose of providing annual
783 updates, we take the median estimate at 0.01°C/decade precision, resulting in an overall best estimate for 2014–2023
784 of 0.26°C/decade. This increased rate relative to the 0.2°C/decade AR6 assessment is broken down in the following
785 way: (i) 0.03°C/decade of the increase is from a change in rounding precision (updating the AR6 assessment for the
786 2010–2019 warming rate from 0.2°C/decade to 0.23°C/decade), (ii) 0.02°C/decade of the increase is due to
787 methodological and dataset updates (updating the 2010–2019 warming rate from 0.23°C/decade to 0.25°C/decade;
788 this includes the effect of adding 4 additional observed years which affect the attribution for the entire historical
789 period), and (iii) only 0.01°C/decade of the increase is due to a substantive increase in rate for the 2014–2023 period
790 since the 2010–2019 period (updating 0.25°C/decade for 2010–2019 to 0.26°C/decade for 2014–2023). The spread of

791 rates across the three attribution methods remains similar to their spread in AR6, and hence do not support a decrease
 792 in the uncertainty range in this update. However, to better reflect the closer agreement of the 5% floors and the larger
 793 spread in the 95% ceilings of the three methods, and high rate from the ROF method, we update the uncertainty range
 794 for the rate of human-induced warming from [0.1–0.3]°C/decade in AR6 to [0.2–0.4]°C/decade, leaving the precision
 795 and range unchanged, noting that this is asymmetric around the central estimate. Therefore, the rate of human-induced
 796 warming for the 2014-2023 decade is concluded to be 0.26°C/decade with a range of [0.2–0.4]°C/decade).

797
 798 **Table 7 Updates to the IPCC AR6 rate of human-induced warming. Results for each method are given as best estimates**
 799 **with 5-95% confidence, as described in the main text; assessment results are given as a best estimate with likely range in**
 800 **brackets. Results from AR6 WGI (Ch.3 Sect. 3.3.1.1.2 Table 3.1) are quoted in column (i), and compared with a repeat**
 801 **calculation using the updated methods and datasets in column (ii), and finally updated for the 2014-2023 period in column**
 802 **(iii). The AR6 assessment result was identical to the SR1.5 assessment result, though the latter was based on a different set**
 803 **of studies and timeframes. * Note that for clarity and ease of comparison with this year’s updated assessment, in the assessed**
 804 **rate in column (i) both quotes the assessment from AR6 and retrospectively applies the median approach adopted in this**
 805 **paper.**

Estimates of anthropogenic warming rate, in °C per decade Results are given as best estimates, with brackets giving the likely range for the assessments, and 5-95% uncertainty for the individual methods			
Definition	IPCC AR6 Anthropogenic Warming Rate Update <i>Linear trend in anthropogenic warming over the trailing 10-year period</i>		
Period	(i) 2010-2019 <i>Quoted from AR6 Chapter 3 Sect. 3.3.1.1.2 Table 3.1</i>	(ii) 2010-2019 <i>Repeat calculation using the updated methods and datasets</i>	(iii) 2014-2023 <i>Updated value using updated methods and datasets</i>
Method			
Anthropogenic Warming Rate Assessment	Quoted from AR6: 0.2 [0.1 to 0.3] Using the median approach: 0.23 [0.1 to 0.3] *	0.25 [0.2 to 0.4]	0.26 [0.2 to 0.4]
GWI	0.23 [0.19 to 0.35] GMST	0.24 [0.18 to 0.29] GMST	0.24 [0.19 to 0.30] GMST
KCC	0.23 [0.18 to 0.29] GSAT	0.25 [0.20 to 0.30] GMST	0.26 [0.20 to 0.31] GMST
ROF	0.35 [0.30 to 0.41] GSAT	0.27 [0.17 to 0.38] GMST	0.38 [0.24 to 0.52] GMST

806
 807 Fig. 8 and Table 7 include a breakdown into well-mixed GHGs and other human forcings (including aerosols), and
 808 natural forcing contributions since pre-industrial times. The rate timeseries with ensemble uncertainty are depicted
 809 from the GWI method, which is based on observed warming and historical forcing. The rate of total attributable
 810 warming (the sum of anthropogenic and natural, not plotted) has good correspondence with the reference plotted
 811 observed warming rates. The rates for the attributed warming also correlate closely with the forcing rates. Warming

812 rates have remained high due to strong GHG warming from high emissions and declining aerosol cooling (Forster et
813 al., 2023, Quaas et al., 2022, Jenkins et al., 2022).

814 **8 Remaining Carbon Budget**

815 AR5 (IPCC, 2013) assessed that global surface temperature increase is close to linearly proportional to the total
816 amount of cumulative CO₂ emissions (Collins et al., 2013). The most recent AR6 report reaffirmed this assessment
817 (Canadell et al., 2021). This near-linear relationship implies that for keeping global warming below a specified
818 temperature level, one can estimate the total amount of CO₂ that can ever be emitted. When expressed relative to a
819 recent reference period, this is referred to as the remaining carbon budget (Rogelj et al., 2018).

820
821 AR6 assessed the remaining carbon budget (RCB) in Chap. 5 of its WGI report (Canadell et al., 2021) for 1.5, 1.7 and
822 2 °C thresholds (see Table 7). They were also reported in its Summary for Policymakers (Table SPM.2, IPCC, 2021b).
823 These are updated in this section using the same method as last year (Forster et al., 2023).

824
825 The RCB is estimated by application of the WGI AR6 method described in Rogelj et al. (2019), which involves the
826 combination of the assessment of five factors: (i) the most recent decade of human-induced warming (given in Sect.
827 7), (ii) the transient climate response to cumulative emissions of CO₂ (TCRE), (iii) the zero emissions commitment
828 (ZEC), (iv) the temperature contribution of non-CO₂ emissions and (v) an adjustment term for Earth system feedbacks
829 that are otherwise not captured through the other factors. AR6 WGI reassessed all five terms (Canadell et al., 2021).
830 The incorporation of Earth system feedbacks was further considered by Lamboll and Rogelj (2022). Lamboll et al.
831 (2023) further considered the temperature contribution of non-CO₂ emissions, while Rogelj and Lamboll (2024)
832 clarified the reductions in non-CO₂ that are assumed in the RCB estimation.

833
834 The RCB for 1.5, 1.7 and 2 °C warming levels is re-assessed based on the most recent available data. Estimated RCBs
835 are reported in Table 8. They are expressed both relative to 2020 to compare to AR6 and relative to the start of 2024
836 for estimates based on the 2014–2023 human-induced warming update (Sect. 7). Note that between the start of 2020
837 and the end of 2023, about 164 GtCO₂ has been emitted (Sect. 2). Based on the variation in non-CO₂ emissions across
838 the scenarios in AR6 WGIII scenario database, the estimated RCB values can be higher or lower by around 200 GtCO₂
839 depending on how deeply non-CO₂ emissions are reduced (Lamboll et al., 2023; Rogelj and Lamboll, 2024). The
840 impact of non-CO₂ emissions on warming includes both the warming effects of other greenhouse gases such as
841 methane and the cooling effects of aerosols such as sulfates. Updating these pathways increased the estimate of the
842 importance of aerosols, which are expected to decline with time in low emissions pathways (Rogelj et al., 2014; Rogelj
843 and Lamboll, 2024), causing a warming and decreasing the RCB (Lamboll et al., 2023). Structural uncertainties give
844 inherent limits to the precision with which remaining carbon budgets can be quantified. These particularly impact the
845 1.5 °C RCB. Overall, the 1.5 °C compatible budget is very small and shrinking fast due to continuing high global CO₂
846 emissions.

847

848 **Table 8 Updated estimates of the remaining carbon budget for 1.5, 1.7 and 2.0 °C, for five levels of likelihood, considering**
849 **only uncertainty in TCRE. Estimates start from AR6 WGI estimates (first row for each warming level), updated with the**
850 **latest MAGICC emulator and scenario information from AR6 WGIII (from second row for each warming level), and an**
851 **update of the anthropogenic historical warming, which is estimated for the 2014–2023 period (third row for each warming**
852 **level). Estimates are expressed relative to either the start of the year 2020 or 2024. The probability includes only the**
853 **uncertainty in how the Earth immediately responds to carbon emissions, not long-term committed warming or uncertainty**
854 **in other emissions. All values are rounded to the nearest 50 GtCO₂.**

Remaining carbon budget case/update	Base year	Estimated remaining carbon budgets from the beginning of base year (GtCO ₂)				
		17%	33%	50%	67%	83%
Likelihood of limiting global warming to temperature limit		17%	33%	50%	67%	83%
1.5 °C from AR6 WG1	2020	900	650	500	400	300
+ AR6 emulators and scenarios	2020	750	500	400	300	200
+ Updated warming estimate	2024	450	300	200	150	100
1.7 °C from AR6 WG1	2020	1450	1050	850	700	550
+ AR6 emulators and scenarios	2020	1300	950	750	600	500
+ Updated warming estimate	2024	1000	700	550	450	350
2 °C from AR6 WG1	2020	2300	1700	1350	1150	900
+ AR6 emulators and scenarios	2020	2200	1650	1300	1100	900
+ Updated warming estimate	2024	1900	1400	1100	900	750

855
856 Updated RCB estimates presented in Table 8 for 1.5, 1.7 and 2.0 °C of global warming are smaller than AR6, and
857 geophysical and other uncertainties therefore have become larger in relative terms. This is a feature that will have to
858 be kept in mind when communicating budgets. The estimates presented here differ from those presented in the annual
859 Global Carbon Budget (GCB) publications (Friedlingstein et al., 2023). The GCB 2023 used the average between the
860 AR6 WGI estimate and the Forster et al. (2023) estimates. The RCB estimates presented here consider the same
861 updates in historical CO₂ emissions from the GCB as well as the latest available quantification of human-induced
862 warming to date and a reassessment from AR6 of non-CO₂ warming contributions.

863
864 The RCB for limiting warming to 1.5 °C is rapidly diminishing. It is important, however, to correctly interpret this
865 information. RCB estimates consider projected reductions in non-CO₂ emissions that are aligned with a global
866 transition to net zero CO₂ emissions (Lamboll et al., 2023; Rogelj and Lamboll, 2024). These estimates assume median

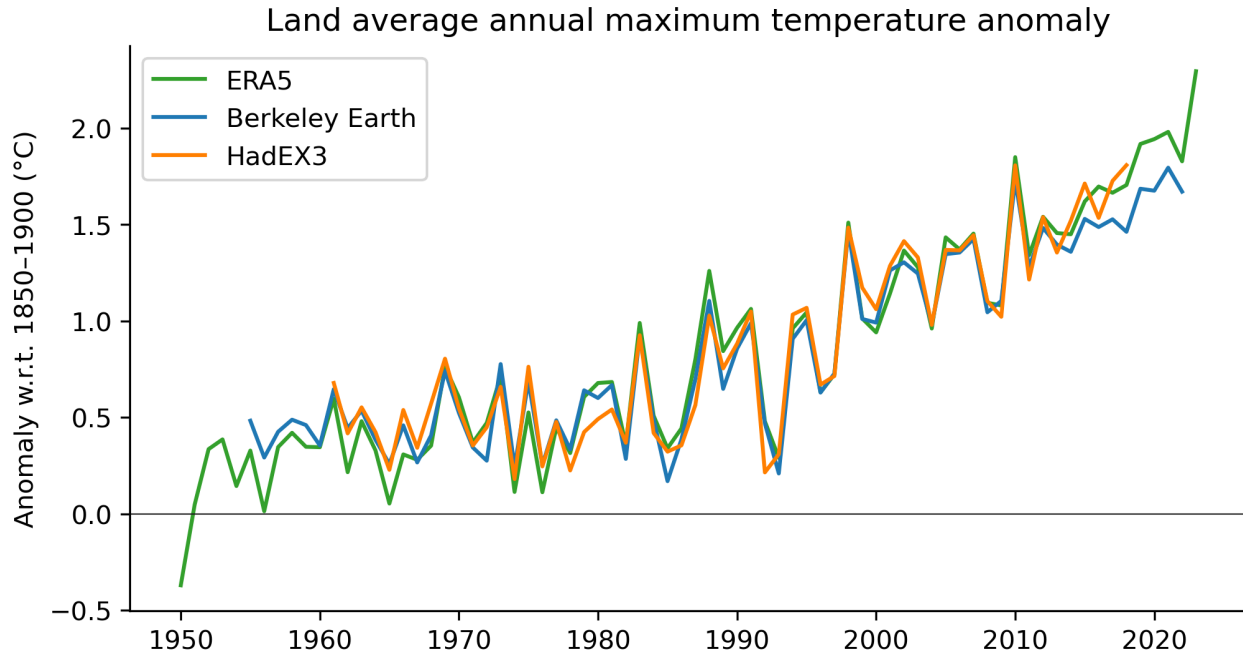
867 reductions in non-CO₂ emissions between 2020–2050 of CH₄ (about 50 %), N₂O (about 20 %) and SO₂ (about 80 %) (Rogelj and Lamboll, 2024) (see Supplement, Sect. S8 and Table S5). If these non-CO₂ greenhouse gas emission reductions are not achieved, the RCB will be smaller (see Lamboll et al., 2023, Rogelj and Lamboll, 2024). This year's update of the 1.5°C budget uses the historical warming level for the 2014-2023 period of 1.19°C, with a 0.13°C future contribution of non-CO₂ warming. Assuming a median estimate of 0.45°C per 1000 GtCO₂ this gives around 400 GtCO₂ from the midpoint of the period, from which we subtract around 200 GtCO₂ (205 GtCO₂ emissions from the middle of the 2014-2023 period and 8 GtCO₂ being the median estimate of the impact of Earth systems feedbacks that would otherwise not be covered). This gives an RCB for 1.5°C with 50% probability of 200 GtCO₂. The full calculation includes the distributions of these values for the uncertainty estimates.

876 Note that the 50 % RCB is expected to be exhausted a few years before the 1.5 °C global warming level is reached due to the way it factors future warming from non-CO₂ emissions into its estimate.

878 **9 Climate and weather extremes**

879 Changes in climate and weather extremes are among the most visible effects of human-induced climate change. Within AR6 WGI, a full chapter was dedicated to the assessment of past and projected changes in extremes on continents (Seneviratne et al., 2021), and the chapter on ocean, cryosphere and sea level changes also provided assessments on changes in marine heatwaves (Fox-Kemper et al., 2021). Global indicators related to climate extremes include averaged changes in climate extremes, for example, the mean increase of annual minimum and maximum temperatures on land (AR6 WGI Chap. 11, Fig. 11.2, Seneviratne et al., 2021) or the area affected by certain types of extremes (AR6 WGI Chap. 11, Box 11.1, Fig. 1, Seneviratne et al., 2021; Sippel et al., 2015). In contrast to global surface temperature, extreme indicators are less established.

887
888 The climate indicator of changes in temperature extremes consists of land average annual maximum temperatures (TXx) (excluding Antarctica). As part of this update, we provide an upgraded version of Fig. 6 from Forster et al. (2023), which in turn is based on Fig. 11.2 from Seneviratne et al. (2021) (Fig. 9). As last year, three datasets are analyzed: HadEX3 (Dunn et al., 2020), Berkeley Earth Surface Temperature (building off Rohde et al., 2013), and the fifth-generation ECMWF atmospheric reanalysis of the global climate (ERA5; Hersbach et al., 2020). HadEX3 is currently static and is not being updated. Berkeley Earth has been updated, resulting in TXx differences for most years (less than 0.1°C), and now includes data for 2022. Of the three datasets, only ERA5 covers the whole of 2023 at the present time. TXx is calculated by averaging the annual maximum temperature over all available land grid points (excluding Antarctica) and then converted to anomalies with respect to a base period of 1961–1990. To express the TXx as anomalies with respect to 1850–1900, we add an offset of 0.52°C to all three datasets. See Supplement Sect. S9 for details on the data selection, averaging and offset computation. We note that Berkeley Earth has slightly smaller trends than ERA5 and that this might warrant further investigation.



900
 901 **Figure 9** Time series of observed temperature anomalies for land average annual maximum temperature (TXx) for ERA5
 902 (1950–2023), Berkeley Earth (1955–2022) and HadEX3 (1961–2018), with respect to 1850–1900. Note that the datasets have
 903 different spatial coverage and are not coverage-matched. All anomalies are calculated relative to 1961–1990, and an offset
 904 of 0.52 °C is added to obtain TXx values relative to 1850–1900. Note that while the HadEX3 numbers are the same as shown
 905 in Seneviratne et al. (2021) Fig. 11.2, these numbers were not specifically assessed.

906
 907 Our climate has warmed rapidly in the last few decades (Sect. 6), which also manifests in changes in the occurrence
 908 and intensity of climate and weather extremes. From about 1980 onwards, all employed datasets point to a strong TXx
 909 increase, which coincides with the transition from global dimming, associated with aerosol increases, to brightening,
 910 associated with aerosol decreases (Wild et al., 2005, Sect. 3). The ERA5 based TXx warming estimate w.r.t. 1850-
 911 1900 for 2023 is at 2.3°C; an increase of more than 0.5°C compared to 2022, and shattering the previous record by
 912 more than 0.3°C. On longer time scales, land average annual maximum temperatures have warmed by more than
 913 0.6 °C in the past 10 years (1.81 °C with respect to pre-industrial conditions) compared to the first decade of the
 914 millennium (1.21°C; Table 9). Since the offset relative to our pre-industrial baseline period is calculated over the
 915 1961–1990, temperature anomalies align by construction over this period but can diverge afterwards. In an extensive
 916 comparison of climate extreme indices across several reanalyses and observational products, Dunn et al. (2022) point
 917 to an overall strong correspondence between temperature extreme indices across reanalysis and observational
 918 products, with ERA5 exhibiting especially high correlations to HadEX3 among all regularly updated datasets.

919
 920 **Table 9** Anomalies of land average annual maximum temperature (TXx) for recent decades based on HadEX3 and ERA5.

Period	Anomaly w.r.t. 1850-1900 (°C)	Anomaly w.r.t. 1961-1990 (°C)	Anomaly w.r.t. 1961-1990 (°C)
--------	-------------------------------	-------------------------------	-------------------------------

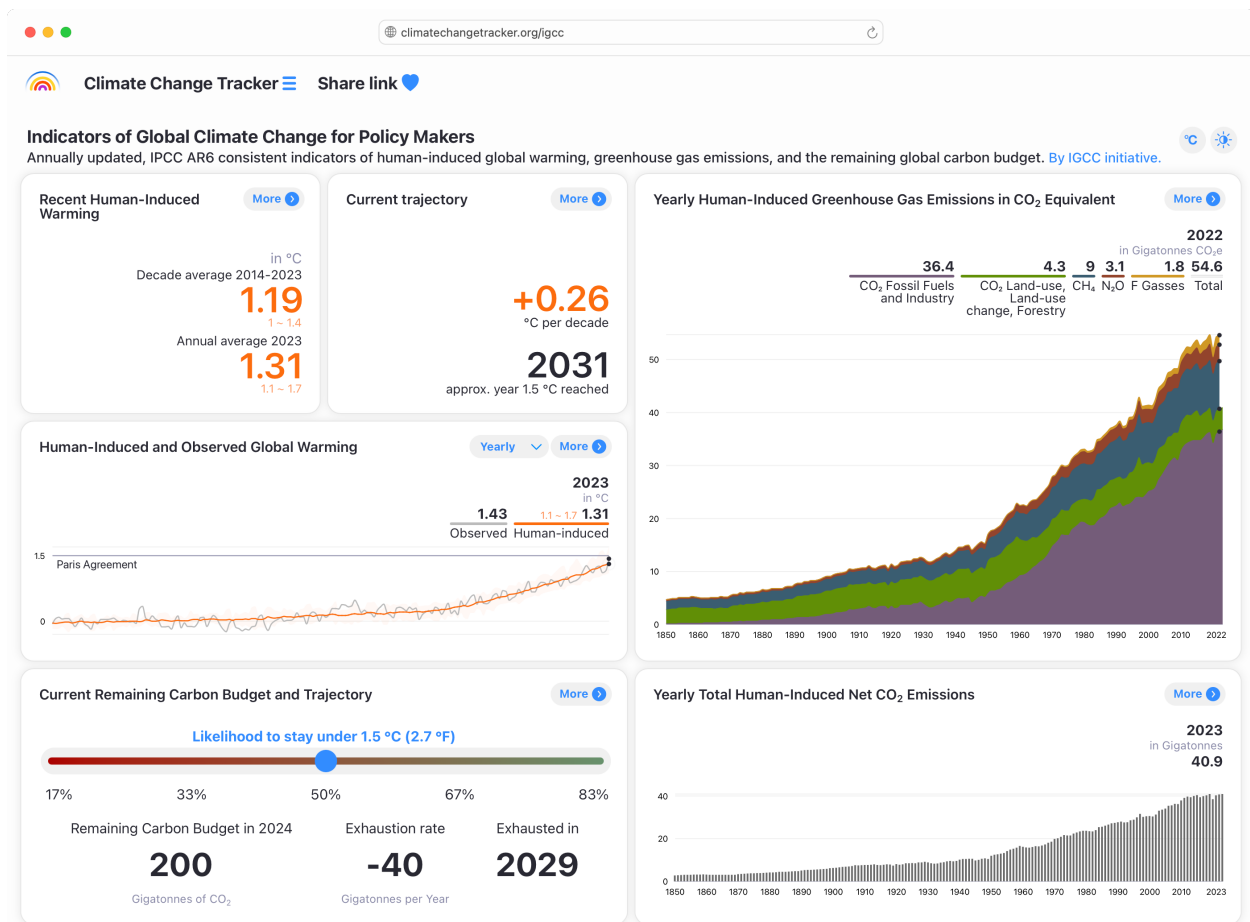
	ERA5	ERA5	HadEX3
2000-2009	1.21	0.69	0.72
2009-2018	1.54	1.02	1.01
2010-2019	1.62	1.11	-
2011-2020	1.63	1.12	-
2012-2021	1.70	1.18	-
2013-2022	1.73	1.21	-
2014-2023	1.81	1.29	-

921 **10 Code, data availability and visualisations**

922 We publish a set of selected key indicators of global climate change via Climate Change Tracker
 923 (<https://climatechangetracker.org/igcc>, Climate Change Tracker, 2024), a platform which aims to provide reliable,
 924 user-friendly, high-quality interactive dashboards, visualisations, data, and easily accessible insights of this paper (see
 925 Figure 10).

926
 927 With Climate Change Tracker we aim to reach a wider public audience, including policymakers involved in UNFCCC
 928 negotiations, and people with significant roles in climate change mitigation and adaptation. Climate Change Tracker
 929 plans to update significant indicators multiple times throughout the year, providing an up-to-date picture of the
 930 indicators of climate change. Within the dashboards, all data is traceable to the underlying sources.

931



932
 933 **Figure 10** Screenshot dashboard, access: <https://climatechangetracker.org/igcc>, Climate Change Tracker
 934 (2024).

935
 936 The carbon budget calculation is available from <https://github.com/RIamboll/AR6CarbonBudgetCalc/tree/v1.0.1>
 937 (Lamboll and Rogelj, 2024). The code and data used to produce other indicators are available in repositories under
 938 <https://github.com/ClimateIndicator/data/tree/v2024.05.29b> (Smith et al., 2024b). All data are available from
 939 <https://doi.org/10.5281/zenodo.11388387> (Smith et al., 2024a). Data are provided under the CC-BY 4.0 Licence.

940
 941 HadEX3 [3.0.4] data were obtained from <https://catalogue.ceda.ac.uk/uuid/115d5e4ebf7148ec941423ec86fa9f26>
 942 (Dunn et al., 2023) on 5 April 2023 and are © British Crown Copyright, Met Office, 2022, provided under an Open
 943 Government Licence; <http://www.nationalarchives.gov.uk/doc/open-government-licence/version/2/> (last access: 2
 944 June 2023).

945 **11 Discussion and conclusions**

946 The second year of the Global Climate Change (IGCC) initiative has built on last year's effort and the AR6 report
 947 cycle to provide a comprehensive update of the climate change indicators required to estimate the human-induced

948 warming and the remaining carbon budget. Table 10 and Figure 11 present a summary of the headline indicators from
 949 each section compared to those given in the AR6 assessment and also summarises methodological updates. The main
 950 substantive dataset change since AR6 is that land-use CO₂ emissions have been revised down by around 2 GtCO₂
 951 (Table 10). However, as CO₂ ERF and human-induced warming estimates depend on concentrations, not emissions,
 952 this does not affect most of the other findings. Note it does slightly increase the remaining carbon budget, but this is
 953 only by 5 GtCO₂, less than the 50 GtCO₂ rounding precision.

954
 955 **Table 10 Summary of headline results and methodological updates from the Indicators of Global Climate Change (IGCC)**
 956 **initiative.**

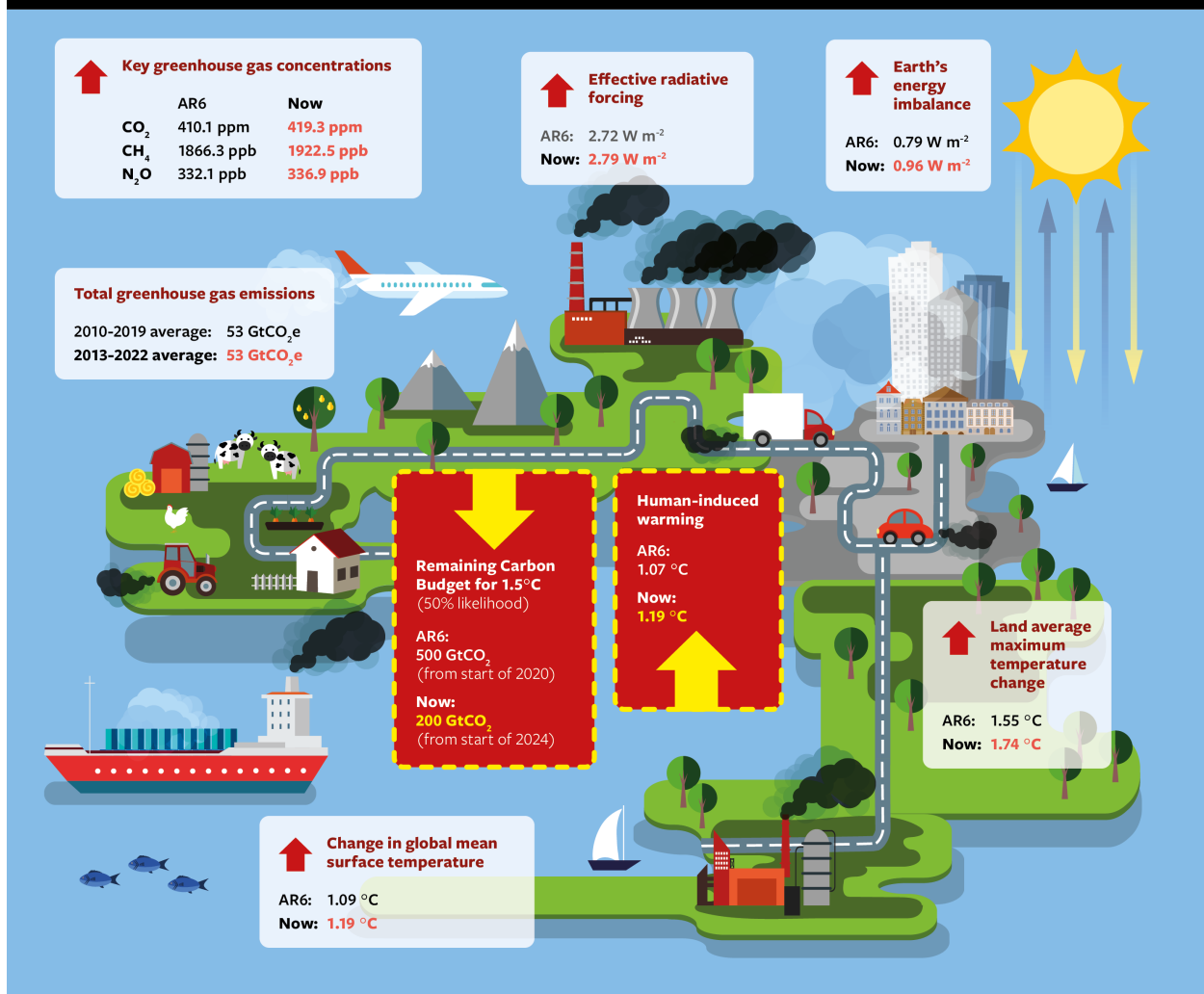
Climate Indicator	AR6 2021 assessment	This 2023 assessment	Explanation of changes	Methodological updates since AR6
Greenhouse gas emissions AR6 WGIII Chapter 2: Dhakal et al. (2022); see also Minx et al. (2021)	2010-2019 average: 56 ± 6 GtCO ₂ e*	2010-2019 average: 53 ± 5.5 GtCO ₂ e 2013-2022 average: 53 ± 5.4 GtCO ₂ e	Average emissions in the past decade grew at a slower rate than in the previous decade. The change from AR6 is due to a systematic downward revision in CO ₂ -LULUCF and CH ₄ estimates. Real-world emissions have slightly increased.	CO ₂ -LULUCF emissions revised down. CO ₂ GCB Fossil Fuel and Industry emissions used instead of EDGAR. PRIMAP-hist CR used in place of EDGAR for CH ₄ and N ₂ O emissions, atmospheric measurements taken for F-gas emissions. These changes reduce estimates by around 3 GtCO ₂ e (Sect. 2). Note following convention, ODS F-gases are excluded from the total.
Greenhouse gas concentrations AR6 WGI Chapter 2: Gulev et al. (2021)	2019: CO ₂ , 410.1 [± 0.36] ppm CH ₄ , 1866.3 [± 3.2] ppb N ₂ O, 332.1 [± 0.7] ppb	2023: CO ₂ , 419.3 [±0.4] ppm CH ₄ , 1922.5 [±3.3] ppb N ₂ O, 336.9 [±0.4] ppb	Increases caused by continued GHG anthropogenic emissions	Updates based on NOAA data and AGAGE (Sect. 3)

<p>Effective radiative forcing change since 1750</p> <p>AR6 WGI Chapter 7: Forster et al. (2021)</p>	<p>2019:</p> <p>2.72 [1.96 to 3.48] W m⁻²</p>	<p>2023:</p> <p>2.79 [1.78 to 3.60] W m⁻²</p>	<p>Trend since 2019 is caused by increases in greenhouse gas concentrations and reductions in aerosol precursors. Shipping emission reductions may have added approximately 0.1 W m⁻² to the ERF in 2023 compared to 2022. However, increases in biomass burning aerosol from Canadian wildfires decreased the ERF by more.</p>	<p>Follows AR6 with minor update to aerosol precursor treatment and emissions dataset that revises 2019 ERF estimate relative to 1750 downwards (more negative) by 0.09 W m⁻². Headline assessment of 1750 to 2005-2014 of -1.3 W m⁻² is unchanged from AR6. Contrails ERF estimate methodology slightly revised which does not make a material difference.</p>
<p>Earth's energy imbalance</p> <p>AR6 WGI Chapter 7: Forster et al. (2021)</p>	<p>2006-2018 average:</p> <p>0.79 [0.52 to 1.06] W m⁻²</p>	<p>2010-2023. average:</p> <p>0.96 [0.67 to 1.26] W m⁻²</p>	<p>Substantial increase in energy imbalance estimated based on increased rate of ocean heating.</p>	<p>Ocean heat content timeseries extended from 2018 to 2023 using 4 of the 5 AR6 datasets. Other heat inventory terms updated following von Schuckmann et al (2023a). Ocean heat content uncertainty is used as a proxy for total uncertainty. Further details in Sect. 5.</p>
<p>Global mean surface temperature change since 1850-1900</p> <p>AR6 WGI Chapter 2: Gulev et al. (2021)</p>	<p>2011-2020 average:</p> <p>1.09 [0.95 to 1.20] °C</p>	<p>2014-2023 average:</p> <p>1.19 [1.06–1.30] °C</p>	<p>An increase of 0.1 °C within three years, indicating a high decadal rate of change which may in part be internal variability.</p>	<p>Methods match four datasets used in AR6 (Sect. 6). Individual datasets have updated historical data, but these changes are not materially affecting results.</p>
<p>Human induced global warming since preindustrial</p> <p>AR6 WGI Chapter 3: Eyring et al. (2021)</p>	<p>2010-2019 average:</p> <p>1.07 [0.8 to 1.3] °C</p>	<p>2010-2019 average:</p> <p>1.09 [0.9 to 1.3] °C</p> <p>2014-2023 average:</p> <p>1.19 [1.0 to 1.4] °C</p>	<p>An increase of 0.1 °C within four years, indicating a high decadal rate of change. GMST increase in 2023 has revised historical estimates upwards.</p>	<p>The three methods for the basis of the AR6 assessment are retained, but each has new input data (Sect. 7)</p>

<p>Remaining carbon budget for 50% likelihood of limiting global warming to 1.5°C</p> <p>AR6 WGI Chapter 5: Canadell et al. (2021)</p>	<p>From the start of 2020:</p> <p>500 GtCO₂</p>	<p>From the start of 2024:</p> <p>200 GtCO₂</p>	<p>The 1.5°C budget is becoming very small. The RCB can exhaust before the 1.5°C threshold is reached due to having to allow for future non-CO₂ warming.</p>	<p>Emulator and scenario change has reduced budget since 2020 by 100 GtCO₂ (Sect. 8)</p>
<p>Land average maximum temperature change compared to pre-industrial.</p> <p>AR6 WGI Chapter 11: Seneviratne et al., 2021</p>	<p>2009-2018 average:</p> <p>1.55 °C</p>	<p>2014-2023 average:</p> <p>1.74 °C</p>	<p>Rising at a substantially faster rate compared to global mean surface temperature</p>	<p>HadEX3 data used in AR6 replaced with reanalysis data employed in this report which is more updatable going forward. Adds 0.01 °C to estimate (Sect. 9)</p>

Key indicators of global climate change 2023: What's changed since AR6?

Human induced warming is increasing at the **unprecedented rate** of over 0.2°C per decade, the result of greenhouse gas emissions being at an all-time high over the last decade, as well as reductions in the strength of aerosol cooling.



959

960 **Figure 11 Infographic for the best estimate of headline indicators assessed in this paper.**

961 Last year witnessed a large increase in GMST (Sect. 6), approaching 1.5°C above 1850-1900 levels that has widely
 962 been reported in the press. The 2022 to 2023 increase was the third largest annual increase in the instrumental record
 963 after 1876-1877 and 1976-1977, two other periods with a strong transition from La Niña to El Niño conditions. The
 964 reasons for the change, especially regarding the potential role of external forcings such as shipping emission reductions
 965 compared to internal variability are currently being investigated (e.g. Schmidt, 2024; Gettelman et al. 2024). Our work
 966 looks at long-term changes and does not directly investigate the reasons for the jump in GMST levels, yet we note
 967 that our best estimate of human induced warming in 2023 is 1.31 (1.1 to 1.7) °C (Table 6), below the observed GMST

968 estimate of 1.43 [1.32 to 1.53] °C in 2023 (Sect. 6). This indicates a potentially large role for El Niño and other wind-
969 driven ocean changes.

970 Methane and biomass emissions had a strong component of change related to climate feedbacks (Sects. 2 and 3). Such
971 changes will become increasingly important over this century, even if the direct human influence declines. These
972 changes need to be properly accounted for to explain atmospheric concentration and energy budget changes. The
973 approach to methane taken in this paper (where changes to natural sources are excluded) is inconsistent with that taken
974 for aerosol emissions (where wildfire changes are included). In future years and in the next IPCC report a consistent
975 approach to attribution of atmospheric emissions, concentration change and radiative forcing should be developed.
976 Similarly, we follow the underlying literature in treating wildfire related CO₂ emissions and removals as natural only
977 (Friedlingstein et al. 2023), even though their intensity and frequency is shifting under anthropogenic climate change.

978 It is hoped that this update can support the science community in its collection and provision of reliable and timely
979 global climate data. In future years we are particularly interested in improving SLCF updating methods to get a more
980 accurate estimate of short-term ERF changes. The work also highlights the importance of high-quality metadata to
981 document changes in methodological approaches over time. In future years we hope to improve the robustness of the
982 indicators presented here but also extend the breadth of indicators reported through coordinated research activities.
983 For example, we could begin to make use of new satellite and ground-based data for better greenhouse monitoring
984 (e.g. via the WMO Global Greenhouse Gas Watch initiative). Parallel efforts could explore how we might update
985 indicators of regional climate extremes and their attribution, which are particularly relevant for supporting actions on
986 adaptation and loss and damage.

987
988 Generally, scientists and scientific organisations have an important role as “watchdogs” to critically inform evidence-
989 based decision-making. This annual update traced to IPCC methods can provide a reliable, timely source of
990 trustworthy information. As well as helping inform decisions, we can use the update to track changes in datasets
991 between their use in one IPCC report and the next. We can also provide information and testing to motivate updates
992 in methods that future IPCC reports might choose to employ.

993
994 This is a critical decade: human-induced global warming rates are at their highest historical level, and 1.5 °C global
995 warming might be expected to be reached or exceeded within the next 10 years in the absence of cooling from major
996 volcanic eruptions (Lee et al., 2021). Yet this is also the decade that global greenhouse gas emissions could be expected
997 to peak and begin to substantially decline. The indicators of global climate change presented here show that the Earth's
998 energy imbalance has increased to around 0.9 W m⁻², averaged over the last 12 years. This also has implications for
999 the committed response of slow components in the climate system (glaciers, deep ocean, ice sheets) and committed
1000 long-term sea level rise, but this is not part of the update here. However, rapid and stringent GHG emission decreases
1001 such as those committed to at COP28 could halve warming rates over the next 20 years (McKenna et al., 2021). Table
1002 1 shows that global GHG emissions are at a long-term high, yet there are signs that their rate of increase has slowed.

1003 Depending on the societal choices made in this critical decade, a continued series of these annual updates could track
1004 an improving trend for some of the the indicators herein discussed.

1005 **Supplement**

1006 The supplement related to this article is available online at: **TBD**

1007 **Author contributions**

1008 PMF, CS, MA, PF, JR and AP developed the concept of an annual update in discussions with the wider IPCC
1009 community over many years. CS led the work of the data repositories. VMD, PZ, SS, JCM, CFS, SIS, VN, AP, NPG,
1010 GP, BT, MDP, KvS, JR, PF, MA,XZ, KZ, RAB, CB, CC, SB and PT provided important IPCC and UNFCCC framing.
1011 PMF coordinated the production of the manuscript with support from DR. WFL led Sect. 2 with contributions from
1012 JCM, PF, GP, JG, JP and RA. CS and BH led Sect. 3 with inputs from XL, JM and PK, CS led Sect. 4 with
1013 contributions from BH, SS, VN, RMH, GM, AG, GW, MVMK, EM, J-P.K, MvM and XL. BT led Sect. 5 with
1014 contributions from PT, CM, CK, JK, RR, and RV. KvS and MDP led Sect. 6 with contributions from LC, MI, TB and
1015 REK. BT led Sect. 6 with contributions from PT, CM, CK, JK, RR, RV and LC. TW led Sect. 7 with contributions
1016 and calculations from AR, NG, SJ and MA. RL led Sect. 8 with contributions from JR and KZ. Sect. 9 was led by
1017 MH, with contributions from SIS, XZ and DS. All authors either edited or commented on the manuscript. DR, AB
1018 and JAB coordinated the data visualisation effort.

1019 **Competing interests**

1020 The contact author has declared that none of the authors has any competing interests.

1021 **Disclaimer**

1022 Publisher's note: Copernicus Publications remains neutral with regard to jurisdictional claims in published maps and
1023 institutional affiliations.

1024 **Acknowledgements**

1025 This research has been supported by the European Union's Horizon Europe research and innovation programme under
1026 Grant Agreement No. 820829, 101081395, 101081661 and 821003), the H2020 European Research Council (grant
1027 no. 951542), the Natural Environment Research Council (NE/T009381/1) and the Engineering and Physical Research
1028 Council (EP/V000772/1). Chris Smith, Matthew D. Palmer, Colin Morice, Rachel E. Killick and Richard A. Betts
1029 were supported by the Met Office Hadley Centre Climate Programme funded by DSIT. Peter Thorne was supported
1030 by Co-Centre award number 22/CC/11103. The Co-Centre award is managed by Science Foundation Ireland (SFI),
1031 Northern Ireland's Department of Agriculture, Environment and Rural Affairs (DAERA) and UK Research and

1032 Innovation (UKRI), and supported via UK's International Science Partnerships Fund (ISPF), and the Irish
1033 Government's Shared Island initiative.

1034 **References**

1035 Allen, M. R., O. P. Dube, W. Solecki, F. Aragón-Durand, W. Cramer, S. Humphreys, M. Kainuma, J. Kala, N.
1036 Mahowald, Y. Mulugetta, R. Perez, M. Wairiu, and K. Zickfeld, 2018: Framing and Context. In: Global Warming of
1037 1.5°C. An IPCC Special Report on the impacts of global warming of 1.5°C above pre-industrial levels and related
1038 global greenhouse gas emission pathways, in the context of strengthening the global response to the threat of climate
1039 change, sustainable development, and efforts to eradicate poverty [Masson-Delmotte, V., P. Zhai, H.-O. Pörtner, D.
1040 Roberts, J. Skea, P.R. Shukla, A. Pirani, W. Moufouma-Okia, C. Péan, R. Pidcock, S. Connors, J.B.R. Matthews, Y.
1041 Chen, X. Zhou, M.I. Gomis, E. Lonnoy, T. Maycock, M. Tignor, and T. Waterfield (eds.)], Cambridge University
1042 Press, Cambridge, UK and New York, NY, USA, 49-92, <https://doi.org/10.1017/9781009157940.003>, 2018.

1043 Allison, L. C., Palmer, M. D., Allan, R. P., Hermanson, L., Liu, C., and Smith, D. M.: Observations of planetary
1044 heating since the 1980s from multiple independent datasets, *Environ. Res. Commun.*, 2, 101001,
1045 <https://doi.org/10.1088/2515-7620/abbb39>, 2020.

1046 Barnes, C., Boulanger, Y., Keeping, T., Gachon, P., Gillett, N., Haas, O., Wang, X., Roberge, F., Kew, S., Heinrich,
1047 D., Singh, R., Vahlberg, M., Van Aalst, M., Otto, F., Kimutai, J., Boucher, J., Kasoar, M., Zachariah, M., and Krikken,
1048 F.: Climate change more than doubled the likelihood of extreme fire weather conditions in Eastern Canada, Imperial
1049 College London, <https://doi.org/10.25561/105981>, 2023.

1050 Basu, S., Lan, X., Dlugokencky, E., Michel, S., Schwietzke, S., Miller, J. B., Bruhwiler, L., Oh, Y., Tans, P. P.,
1051 Apadula, F., Gatti, L. V., Jordan, A., Necki, J., Sasakawa, M., Morimoto, S., Di Iorio, T., Lee, H., Arduini, J., and
1052 Manca, G.: Estimating emissions of methane consistent with atmospheric measurements of methane and $\delta^{13}\text{C}$ of
1053 methane, *Atmos. Chem. Phys.*, 22, 15351–15377, <https://doi.org/10.5194/acp-22-15351-2022>, 2022.

1054 Bellouin, N., Davies, W., Shine, K. P., Quaas, J., Mülmenstädt, J., Forster, P. M., Smith, C., Lee, L., Regayre, L.,
1055 Brasseur, G., Sudarchikova, N., Bouarar, I., Boucher, O., and Myhre, G.: Radiative forcing of climate change from
1056 the Copernicus reanalysis of atmospheric composition, *Earth Syst. Sci. Data*, 12, 1649–1677,
1057 <https://doi.org/10.5194/essd-12-1649-2020>, 2020.

1058 Betts, R. A., Belcher, S. E., Hermanson, L., Klein Tank, A., Lowe, J. A., Jones, C. D., Morice, C. P., Rayner, N. A.,
1059 Scaife, A. A., and Stott, P. A.: Approaching 1.5 °C: how will we know we've reached this crucial warming mark?,
1060 *Nature*, 624, 33–35, <https://doi.org/10.1038/d41586-023-03775-z>, 2023.

1061 Bond, T. C., Doherty, S. J., Fahey, D. W., Forster, P. M., Berntsen, T., DeAngelo, B. J., Flanner, M. G., Ghan, S.,
1062 Kärcher, B., Koch, D., Kinne, S., Kondo, Y., Quinn, P. K., Sarofim, M. C., Schultz, M. G., Schulz, M., Venkataraman,
1063 C., Zhang, H., Zhang, S., Bellouin, N., Guttikunda, S. K., Hopke, P. K., Jacobson, M. Z., Kaiser, J. W., Klimont, Z.,
1064 Lohmann, U., Schwarz, J. P., Shindell, D., Storelvmo, T., Warren, S. G., and Zender, C. S.: Bounding the role of black
1065 carbon in the climate system: A scientific assessment, *J. Geophys. Res.-Atmos.*, 118, 5380–5552,
1066 <https://doi.org/10.1002/jgrd.50171>, 2013.

1067 Bun, R., Marland, G., Oda, T., See, L., Puliafito, E., Nahorski, Z., Jonas, M., Kovalyshyn, V., Ialongo, I., Yashchun,
1068 O., and Romanchuk, Z.: Tracking unaccounted greenhouse gas emissions due to the war in Ukraine since 2022,
1069 Science of The Total Environment, 914, 169879, <https://doi.org/10.1016/j.scitotenv.2024.169879>, 2024.

1070 Canadell, J.G., P. M. S. Monteiro, M. H. Costa, L. Cotrim da Cunha, P. M. Cox, A.V. Eliseev, S. Henson, M. Ishii, S.
1071 Jaccard, C. Koven, A. Lohila, P. K. Patra, S. Piao, J. Rogelj, S. Syampungani, S. Zaehle, and K. Zickfeld: Global
1072 Carbon and other Biogeochemical Cycles and Feedbacks. In Climate Change 2021: The Physical Science Basis.
1073 Contribution of Working Group I to the Sixth Assessment Report of the Intergovernmental Panel on Climate Change
1074 [Masson-Delmotte, V., P. Zhai, A. Pirani, S.L. Connors, C. Péan, S. Berger, N. Caud, Y. Chen, L. Goldfarb, M.I.
1075 Gomis, M. Huang, K. Leitzell, E. Lonnoy, J.B.R. Matthews, T.K. Maycock, T. Waterfield, O. Yelekçi, R. Yu, and B.
1076 Zhou (eds.)]. Cambridge University Press, Cambridge, United Kingdom and New York, NY, USA, pp. 673–816,
1077 <https://doi.org/10.1017/9781009157896.007>, 2021.

1078 Cheng, L., Abraham, J., Hausfather, Z., and Trenberth, K. E.: How fast are the oceans warming?, Science, 363, 128–
1079 129, <https://doi.org/10.1126/science.aav7619>, 2019.

1080 Cheng, L., Von Schuckmann, K., Abraham, J. P., Trenberth, K. E., Mann, M. E., Zanna, L., England, M. H., Zika, J.
1081 D., Fasullo, J. T., Yu, Y., Pan, Y., Zhu, J., Newsom, E. R., Bronselaer, B., and Lin, X.: Past and future ocean warming,
1082 Nat. Rev. Earth. Environ., 3, 776–794, <https://doi.org/10.1038/s43017-022-00345-1>, 2022.

1083 Climate Change Tracker, <https://climatechangetracker.org/igcc>, accessed 20.05.2024, 2024.

1084 Collins, M., Knutti, R., Arblaster, J., Dufresne, J.-L., Fichet, T., Friedlingstein, P., Gao, X., Gutowski, W.J., Johns,
1085 T., Krinner, G., Shongwe, M., Tebaldi, C., Weaver, A.J. & Wehner, M.: Long-term Climate Change: Projections,
1086 Commitments and Irreversibility. In: V.B. Stocker T.F., .D. Qin, G.K. Plattner, M. Tignor, S.K. Allen, J. Boschung,
1087 A. Nauels, Y. Xia & P.M. Midgley (eds.). Climate Change 2013: The Physical Science Basis. Contribution of Working
1088 Group I to the Fifth Assessment Report of the Intergovernmental Panel on Climate Change. Cambridge, United
1089 Kingdom and New York, NY, USA, Cambridge University Press. pp. 1029–1136, 2013.

1090 Crippa, M., Guizzardi, D., Schaaf, E., Monforti-Ferrario, F., Quadrelli, R., Risquez Martin, A., Rossi, S., Vignati, E.,
1091 Muntean, M., Brandao De Melo, J., Oom, D., Pagani, F., Banja, M., Taghavi-Moharamli, P., Köykkä, J., Grassi, G.,
1092 Branco, A., and San-Miguel, J.: GHG emissions of all world countries – 2023, Publications Office of the European
1093 Union, <https://doi.org/doi/10.2760/953322>, 2023.

1094 Cuesta-Valero, F. J., Beltrami, H., García-García, A., Krinner, G., Langer, M., MacDougall, A., Nitzbon, J., Peng, J.,
1095 von Schuckmann, K., Seneviratne, S., Thiery, W., Vanderkelen, I., Wu, T.: GCOS EHI 1960-2020 Continental Heat
1096 Content (Version 2), World Data Center for Climate (WDCC) at DKRZ,
1097 https://doi.org/10.26050/WDCC/GCOS_EHI_1960-2020_CoHC_v2, 2023.

1098 Deng, Z., Ciais, P., Tzompa-Sosa, Z. A., Saunio, M., Qiu, C., Tan, C., Sun, T., Ke, P., Cui, Y., Tanaka, K., Lin, X.,
1099 Thompson, R. L., Tian, H., Yao, Y., Huang, Y., Lauerwald, R., Jain, A. K., Xu, X., Bastos, A., Sitch, S., Palmer, P.
1100 I., Lauvaux, T., d’Aspremont, A., Giron, C., Benoit, A., Poulter, B., Chang, J., Petrescu, A. M. R., Davis, S. J., Liu,
1101 Z., Grassi, G., Albergel, C., Tubiello, F. N., Perugini, L., Peters, W., and Chevallier, F.: Comparing national

1102 greenhouse gas budgets reported in UNFCCC inventories against atmospheric inversions, *Earth System Science Data*,
1103 14, 1639–1675, <https://doi.org/10.5194/essd-14-1639-2022>, 2022.

1104 Dhakal, S., J. C. Minx, F. L. Toth, A. Abdel-Aziz, M. J. Figueroa Meza, K. Hubacek, I. G. C. Jonckheere, Yong-Gun
1105 Kim, G. F. Nemet, S. Pachauri, X. C. Tan, T. Wiedmann: Emissions Trends and Drivers. In IPCC, 2022: Climate
1106 Change 2022: Mitigation of Climate Change. Contribution of Working Group III to the Sixth Assessment Report of
1107 the Intergovernmental Panel on Climate Change [P.R. Shukla, J. Skea, R. Slade, A. Al Khourdajie, R. van Diemen,
1108 D. McCollum, M. Pathak, S. Some, P. Vyas, R. Fradera, M. Belkacemi, A. Hasija, G. Lisboa, S. Luz, J. Malley,
1109 (eds.)]. Cambridge University Press, Cambridge, UK and New York, NY, USA,
1110 <https://doi.org/10.1017/9781009157926.004>, 2022.

1111 Douville, H., K. Raghavan, J. Renwick, R.P. Allan, P.A. Arias, M. Barlow, R. Cerezo-Mota, A. Cherchi, T.Y. Gan, J.
1112 Gergis, D. Jiang, A. Khan, W. Pokam Mba, D. Rosenfeld, J. Tierney, and O. Zolina: Water Cycle Changes. In Climate
1113 Change 2021: The Physical Science Basis. Contribution of Working Group I to the Sixth Assessment Report of the
1114 Intergovernmental Panel on Climate Change [Masson-Delmotte, V., P. Zhai, A. Pirani, S.L. Connors, C. Péan, S.
1115 Berger, N. Caud, Y. Chen, L. Goldfarb, M.I. Gomis, M. Huang, K. Leitzell, E. Lonnoy, J.B.R. Matthews, T.K.
1116 Maycock, T. Waterfield, O. Yelekçi, R. Yu, and B. Zhou (eds.)]. Cambridge University Press, Cambridge, United
1117 Kingdom and New York, NY, USA, pp. 1055–1210, <https://doi.org/10.1017/9781009157896.010>, 2021.

1118 Droste, E. S., Adcock, K. E., Ashfold, M. J., Chou, C., Fleming, Z., Fraser, P. J., Gooch, L. J., Hind, A. J., Langenfelds,
1119 R. L., Leedham Elvidge, E. C., Mohd Hanif, N., O'Doherty, S., Oram, D. E., Ou-Yang, C.-F., Panagi, M., Reeves, C.
1120 E., Sturges, W. T., and Laube, J. C.: Trends and emissions of six perfluorocarbons in the Northern Hemisphere and
1121 Southern Hemisphere, *Atmos. Chem. Phys.*, 20, 4787–4807, <https://doi.org/10.5194/acp-20-4787-2020>, 2020.

1122 Dunn, R. J. H., Alexander, L. V., Donat, M. G., Zhang, X., Bador, M., Herold, N., Lippmann, T., Allan, R., Aguilar,
1123 E., Barry, A. A., Brunet, M., Caesar, J., Chagnaud, G., Cheng, V., Cinco, T., Durre, I., Guzman, R., Htay, T. M., Wan
1124 Ibadullah, W. M., Bin Ibrahim, M. K. I., Khoshkam, M., Kruger, A., Kubota, H., Leng, T. W., Lim, G., Li-Sha, L.,
1125 Marengo, J., Mbatha, S., McGree, S., Menne, M., Milagros Skansi, M., Ngwenya, S., Nkrumah, F., Oonariya, C.,
1126 Pabon-Caicedo, J. D., Panthou, G., Pham, C., Rahimzadeh, F., Ramos, A., Salgado, E., Salinger, J., Sané, Y.,
1127 Sopaheluwakan, A., Srivastava, A., Sun, Y., Timbal, B., Trachow, N., Trewin, B., Schrier, G., Vazquez-Aguirre, J.,
1128 Vasquez, R., Villarroel, C., Vincent, L., Vischel, T., Vose, R., and Bin Hj Yussof, M. N.: Development of an updated
1129 global land in situ-based data set of temperature and precipitation extremes: HadEX3, *J. Geophys. Res.-Atmos.*, 125,
1130 e2019JD032263, <https://doi.org/10.1029/2019JD032263>, 2020.

1131 Dunn, R. J. H., Donat, M. G., and Alexander, L. V.: Comparing extremes indices in recent observational and reanalysis
1132 products, *Front. Clim.*, 4, 98905, <https://doi.org/10.3389/fclim.2022.989505>, 2022.

1133 Dunn, R.J.H., Alexander, L., Donat, M., Zhang, X., Bador, M., Herold, N., Lippmann, T., Allan, R.J., Aguilar, E.,
1134 Aziz, A., Brunet, M., Caesar, J., Chagnaud, G., Cheng, V., Cinco, T., Durre, I., de Guzman, R., Htay, T.M., Wan
1135 Ibadullah, W.M., Bin Ibrahim, M.K.I., Khoshkam, M., Kruge, A., Kubota, H., Leng, T.W., Lim, G., Li-Sha, L.,
1136 Marengo, J., Mbatha, S., McGree, S., Menne, M., de los Milagros Skansi, M., Ngwenya, S., Nkrumah, F., Oonariya,
1137 C., Pabon-Caicedo, J.D., Panthou, G., Pham, C., Rahimzadeh, F., Ramos, A., Salgado, E., Salinger, J., Sane, Y.,

1138 Sopaheluwakan, A., Srivastava, A., Sun, Y., Trimbal, B., Trachow, N., Trewin, B., van der Schrier, G., Vazquez-
1139 Aguirre, J., Vasquez, R., Villarroel, C., Vincent, L., Vischel, T., Vose, R., Bin Hj Yussof, and M.N.A.: HadEX3:
1140 Global land-surface climate extremes indices v3.0.4 (1901-2018), NERC EDS Centre for Environmental Data
1141 Analysis [data set], <https://dx.doi.org/10.5285/115d5e4ebf7148ec941423ec86fa9f26>, 2023.

1142 Dutton, G.S., B. D. Hall, S.A. Montzka, J. D. Nance, S. D. Clingan, K. M. Petersen, Combined Atmospheric
1143 Chlorofluorocarbon-12 Dry Air Mole Fractions from the NOAA GML Halocarbons Sampling Network, 1977-2024,
1144 Version: 2024-03-07, <https://doi.org/10.15138/PJ63-H440>, 2024.

1145 Eyring, V., N. P. Gillett, K.M. Achuta Rao, R. Barimalala, M. Barreiro Parrillo, N. Bellouin, C. Cassou, P. J. Durack,
1146 Y. Kosaka, S. McGregor, S. Min, O. Morgenstern, and Y. Sun: Human Influence on the Climate System. In Climate
1147 Change 2021: The Physical Science Basis. Contribution of Working Group I to the Sixth Assessment Report of the
1148 Intergovernmental Panel on Climate Change [Masson-Delmotte, V., P. Zhai, A. Pirani, S.L. Connors, C. Péan, S.
1149 Berger, N. Caud, Y. Chen, L. Goldfarb, M.I. Gomis, M. Huang, K. Leitzell, E. Lonnoy, J.B.R. Matthews, T.K.
1150 Maycock, T. Waterfield, O. Yelekçi, R. Yu, and B. Zhou (eds.)]. Cambridge University Press, Cambridge, United
1151 Kingdom and New York, NY, USA, pp. 423–552, <http://doi:10.1017/9781009157896.005>, 2021.

1152 Feron, S., Malhotra, A., Bansal, S., Fluet-Chouinard, E., McNicol, G., Knox, S. H., Delwiche, K. B., Cordero, R. R.,
1153 Ouyang, Z., Zhang, Z., Poulter, B., and Jackson, R. B.: Recent increases in annual, seasonal, and extreme methane
1154 fluxes driven by changes in climate and vegetation in boreal and temperate wetland ecosystems, *Global Change*
1155 *Biology*, 30, e17131, <https://doi.org/10.1111/gcb.17131>, 2024.

1156 Forster, P. M., Forster, H. I., Evans, M. J., Gidden, M. J., Jones, C. D., Keller, C. A., Lamboll, R. D., Le Quéré, C.,
1157 Rogelj, J., Rosen, D., Schleussner, C. F., Richardson, T. B., Smith, C. J. and Turnock, S. T.: Current and future global
1158 climate impacts resulting from COVID-19, *Nature Clim. Chang*, 10, 913–919, [https://doi.org/10.1038/s41558-020-](https://doi.org/10.1038/s41558-020-0883-0)
1159 [0883-0](https://doi.org/10.1038/s41558-020-0883-0), 2020.

1160 Forster, P., T. Storelvmo, K. Armour, W. Collins, J.-L. Dufresne, D. Frame, D.J. Lunt, T. Mauritsen, M.D. Palmer,
1161 M. Watanabe, M. Wild, and H. Zhang, 2021: The Earth’s Energy Budget, Climate Feedbacks, and Climate Sensitivity.
1162 In *Climate Change 2021: The Physical Science Basis. Contribution of Working Group I to the Sixth Assessment*
1163 *Report of the Intergovernmental Panel on Climate Change* [Masson-Delmotte, V., P. Zhai, A. Pirani, S.L. Connors,
1164 C. Péan, S. Berger, N. Caud, Y. Chen, L. Goldfarb, M.I. Gomis, M. Huang, K. Leitzell, E. Lonnoy, J.B.R. Matthews,
1165 T.K. Maycock, T. Waterfield, O. Yelekçi, R. Yu, and B. Zhou (eds.)]. Cambridge University Press, Cambridge, United
1166 Kingdom and New York, NY, USA, pp. 923–1054, <https://doi.org/10.1017/9781009157896.009>, 2021.

1167 Forster, P., Smith, C., Walsh, T., Lamb, W., Lamboll, R., Hauser, M., Ribes, A., Rosen, D., Gillett, N., Palmer, M.,
1168 Rogelj, J., von Schuckmann, K., Seneviratne, S., Trewin, B., Zhang, X., Allen, M., Andrew, R., Birt, A., Borger, A.,
1169 Boyer, T., Broersma, J., Cheng, L., Dentener, F., Friedlingstein, P., Gutiérrez, J., Gütschow, J., Hall, B., Ishii, M.,
1170 Jenkins, S., Lan, X., Lee, J.-Y., Morice, C., Kadow, C., Kennedy, J., Killick, R., Minx, J., Naik, V., Peters, G., Pirani,
1171 A., Pongratz, J., Schleussner, C.-F., Szopa, S., Thorne, P., Rohde, R., Rojas Corradi, M., Schumacher, D., Vose, R.,
1172 Zickfeld, K., Masson-Delmotte, V., and Zhai, P.: Indicators of Global Climate Change 2022: annual update of large-

1173 scale indicators of the state of the climate system and human influence, *Earth System Science Data*, 15, 2295–2327,
1174 <https://doi.org/10.5194/essd-15-2295-2023>, 2023.

1175 Fox-Kemper, B., Fox-Kemper, B., H. T. Hewitt, C. Xiao, G. Aðalgeirsdóttir, S.S. Drijfhout, T. L. Edwards, N. R.
1176 Golledge, M. Hemer, R. E. Kopp, G. Krinner, A. Mix, D. Notz, S. Nowicki, I. S. Nurhati, L. Ruiz, J.-B. Sallée, A. B.
1177 A. Slangen, and Y. Yu: Ocean, Cryosphere and Sea Level Change. In *Climate Change 2021: The Physical Science*
1178 *Basis. Contribution of Working Group I to the Sixth Assessment Report of the Intergovernmental Panel on Climate*
1179 *Change* [Masson-Delmotte, V., P. Zhai, A. Pirani, S.L. Connors, C. Péan, S. Berger, N. Caud, Y. Chen, L. Goldfarb,
1180 M.I. Gomis, M. Huang, K. Leitzell, E. Lonnoy, J. B. R. Matthews, T. K. Maycock, T. Waterfield, O. Yelekçi, R. Yu,
1181 and B. Zhou (eds.)]. Cambridge University Press, Cambridge, United Kingdom and New York, NY, USA, pp. 1211–
1182 1362, <https://doi.org/10.1017/9781009157896.011>, 2021.

1183 Francey, R.J., L.P. Steele, R.L. Langenfelds and B.C. Pak, High precision long-term monitoring of radiatively-active
1184 trace gases at surface sites and from ships and aircraft in the Southern Hemisphere atmosphere, *J. Atmos. Science*, 56,
1185 279-285 [https://doi.org/10.1175/1520-0469\(1999\)056<0279:HPLTMO>2.0.CO;2](https://doi.org/10.1175/1520-0469(1999)056<0279:HPLTMO>2.0.CO;2), 1999.

1186 Friedlingstein, P., O’Sullivan, M., Jones, M. W., Andrew, R. M., Hauck, J., Olsen, A., Peters, G. P., Peters, W.,
1187 Pongratz, J., Sitch, S., Le Quéré, C., Canadell, J. G., Ciais, P., Jackson, R. B., Alin, S., Aragão, L. E. O. C., Arneeth,
1188 A., Arora, V., Bates, N. R., Becker, M., Benoit-Cattin, A., Bittig, H. C., Bopp, L., Bultan, S., Chandra, N., Chevallier,
1189 F., Chini, L. P., Evans, W., Florentie, L., Forster, P. M., Gasser, T., Gehlen, M., Gilfillan, D., Gkritzalis, T., Gregor,
1190 L., Gruber, N., Harris, I., Hartung, K., Haverd, V., Houghton, R. A., Ilyina, T., Jain, A. K., Joetzjer, E., Kadono, K.,
1191 Kato, E., Kitidis, V., Korsbakken, J. I., Landschützer, P., Lefèvre, N., Lenton, A., Lienert, S., Liu, Z., Lombardozzi,
1192 D., Marland, G., Metzl, N., Munro, D. R., Nabel, J. E. M. S., Nakaoka, S.-I., Niwa, Y., O’Brien, K., Ono, T., Palmer,
1193 P. I., Pierrot, D., Poulter, B., Resplandy, L., Robertson, E., Rödenbeck, C., Schwinger, J., Séférian, R., Skjelvan, I.,
1194 Smith, A. J. P., Sutton, A. J., Tanhua, T., Tans, P. P., Tian, H., Tilbrook, B., van der Werf, G., Vuichard, N., Walker,
1195 A. P., Wanninkhof, R., Watson, A. J., Willis, D., Wiltshire, A. J., Yuan, W., Yue, X., and Zaehle, S.: Global carbon
1196 budget 2020, *Earth Syst. Sci. Data*, 12, 3269–3340, <https://doi.org/10.5194/essd-12-3269-2020>, 2020.

1197 Friedlingstein, P., O’Sullivan, M., Jones, M. W., Andrew, R. M., Gregor, L., Hauck, J., Le Quéré, C., Luijkx, I. T.,
1198 Olsen, A., Peters, G. P., Peters, W., Pongratz, J., Schwingshackl, C., Sitch, S., Canadell, J. G., Ciais, P., Jackson, R.
1199 B., Alin, S. R., Alkama, R., Arneeth, A., Arora, V. K., Bates, N. R., Becker, M., Bellouin, N., Bittig, H. C., Bopp, L.,
1200 Chevallier, F., Chini, L. P., Cronin, M., Evans, W., Falk, S., Feely, R. A., Gasser, T., Gehlen, M., Gkritzalis, T.,
1201 Gloege, L., Grassi, G., Gruber, N., Gürses, Ö., Harris, I., Hefner, M., Houghton, R. A., Hurtt, G. C., Iida, Y., Ilyina,
1202 T., Jain, A. K., Jersild, A., Kadono, K., Kato, E., Kennedy, D., Klein Goldewijk, K., Knauer, J., Korsbakken, J. I.,
1203 Landschützer, P., Lefèvre, N., Lindsay, K., Liu, J., Liu, Z., Marland, G., Mayot, N., McGrath, M. J., Metzl, N.,
1204 Monacci, N. M., Munro, D. R., Nakaoka, S.-I., Niwa, Y., O’Brien, K., Ono, T., Palmer, P. I., Pan, N., Pierrot, D.,
1205 Pockock, K., Poulter, B., Resplandy, L., Robertson, E., Rödenbeck, C., Rodriguez, C., Rosan, T. M., Schwinger, J.,
1206 Séférian, R., Shutler, J. D., Skjelvan, I., Steinhoff, T., Sun, Q., Sutton, A. J., Sweeney, C., Takao, S., Tanhua, T., Tans,
1207 P. P., Tian, X., Tian, H., Tilbrook, B., Tsujino, H., Tubiello, F., van der Werf, G. R., Walker, A. P., Wanninkhof, R.,
1208 Whitehead, C., Willstrand Wranne, A., et al.: Global Carbon Budget 2022, *Earth Syst. Sci. Data*, 14, 4811–4900,
1209 <https://doi.org/10.5194/essd-14-4811-2022>, 2022.

1210 Friedlingstein, P., O'Sullivan, M., Jones, M. W., Andrew, R. M., Bakker, D. C. E., Hauck, J., Landschützer, P., Le
1211 Quéré, C., Lujikx, I. T., Peters, G. P., Peters, W., Pongratz, J., Schwingshackl, C., Sitch, S., Canadell, J. G., Ciais, P.,
1212 Jackson, R. B., Alin, S. R., Anthoni, P., Barbero, L., Bates, N. R., Becker, M., Bellouin, N., Decharme, B., Bopp, L.,
1213 Brasika, I. B. M., Cadule, P., Chamberlain, M. A., Chandra, N., Chau, T.-T.-T., Chevallier, F., Chini, L. P., Cronin,
1214 M., Dou, X., Enyo, K., Evans, W., Falk, S., Feely, R. A., Feng, L., Ford, D. J., Gasser, T., Ghattas, J., Gkritzalis, T.,
1215 Grassi, G., Gregor, L., Gruber, N., Gürses, Ö., Harris, I., Hefner, M., Heinke, J., Houghton, R. A., Hurtt, G. C., Iida,
1216 Y., Ilyina, T., Jacobson, A. R., Jain, A., Jarníková, T., Jersild, A., Jiang, F., Jin, Z., Joos, F., Kato, E., Keeling, R. F.,
1217 Kennedy, D., Klein Goldewijk, K., Knauer, J., Korsbakken, J. I., Körtzinger, A., Lan, X., Lefèvre, N., Li, H., Liu, J.,
1218 Liu, Z., Ma, L., Marland, G., Mayot, N., McGuire, P. C., McKinley, G. A., Meyer, G., Morgan, E. J., Munro, D. R.,
1219 Nakaoka, S.-I., Niwa, Y., O'Brien, K. M., Olsen, A., Omar, A. M., Ono, T., Paulsen, M., Pierrot, D., Pockock, K.,
1220 Poulter, B., Powis, C. M., Rehder, G., Resplandy, L., Robertson, E., Rödenbeck, C., Rosan, T. M., Schwinger, J.,
1221 Séférian, R., et al.: Global Carbon Budget 2023, *Earth System Science Data*, 15, 5301–5369,
1222 <https://doi.org/10.5194/essd-15-5301-2023>, 2023.

1223 Gasser, T., Crepin, L., Quilcaille, Y., Houghton, R. A., Ciais, P., and Obersteiner, M.: Historical CO₂ emissions from
1224 land use and land cover change and their uncertainty, *Biogeosciences*, 17, 4075–4101, [https://doi.org/10.5194/bg-17-](https://doi.org/10.5194/bg-17-4075-2020)
1225 [4075-2020](https://doi.org/10.5194/bg-17-4075-2020), 2020.

1226 Gettelman, A., Christensen, M. A., Diamond, M. S., Gryspeerdt, E., Manshausen, P., Sieir, P., Watson-Parris, D.,
1227 Yang, M., Yoshioka, M., and Yuan, T.: Has Reducing Ship Emissions Brought Forward Global Warming?, *Geophys.*
1228 *Res. Lett.*, 2024.

1229 Gillett, N.P., Kirchmeier-Young, M., Ribes, A., Shiogama, H., Hegerl, G.C., Knutti, R., Gastineau, G., John, J.G., Li,
1230 L., Nazarenko, L., Rosenbloom, N., Seland, Ø., Wu, T., Yukimoto, S., and Ziehn, T.: Constraining human
1231 contributions to observed warming since the pre-industrial period, *Nat. Clim. Chang.*, 11, 207–212,
1232 <https://doi.org/10.1038/s41558-020-00965-9>, 2021.

1233 Gleckler, P. J., Durack, P. J., Stouffer, R. J., Johnson, G. C., and Forest, C. E.: Industrial-era global ocean heat uptake
1234 doubles in recent decades, *Nat. Clim. Chang.*, 6, 394–398, <https://doi.org/10.1038/nclimate2915>, 2016.

1235 Grassi, G., Schwingshackl, C., Gasser, T., Houghton, R. A., Sitch, S., Canadell, J. G., Cescatti, A., Ciais, P., Federici,
1236 S., Friedlingstein, P., Kurz, W. A., Sanz Sanchez, M. J., Abad Viñas, R., Alkama, R., Bultan, S., Ceccherini, G., Falk,
1237 S., Kato, E., Kennedy, D., Knauer, J., Korosuo, A., Melo, J., McGrath, M. J., Nabel, J. E. M. S., Poulter, B.,
1238 Romanovskaya, A. A., Rossi, S., Tian, H., Walker, A. P., Yuan, W., Yue, X., and Pongratz, J.: Harmonising the land-
1239 use flux estimates of global models and national inventories for 2000–2020, *Earth Syst. Sci. Data*, 15, 1093–1114,
1240 <https://doi.org/10.5194/essd-15-1093-2023>, 2023.

1241 Gulev, S. K., P. W. Thorne, J. Ahn, F. J. Dentener, C. M. Domingues, S. Gerland, D. Gong, D. S. Kaufman, H. C.
1242 Nnamchi, J. Quaas, J.A. Rivera, S. Sathyendranath, S.L. Smith, B. Trewin, K. von Schuckmann, and R. S. Vose:
1243 Changing State of the Climate System. In *Climate Change 2021: The Physical Science Basis. Contribution of Working*
1244 *Group I to the Sixth Assessment Report of the Intergovernmental Panel on Climate Change*[Masson-Delmotte, V., P.
1245 Zhai, A. Pirani, S.L. Connors, C. Péan, S. Berger, N. Caud, Y. Chen, L. Goldfarb, M.I. Gomis, M. Huang, K. Leitzell,

1246 E. Lonnoy, J.B.R. Matthews, T.K. Maycock, T. Waterfield, O. Yelekçi, R. Yu, and B. Zhou (eds.]. Cambridge
1247 University Press, Cambridge, United Kingdom and New York, NY, USA, pp. 287–422,
1248 <https://doi.org/10.1017/9781009157896.004>, 2021.

1249 Gütschow, J., Jeffery, M. L., Gieseke, R., Gebel, R., Stevens, D., Krapp, M., and Rocha, M.: The PRIMAP-hist
1250 national historical emissions time series, *Earth Syst. Sci. Data*, 8, 571–603, <https://doi.org/10.5194/essd-8-571-2016>,
1251 2016.

1252 Gütschow, J., Pflüger, M., and Busch, D.: The PRIMAP-hist national historical emissions time series v2.5.1 (1750-
1253 2022) (2.5.1), Zenodo [data set] <https://doi.org/10.5281/zenodo.10705513>, 2024.

1254 Hakuba, M. Z., Frederikse, T., and Landerer, F. W.: Earth's energy imbalance from the ocean perspective (2005–
1255 2019), *Geophys Res Lett*, 48, e2021GL093624, <https://doi.org/10.1029/2021GL093624>, 2021.

1256 Hansen, J. E., Sato, M., Simons, L., Nazarenko, L. S., Sangha, I., Kharecha, P., Zachos, J. C., von Schuckmann, K.,
1257 Loeb, N. G., Osman, M. B., Jin, Q., Tselioudis, G., Jeong, E., Lacis, A., Ruedy, R., Russell, G., Cao, J., and Li, J.:
1258 Global warming in the pipeline, *Oxford Open Climate Change*, 3, kgad008, <https://doi.org/10.1093/oxfclm/kgad008>,
1259 2023.

1260 Hansis, E., Davis, S. J., and Pongratz, J.: Relevance of methodological choices for accounting of land use change
1261 carbon fluxes, *Global Biogeochem. Cy.*, 29, 1230–1246, <https://doi.org/10.1002/2014GB004997>, 2015.

1262 Haustein, K., Allen, M. R., Forster, P. M., Otto, F. E. L., Mitchell, D. M., Matthews, H. D., and Frame, D. J.: A real-
1263 time Global Warming Index, *Sci Rep*, 7, 15417, <https://doi.org/10.1038/s41598-017-14828-5>, 2017.

1264 Hersbach, H., Bell, B., Berrisford, P., Hirahara, S., Horányi, A., Muñoz-Sabater, J., Nicolas, J., Peubey, C., Radu, R.,
1265 Schepers, D., Simmons, A., Soci, C., Abdalla, S., Abellan, X., Balsamo, G., Bechtold, P., Biavati, G., Bidlot, J.,
1266 Bonavita, M., De Chiara, G., Dahlgren, P., Dee, D., Diamantakis, M., Dragani, R., Flemming, J., Forbes, R., Fuentes,
1267 M., Geer, A., Haimberger, L., Healy, S., Hogan, R. J., Hólm, E., Janisková, M., Keeley, S., Laloyaux, P., Lopez, P.,
1268 Lupu, C., Radnoti, G., de Rosnay, P., Rozum, I., Vamborg, F., Villaume, S., and Thépaut, J.-N.: The ERA5 global
1269 reanalysis, *Q. J. R. Meteorol. Soc.*, 146, 1999–2049, <https://doi.org/10.1002/qj.3803>, 2020.

1270 Hodnebrog, Ø., Aamaas, B., Fuglestedt, J. S., Marston, G., Myhre, G., Nielsen, C. J., Sandstad, M., Shine, K. P., and
1271 Wallington, T. J.: Updated Global Warming Potentials and Radiative Efficiencies of Halocarbons and Other Weak
1272 Atmospheric Absorbers, *Rev. Geophys.*, 58, e2019RG000691, <https://doi.org/10.1029/2019RG000691>, 2020.

1273 Hodnebrog, Ø., Myhre, G., Jouan, C., Andrews, T., Forster, P. M., Jia, H., Loeb, N. G., Olivie, D. J. L., Paynter, D.,
1274 Quaas, J., Raghuraman, S. P., and Schulz, M.: Recent reductions in aerosol emissions have increased Earth's energy
1275 imbalance, *Communications Earth & Environment*, 5, 166, <https://doi.org/10.1038/s43247-024-01324-8>, 2024.

1276 Hoesly, R. M., Smith, S. J., Feng, L., Klimont, Z., Janssens-Maenhout, G., Pitkanen, T., Seibert, J. J., Vu, L., Andres,
1277 R. J., Bolt, R. M., Bond, T. C., Dawidowski, L., Kholod, N., Kurokawa, J.-I., Li, M., Liu, L., Lu, Z., Moura, M. C. P.,
1278 O'Rourke, P. R., and Zhang, Q.: Historical (1750–2014) anthropogenic emissions of reactive gases and aerosols from
1279 the Community Emissions Data System (CEDS), *Geosci. Model. Dev.*, 11, 369–408, [https://doi.org/10.5194/gmd-11-
1280 369-2018](https://doi.org/10.5194/gmd-11-369-2018), 2018.

1281 Hoesly, R., & Smith, S., CEDS v_2024_04_01 Release Emission Data (v_2024_04_01) [Data set], Zenodo.
1282 <https://doi.org/10.5281/zenodo.10904361>, 2024.

1283 Houghton, R. A., and Nassikas, A. A.: Global and regional fluxes of carbon from land use and land cover change
1284 1850–2015, *Global Biogeochem. Cy.*, 31, 456–472, <https://doi.org/10.1002/2016GB005546>, 2017.

1285 Houghton, R. A. and Castanho, A.: Annual emissions of carbon from land use, land-use change, and forestry from
1286 1850 to 2020, *Earth System Science Data*, 15, 2025–2054, <https://doi.org/10.5194/essd-15-2025-2023>, 2023.

1287 Hu, Y., Yue, X., Tian, C., Zhou, H., Fu, W., Zhao, X., Zhao, Y., and Chen, Y.: Identifying the main drivers of the
1288 spatiotemporal variations in wetland methane emissions during 2001–2020, *Frontiers in Environmental Science*, 11,
1289 <https://doi.org/10.3389/fenvs.2023.1275742>, 2023.

1290 IATA: Air Passenger Monthly Analysis March 2024, [https://www.iata.org/en/iata-repository/publications/economic-](https://www.iata.org/en/iata-repository/publications/economic-reports/air-passenger-market-analysis-march-2024/)
1291 [reports/air-passenger-market-analysis-march-2024/](https://www.iata.org/en/iata-repository/publications/economic-reports/air-passenger-market-analysis-march-2024/), accessed 20.05.2024, 2024.

1292 IEA: CO2 Emissions in 2023. <https://www.iea.org/reports/co2-emissions-in-2023>, accessed 20.04.2024, 2024.

1293 IPCC: Climate Change 2013: The Physical Science Basis. Contribution of Working Group I to the Fifth Assessment
1294 Report of the Intergovernmental Panel on Climate Change [Stocker, T.F., D. Qin, G.-K. Plattner, M. Tignor, S.K.
1295 Allen, J. Boschung, A. Nauels, Y. Xia, V. Bex and P.M. Midgley (eds.)]. Cambridge University Press, Cambridge,
1296 United Kingdom and New York, NY, USA, 1535 pp, <https://doi:10.1017/CBO9781107415324>, 2013.

1297 IPCC: Summary for Policymakers. In: Global Warming of 1.5°C. An IPCC Special Report on the impacts of global
1298 warming of 1.5°C above pre-industrial levels and related global greenhouse gas emission pathways, in the context of
1299 strengthening the global response to the threat of climate change, sustainable development, and efforts to eradicate
1300 poverty [Masson-Delmotte, V., P. Zhai, H.-O. Pörtner, D. Roberts, J. Skea, P.R. Shukla, A. Pirani, W. Moufouma-
1301 Okia, C. Péan, R. Pidcock, S. Connors, J.B.R. Matthews, Y. Chen, X. Zhou, M.I. Gomis, E. Lonnoy, T. Maycock, M.
1302 Tignor, and T. Waterfield (eds.)]. Cambridge University Press, Cambridge, UK and New York, NY, USA, pp. 3-24,
1303 <https://doi.org/10.1017/9781009157940.001>, 2018.

1304 IPCC: Climate Change 2021: The Physical Science Basis. Contribution of Working Group I to the Sixth Assessment
1305 Report of the Intergovernmental Panel on Climate Change, Cambridge University Press, Cambridge, United Kingdom
1306 and New York, NY, USA, <https://doi.org/10.1017/9781009157896>, 2021a.

1307 IPCC: Summary for Policymakers, in: Climate Change 2021: The Physical Science Basis. Contribution of Working
1308 Group I to the Sixth Assessment Report of the Intergovernmental Panel on Climate Change, edited by: Masson-
1309 Delmotte, V., Zhai, P., Pirani, A., Connors, S. L., Péan, C., Berger, S., Caud, N., Chen, Y., Goldfarb, L., Gomis, M.
1310 I., Huang, M., Leitzell, K., Lonnoy, E., Matthews, J. B. R., Maycock, T. K., Waterfield, T., Yelekçi, O., Yu, R., and
1311 Zhou, B., Cambridge University Press, Cambridge, United Kingdom and New York, NY, USA, pp.3–32
1312 <https://doi.org/10.1017/9781009157896.001>, 2021b.

1313 IPCC: Climate Change 2022: Impacts, Adaptation, and Vulnerability. Contribution of Working Group II to the Sixth
1314 Assessment Report of the Intergovernmental Panel on Climate Change [H.-O. Pörtner, D.C. Roberts, M. Tignor, E.S.
1315 Poloczanska, K. Mintenbeck, A. Alegría, M. Craig, S. Langsdorf, S. Lösschke, V. Möller, A. Okem, B. Rama (eds.)].

1316 Cambridge University Press. Cambridge University Press, Cambridge, UK and New York, NY, USA, 3056 pp.,
1317 <https://doi.org/10.1017/9781009325844>, 2022.

1318 IPCC, 2023: Climate Change 2023: Synthesis Report. Contribution of Working Groups I, II and III to the Sixth
1319 Assessment Report of the Intergovernmental Panel on Climate Change [Core Writing Team, H. Lee and J. Romero
1320 (eds.)]. IPCC, Geneva, Switzerland., Intergovernmental Panel on Climate Change (IPCC),
1321 <https://doi.org/10.59327/IPCC/AR6-9789291691647>, 2023a.

1322 IPCC, 2023: Climate Change 2023: Summary for Policy Makers. Contribution of Working Groups I, II and III to the
1323 Sixth Assessment Report of the Intergovernmental Panel on Climate Change [Core Writing Team, H. Lee and J.
1324 Romero (eds.)]. IPCC, Geneva, Switzerland., Intergovernmental Panel on Climate Change (IPCC),
1325 <https://doi.org/10.59327/IPCC/AR6-9789291691647>, 2023b.

1326 Iturbide, M., Fernández, J., Gutiérrez, J. M., Pirani, A., Huard, D., Al Khourdajie, A., Baño-Medina, J., Bedia, J.,
1327 Casanueva, A., Cimadevilla, E., Cofiño, A. S., De Felice, M., Díez-Sierra, J., García-Díez, M., Goldie, J., Herrera, D.
1328 A., Herrera, S., Manzanas, R., Milovac, J., Radhakrishnan, A., San-Martín, D., Spinuso, A., Thyng, K. M., Trenham,
1329 C., and Yelekçi, Ö.: Implementation of FAIR principles in the IPCC: the WGI AR6 Atlas repository, *Sci Data*, 9, 629,
1330 <https://doi.org/10.1038/s41597-022-01739-y>, 2022.

1331 Janardanan, R., Maksyutov, S., Wang, F., Nayagam, L., Sahu, S. K., Mangaraj, P., Saunio, M., Lan, X., and
1332 Matsunaga, T.: Country-level methane emissions and their sectoral trends during 2009–2020 estimated by high-
1333 resolution inversion of GOSAT and surface observations, *Environ. Res. Lett.*, 19, 034007,
1334 <https://doi.org/10.1088/1748-9326/ad2436>, 2024.

1335 Jenkins, S., Povey, A., Gettelman, A., Grainger, R., Stier, P., and Allen, M.: Is Anthropogenic Global Warming
1336 Accelerating?, *Journal of Climate*, 35, 7873–7890, <https://doi.org/10.1175/JCLI-D-22-0081.1>, 2022.

1337 Jenkins, S., Smith, C., Allen, M., and Grainger, R.: Tonga eruption increases chance of temporary surface temperature
1338 anomaly above 1.5 °C, *Nature Clim. Chang.*, 13, 127–129, <https://doi.org/10.1038/s41558-022-01568-2>, 2023.

1339 Kirchengast, G., Gorfer, M., Mayer, M., Steiner, A. K., and Haimberger, L.: GCOS EHI 1960-2020 Atmospheric Heat
1340 Content, https://doi.org/10.26050/WDC/GCOS_EHI_1960-2020_AHC, 2022.

1341 Kramer, R. J., He, H., Soden, B. J., Oreopoulos, L., Myhre, G., Forster, P. M., and Smith, C. J.: Observational evidence
1342 of increasing global radiative forcing, *Geophys. Res. Lett.*, 48, e2020GL091585,
1343 <https://doi.org/10.1029/2020GL091585>, 2021.

1344 Lamboll, R. D., Jones, C. D., Skeie, R. B., Fiedler, S., Samset, B. H., Gillett, N. P., Rogelj, J., and Forster, P. M.:
1345 Modifying emissions scenario projections to account for the effects of COVID-19: protocol for CovidMIP,
1346 *Geoscientific Model Development*, 14, 3683–3695, <https://doi.org/10.5194/gmd-14-3683-2021>, 2021.

1347 Lamboll, R. D. and Rogelj, J.: Code for estimation of remaining carbon budget in IPCC AR6 WGI, Zenodo [code],
1348 <https://doi.org/10.5281/zenodo.6373365>, 2022.

1349 Lamboll, R. and Rogelj, J.: Carbon Budget Calculator, 2024, Github [code],
1350 <https://github.com/Rlamboll/AR6CarbonBudgetCalc/tree/v1.0.1>, last access: 25 April 2024.

1351 Lamboll, R. D., Nicholls, Z. R. J., Smith, C. J., Kikstra, J. S., Byers, E., and Rogelj, J.: Assessing the size and
1352 uncertainty of remaining carbon budgets, *Nature Climate Change*, 13, 1360–1367, [https://doi.org/10.1038/s41558-](https://doi.org/10.1038/s41558-023-01848-5)
1353 [023-01848-5](https://doi.org/10.1038/s41558-023-01848-5), 2023.

1354 Lan, X., Tans, P. and Thoning, K.W.: Trends in globally-averaged CO₂ determined from NOAA Global Monitoring
1355 Laboratory measurements, Version 2023-04, <https://doi.org/10.15138/9N0H-ZH07>, 2023a.

1356 Lan, X., Thoning, K. W., and Dlugokencky, E.J.: Trends in globally-averaged CH₄ N₂O, and SF₆ determined from
1357 NOAA Global Monitoring Laboratory measurements, Version 2023-04, <https://doi.org/10.15138/P8XG-AA10>,
1358 2023b.

1359 Laube, J., Newland, M., Hogan, C., Brenninkmeijer, A.M., Fraser, P.J., Martinerie, P., Oram, D.E., Reeves, C.E.,
1360 Röckmann, T., Schwander, J., Witrant, E., Sturges, W.T.: Newly detected ozone-depleting substances in the
1361 atmosphere. *Nature Geosci.*, 7, 266–269, <https://doi.org/10.1038/ngeo2109>, 2014.

1362 Lee, J.-Y., J. Marotzke, G. Bala, L. Cao, S. Corti, J.P. Dunne, F. Engelbrecht, E. Fischer, J.C. Fyfe, C. Jones, A.
1363 Maycock, J. Mutemi, O. Ndiaye, S. Panickal, and T. Zhou: Future Global Climate: Scenario-Based Projections and
1364 Near-Term Information. In *Climate Change 2021: The Physical Science Basis. Contribution of Working Group I to*
1365 *the Sixth Assessment Report of the Intergovernmental Panel on Climate Change*[Masson-Delmotte, V., P. Zhai, A.
1366 Pirani, S.L. Connors, C. Péan, S. Berger, N. Caud, Y. Chen, L. Goldfarb, M.I. Gomis, M. Huang, K. Leitzell, E.
1367 Lonnoy, J.B.R. Matthews, T.K. Maycock, T. Waterfield, O. Yelekçi, R. Yu, and B. Zhou (eds.)]. Cambridge
1368 University Press, Cambridge, United Kingdom and New York, NY, USA, pp. 553–
1369 672,<https://doi.org/10.1017/9781009157896.006>, 2021.

1370 Lee, H., K. Calvin, D. Dasgupta, G. Krinner, A. Mukherji, P. Thorne, C. Trisos, J. Romero, P. Aldunce, K. Barrett,
1371 G. Blanco, W.W.L. Cheung, S.L. Connors, F. Denton, A. Diongue-Niang, D. Dodman, M. Garschagen, O. Geden, B.
1372 Hayward, C. Jones, F. Jotzo, T. Krug, R. Lasco, J.-Y. Lee, V. Masson-Delmotte, M. Meinshausen, K. Mintenbeck, A.
1373 Mokssit, F.E.L. Otto, M. Pathak, A. Pirani, E. Poloczanska, H.-O. Pörtner, A. Revi, D.C. Roberts, J. Roy, A.C. Ruane,
1374 J. Skea, P.R. Shukla, R. Slade, A. Slangen, Y. Sokona, A.A. Sörensson, M. Tignor, D. van Vuuren, Y.-M. Wei, H.
1375 Winkler, P. Zhai, and Z. Zommers: Synthesis Report of the IPCC Sixth Assessment Report (AR6): Summary for
1376 Policymakers. Intergovernmental Panel on Climate Change [accepted], available at
1377 <https://www.ipcc.ch/report/ar6/syr/>, 2023.

1378 Liu, Z., Deng, Z., Davis, S. J., and Ciais, P.: Global carbon emissions in 2023, *Nature Reviews Earth & Environment*,
1379 5, 253–254, <https://doi.org/10.1038/s43017-024-00532-2>, 2024.

1380 Loeb, N. G., Johnson, G. C., Thorsen, T. J., Lyman, J. M., Rose, F. G., Kato, S.: Satellite and ocean data reveal marked
1381 increase in Earth’s heating rate. *Geophys. Res. Lett.*, 48, e2021GL093047, <https://doi.org/10.1029/2021GL093047>,
1382 2021.

1383 van Marle, M. J. E., Kloster, S., Magi, B. I., Marlon, J. R., Daniau, A.-L., Field, R. D., Arneth, A., Forrest, M.,
1384 Hantson, S., Kehrwald, N. M., Knorr, W., Lasslop, G., Li, F., Mangeon, S., Yue, C., Kaiser, J. W., and van der Werf,
1385 G. R.: Historic global biomass burning emissions for CMIP6 (BB4CMIP) based on merging satellite observations

1386 with proxies and fire models (1750–2015), *Geosci. Model Dev.*, 10, 3329–3357, [https://doi.org/10.5194/gmd-10-](https://doi.org/10.5194/gmd-10-3329-2017)
1387 [3329-2017](https://doi.org/10.5194/gmd-10-3329-2017), 2017.

1388 McKenna, C. M., Maycock, A. C., Forster, P. M., Smith, C. J., and Tokarska, K. B.: Stringent mitigation substantially
1389 reduces risk of unprecedented near-term warming rates, *Nature Climate Change*, 11, 126–131,
1390 <https://doi.org/10.1038/s41558-020-00957-9>, 2021.

1391 Minière, A., von Schuckmann, K., Sallée, J.-B., and Vogt, L.: Robust acceleration of Earth system heating observed
1392 over the past six decades, *Scientific Reports*, 13, 22975, <https://doi.org/10.1038/s41598-023-49353-1>, 2023.

1393 Minx, J. C., Lamb, W. F., Andrew, R. M., Canadell, J. G., Crippa, M., Döbbling, N., Forster, P. M., Guizzardi, D.,
1394 Olivier, J., Peters, G. P., Pongratz, J., Reisinger, A., Rigby, M., Saunio, M., Smith, S. J., Solazzo, E., and Tian, H.:
1395 A comprehensive and synthetic dataset for global, regional, and national greenhouse gas emissions by sector 1970–
1396 2018 with an extension to 2019, *Earth Syst. Sci. Data*, 13, 5213–5252, <https://doi.org/10.5194/essd-13-5213-2021>,
1397 2021.

1398 Nickolay A. Krotkov, Lok N. Lamsal, Sergey V. Marchenko, Edward A. Celarier, Eric J. Bucsela, William H. Swartz,
1399 Joanna Joiner and the OMI core team, OMI/Aura NO2 Cloud-Screened Total and Tropospheric Column L3 Global
1400 Gridded 0.25 degree x 0.25 degree V3, NASA Goddard Space Flight Center, Goddard Earth Sciences Data and
1401 Information Services Center (GES DISC), Accessed: [Data Access 22 April 2024],
1402 <https://doi.org/10.5067/Aura/OMI/DATA3007>, 2019. Nisbet, E. G., Manning, M. R., Dlugokencky, E. J., Michel, S.
1403 E., Lan, X., Roeckmann, T., Gon, H. A. D. V. D., Palmer, P., Oh, Y., Fisher, R., Lowry, D., France, J. L., and White,
1404 J. W. C.: Atmospheric methane: Comparison between methane’s record in 2006–2022 and during glacial terminations,
1405 Preprints, <https://doi.org/10.22541/essoar.167689502.25042797/v1>, 2023.

1406 Nitzbon, J., Krinner, G., Langer, M.: GCOS EHI 1960–2020 Permafrost Heat Content, World Data Center for Climate
1407 (WDCC) at DKRZ, https://doi.org/10.26050/WDCC/GCOS_EHI_1960-2020_PHC, 2022.

1408 Palmer, M. D. and McNeall, D. J.: Internal variability of Earth’s energy budget simulated by CMIP5 climate models,
1409 *Environ. Res. Lett.*, 9, 034016, <https://doi.org/10.1088/1748-9326/9/3/034016>, 2014.

1410 Peng, S., Lin, X., Thompson, R. L., Xi, Y., Liu, G., Hauglustaine, D., Lan, X., Poulter, B., Ramonet, M., Saunio, M.,
1411 Yin, Y., Zhang, Z., Zheng, B., and Ciais, P.: Wetland emission and atmospheric sink changes explain methane growth
1412 in 2020, *Nature*, 612, 477–482, <https://doi.org/10.1038/s41586-022-05447-w>, 2022.

1413 Pirani, A., Alegria, A., Khourdajie, A. A., Gunawan, W., Gutiérrez, J. M., Holsman, K., Huard, D., Juckes, M.,
1414 Kawamiya, M., Klutse, N., Krey, V., Matthews, R., Milward, A., Pascoe, C., Van Der Shrier, G., Spinuso, A.,
1415 Stockhause, M., and Xiaoshi Xing: The implementation of FAIR data principles in the IPCC AR6 assessment process,
1416 <https://doi.org/10.5281/ZENODO.6504469>, 2022.

1417 Pongratz, J., Schwingshackl, C., Bultan, S., Obermeier, W., Havermann, F., and Guo, S.: Land Use Effects on Climate:
1418 Current State, Recent Progress, and Emerging Topics, *Curr. Clim. Change Rep.*, 7, 99–120,
1419 <https://doi.org/10.1007/s40641-021-00178-y>, 2021.

1420 Prinn, R. G., Weiss, R. F., Arduini, J., Arnold, T., DeWitt, H. L., Fraser, P. J., Ganesan, A. L., Gasore, J., Harth, C.
1421 M., Hermansen, O., Kim, J., Krummel, P. B., Li, S., Loh, Z. M., Lunder, C. R., Maione, M., Manning, A. J., Miller,
1422 B. R., Mitrevski, B., Mühle, J., O'Doherty, S., Park, S., Reimann, S., Rigby, M., Saito, T., Salameh, P. K., Schmidt,
1423 R., Simmonds, P. G., Steele, L. P., Vollmer, M. K., Wang, R. H., Yao, B., Yokouchi, Y., Young, D., and Zhou, L.:
1424 History of chemically and radiatively important atmospheric gases from the Advanced Global Atmospheric Gases
1425 Experiment (AGAGE), *Earth Syst. Sci. Data*, 10, 985–1018, <https://doi.org/10.5194/essd-10-985-2018>, 2018.

1426 Quaas, J., Jia, H., Smith, C., Albright, A. L., Aas, W., Bellouin, N., Boucher, O., Doutriaux-Boucher, M., Forster, P.
1427 M., Grosvenor, D., Jenkins, S., Klimont, Z., Loeb, N. G., Ma, X., Naik, V., Paulot, F., Stier, P., Wild, M., Myhre, G.,
1428 and Schulz, M.: Robust evidence for reversal of the trend in aerosol effective climate forcing, *Atmos. Chem. Phys.*,
1429 22, 12221–12239, <https://doi.org/10.5194/acp-22-12221-2022>, 2022.

1430 Raghuraman, S.P., Paynter, D. and Ramaswamy, V.: Anthropogenic forcing and response yield observed positive
1431 trend in Earth's energy imbalance, *Nat. Commun.* 12, 4577, <https://doi.org/10.1038/s41467-021-24544-4>, 2021.

1432 Ribes, A., Qasmi, S., and Gillett, N. P.: Making climate projections conditional on historical observations, *Sci. Adv.*,
1433 7, eabc0671, <https://doi.org/10.1126/sciadv.abc0671>, 2021.

1434 Rogelj, J., D. Shindell, K. Jiang, S. Fifita, P. Forster, V. Ginzburg, C. Handa, H. Kheshgi, S. Kobayashi, E. Kriegler,
1435 L. Mundaca, R. Séférian, and M. V. Vilariño: Mitigation Pathways Compatible with 1.5°C in the Context of
1436 Sustainable Development. In: *Global Warming of 1.5°C. An IPCC Special Report on the impacts of global warming
1437 of 1.5°C above pre-industrial levels and related global greenhouse gas emission pathways, in the context of
1438 strengthening the global response to the threat of climate change, sustainable development, and efforts to eradicate
1439 poverty* [Masson-Delmotte, V., P. Zhai, H.-O. Pörtner, D. Roberts, J. Skea, P.R. Shukla, A. Pirani, W. Moufouma-
1440 Okia, C. Péan, R. Pidcock, S. Connors, J. B. R. Matthews, Y. Chen, X. Zhou, M. I. Gomis, E. Lonnoy, T. Maycock,
1441 M. Tignor, and T. Waterfield (eds.)]. Cambridge University Press, Cambridge, UK and New York, NY, USA, pp. 93-
1442 174, <https://doi.org/10.1017/9781009157940.004>, 2018.

1443 Rogelj, J., Forster, P. M., Kriegler, E., Smith, C. J., and Séférian, R.: Estimating and tracking the remaining carbon
1444 budget for stringent climate targets, *Nature*, 571, 335–342, <https://doi.org/10.1038/s41586-019-1368-z>, 2019.

1445 Rogelj, J., Lamboll, R.D.: Substantial reductions in non-CO2 greenhouse gas emissions reductions implied by IPCC
1446 estimates of the remaining carbon budget. *Communications Earth Environ* 5, 35. [https://doi.org/10.1038/s43247-023-](https://doi.org/10.1038/s43247-023-01168-8)
1447 [01168-8](https://doi.org/10.1038/s43247-023-01168-8), 2024.

1448 Rogelj, J., Rao, S., McCollum, D. L., Pachauri, S., Klimont, Z., Krey, V., and Riahi, K: Air-pollution emission ranges
1449 consistent with the representative concentration pathways, *Nature Clim. Chang.*, 4 (6), 446–450,
1450 <https://doi.org/10.1038/nclimate2178>, 2014.

1451 Rohde, R., Muller, R., Jacobsen, R., Perlmutter, S., Rosenfeld, A. et al.: Berkeley Earth Temperature Averaging
1452 Process, *Geoinfor. Geostat.: An Overview 1:2.*, <http://dx.doi.org/10.4172/gigs.1000103>, 2013.

1453 Scarpelli, T. R., Jacob, D. J., Grossman, S., Lu, X., Qu, Z., Sulprizio, M. P., Zhang, Y., Reuland, F., Gordon, D., and
1454 Worden, J. R.: Updated Global Fuel Exploitation Inventory (GFEI) for methane emissions from the oil, gas, and coal

1455 sectors: evaluation with inversions of atmospheric methane observations, *Atmos. Chem. Phys.*, 22, 3235–3249,
1456 <https://doi.org/10.5194/acp-22-3235-2022>, 2022.

1457 Schmidt, G.: Climate models can't explain 2023's huge heat anomaly — we could be in uncharted territory, *Nature*,
1458 627, 467–467, <https://doi.org/10.1038/d41586-024-00816-z>, 2024.

1459 von Schuckmann, K., Cheng, L., Palmer, M. D., Hansen, J., Tassone, C., Aich, V., Adusumilli, S., Beltrami, H., Boyer,
1460 T., Cuesta-Valero, F. J., Desbruyères, D., Domingues, C., García-García, A., Gentine, P., Gilson, J., Gorfer, M.,
1461 Haimberger, L., Ishii, M., Johnson, G. C., Killick, R., King, B. A., Kirchengast, G., Kolodziejczyk, N., Lyman, J.,
1462 Marzeion, B., Mayer, M., Monier, M., Monselesan, D. P., Purkey, S., Roemmich, D., Schweiger, A., Seneviratne, S.
1463 I., Shepherd, A., Slater, D. A., Steiner, A. K., Straneo, F., Timmermans, M.-L., and Wijffels, S. E.: Heat stored in the
1464 Earth system: where does the energy go?, *Earth Syst. Sci. Data*, 12, 2013–2041, [https://doi.org/10.5194/essd-12-2013-](https://doi.org/10.5194/essd-12-2013-2020)
1465 [2020](https://doi.org/10.5194/essd-12-2013-2020), 2020.

1466 von Schuckmann, K., Minière, A., Gues, F., Cuesta-Valero, F. J., Kirchengast, G., Adusumilli, S., Straneo, F., Ablain,
1467 M., Allan, R. P., Barker, P. M., Beltrami, H., Blazquez, A., Boyer, T., Cheng, L., Church, J., Desbruyeres, D., Dolman,
1468 H., Domingues, C. M., García-García, A., Giglio, D., Gilson, J. E., Gorfer, M., Haimberger, L., Hakuba, M. Z.,
1469 Hendricks, S., Hosoda, S., Johnson, G. C., Killick, R., King, B., Kolodziejczyk, N., Korosov, A., Krinner, G., Kuusela,
1470 M., Landerer, F. W., Langer, M., Lavergne, T., Lawrence, I., Li, Y., Lyman, J., Marti, F., Marzeion, B., Mayer, M.,
1471 MacDougall, A. H., McDougall, T., Monselesan, D. P., Nitzbon, J., Otosaka, I., Peng, J., Purkey, S., Roemmich, D.,
1472 Sato, K., Sato, K., Savita, A., Schweiger, A., Shepherd, A., Seneviratne, S. I., Simons, L., Slater, D. A., Slater, T.,
1473 Steiner, A. K., Suga, T., Szekely, T., Thiery, W., Timmermans, M.-L., Vanderkelen, I., Wijffels, S. E., Wu, T., and
1474 Zemp, M.: Heat stored in the Earth system 1960–2020: where does the energy go?, *Earth System Science Data*, 15,
1475 1675–1709, <https://doi.org/10.5194/essd-15-1675-2023>, 2023a.

1476 von Schuckmann, K., Minière, A., Gues, F., Cuesta-Valero, F. J., Kirchengast, G., Adusumilli, S., Straneo, F., Ablain,
1477 M., Allan, R. P., Barker, P. M., Beltrami, H., Blazquez, A., Boyer, T., Cheng, L., Church, J., Desbruyeres, D., Dolman,
1478 H., Domingues, C. M., García-García, A., Giglio, D., Gilson, J. E., Gorfer, M., Haimberger, L., Hakuba, M. Z.,
1479 Hendricks, S., Hosoda, S., Johnson, G. C., Killick, R., King, B., Kolodziejczyk, N., Korosov, A., Krinner, G., Kuusela,
1480 M., Landerer, F. W., Langer, M., Lavergne, T., Lawrence, I., Li, Y., Lyman, J., Marti, F., Marzeion, B., Mayer, M.,
1481 MacDougall, A. H., McDougall, T., Monselesan, D. P., Nitzbon, J., Otosaka, I., Peng, J., Purkey, S., Roemmich, D.,
1482 Sato, K., Sato, K., Savita, A., Schweiger, A., Shepherd, A., Seneviratne, S. I., Simons, L., Slater, D. A., Slater, T.,
1483 Steiner, A. K., Suga, T., Szekely, T., Thiery, W., Timmermans, M.-L., Vanderkelen, I., Wijffels, S. E., Wu, T., and
1484 Zemp, M.: GCOS EHI 1960-2020 Earth Heat Inventory Ocean Heat Content (Version 2),
1485 https://doi.org/10.26050/WDCC/GCOS_EHI_1960-2020_OHC_v2, 2023b.

1486 Seneviratne, S.I., X. Zhang, M. Adnan, W. Badi, C. Dereczynski, A. Di Luca, S. Ghosh, I. Iskandar, J. Kossin, S.
1487 Lewis, F. Otto, I. Pinto, M. Satoh, S. M. Vicente-Serrano, M. Wehner, and B. Zhou: Weather and Climate Extreme
1488 Events in a Changing Climate. In *Climate Change 2021: The Physical Science Basis. Contribution of Working Group*
1489 *I to the Sixth Assessment Report of the Intergovernmental Panel on Climate Change* [Masson-Delmotte, V., P. Zhai,
1490 A. Pirani, S.L. Connors, C. Péan, S. Berger, N. Caud, Y. Chen, L. Goldfarb, M.I. Gomis, M. Huang, K. Leitzell, E.

1491 Lonnoy, J.B.R. Matthews, T.K. Maycock, T. Waterfield, O. Yelekçi, R. Yu, and B. Zhou (eds.]. Cambridge
1492 University Press, Cambridge, United Kingdom and New York, NY, USA, pp. 1513–1766,
1493 doi:10.1017/9781009157896.013.1513–1766, <https://doi.org/10.1017/9781009157896.013>, 2021.

1494 Sherwin, E. D., Rutherford, J. S., Zhang, Z., Chen, Y., Wetherley, E. B., Yakovlev, P. V., Berman, E. S. F., Jones, B.
1495 B., Cusworth, D. H., Thorpe, A. K., Ayasse, A. K., Duren, R. M., and Brandt, A. R.: US oil and gas system emissions
1496 from nearly one million aerial site measurements, *Nature*, 627, 328–334, [https://doi.org/10.1038/s41586-024-07117-](https://doi.org/10.1038/s41586-024-07117-5)
1497 [5](https://doi.org/10.1038/s41586-024-07117-5), 2024.

1498 Simmonds, P. G., Rigby, M., McCulloch, A., O'Doherty, S., Young, D., Mühle, J., Krummel, P. B., Steele, P., Fraser,
1499 P. J., Manning, A. J., Weiss, R. F., Salameh, P. K., Harth, C. M., Wang, R. H. J., and Prinn, R. G.: Changing trends
1500 and emissions of hydrochlorofluorocarbons (HCFCs) and their hydrofluorocarbon (HFCs) replacements, *Atmos.*
1501 *Chem. Phys.*, 17, 4641–4655, <https://doi.org/10.5194/acp-17-4641-2017>, 2017.

1502 Sippel, S., Zscheischler, J., Heimann, M., Otto, F. E. L., Peters, J., and Mahecha, M. D.: Quantifying changes in
1503 climate variability and extremes: Pitfalls and their overcoming, *Geophys. Res. Lett.*, 42, 9990–9998,
1504 <https://doi.org/10.1002/2015GL066307>, 2015.

1505 Smith, C., Walsh, T., Gillett, N., Hall, B., Hauser, M., Krummel, P., Lamb, W., Lamboll, R., Lan, X., Muhle, J.,
1506 Palmer, M., Ribes, A., Schumacher, D., Seneviratne, S., Trewin, B., von Schuckmann, K., and Forster, P.:
1507 ClimateIndicator/data: Indicators of Global Climate Change 2023 revision (v2024.05.29b), Zenodo [Data set],
1508 <https://doi.org/10.5281/zenodo.11388387>, 2024a.

1509 Smith, C., Walsh, T., Gillett, N., Hall, B., Hauser, M., Krummel, P., Lamb, W., Lamboll, R., Lan, X., Muhle, J.,
1510 Palmer, M., Ribes, A., Schumacher, D., Seneviratne, S., Trewin, B., von Schuckmann, K., and Forster, P.: Indicators
1511 of Global Climate Change 2023, Github [code], <https://github.com/ClimateIndicator/data/tree/v2024.05.29b>, last
1512 access: 25 April 2024b

1513 Smith, C., Nicholls, Z. R. J., Armour, K., Collins, W., Forster, P., Meinshausen, M., Palmer, M. D., and Watanabe,
1514 M.: The Earth's Energy Budget, Climate Feedbacks, and Climate Sensitivity Supplementary Material, in: *Climate*
1515 *Change 2021: The Physical Science Basis. Contribution of Working Group I to the Sixth Assessment Report of the*
1516 *Intergovernmental Panel on Climate Change*, edited by: Masson-Delmotte, V., Zhai, P., Pirani, A., Connors, S. L.,
1517 Péan, C., Berger, S., Caud, N., Chen, Y., Goldfarb, L., Gomis, M. I., Huang, M., Leitzell, K., Lonnoy, E., Matthews,
1518 J. B. R., Maycock, T. K., Waterfield, T., Yelekçi, O., Yu, R., and Zhou, B., 2021.

1519 Smith, S. J., van Aardenne, J., Klimont, Z., Andres, R. J., Volke, A., and Delgado Arias, S.: Anthropogenic sulfur
1520 dioxide emissions: 1850–2005, *Atmos. Chem. and Phys.*, 11, 1101–1116, <https://doi.org/10.5194/acp-11-1101-2011>,
1521 2011.

1522 Storto, A. and Yang, C.: Acceleration of the ocean warming from 1961 to 2022 unveiled by large-ensemble reanalyses,
1523 *Nature Communications*, 15, 545, <https://doi.org/10.1038/s41467-024-44749-7>, 2024.

1524 Szopa, S., V. Naik, B. Adhikary, P. Artaxo, T. Berntsen, W.D. Collins, S. Fuzzi, L. Gallardo, A. Kiendler-Scharr, Z.
1525 Klimont, H. Liao, N. Unger, and P. Zanis: Short-Lived Climate Forcers. In *Climate Change 2021: The Physical*

1526 Science Basis. Contribution of Working Group I to the Sixth Assessment Report of the Intergovernmental Panel on
1527 Climate Change [Masson-Delmotte, V., P. Zhai, A. Pirani, S.L. Connors, C. Péan, S. Berger, N. Caud, Y. Chen, L.
1528 Goldfarb, M.I. Gomis, M. Huang, K. Leitzell, E. Lonnoy, J.B.R. Matthews, T.K. Maycock, T. Waterfield, O. Yelekçi,
1529 R. Yu, and B. Zhou (eds.)]. Cambridge University Press, Cambridge, United Kingdom and New York, NY, USA, pp.
1530 817–922, <https://doi.org/10.1017/9781009157896.008>, 2021.

1531 Tibrewal, K., Ciais, P., Saunois, M., Martinez, A., Lin, X., Thanwerdas, J., Deng, Z., Chevallier, F., Giron, C.,
1532 Albergel, C., Tanaka, K., Patra, P., Tsuruta, A., Zheng, B., Belikov, D., Niwa, Y., Janardan, R., Maksyutov, S.,
1533 Segers, A., Tzompa-Sosa, Z. A., Bousquet, P., and Sciare, J.: Assessment of methane emissions from oil, gas and coal
1534 sectors across inventories and atmospheric inversions, *Communications Earth & Environment*, 5, 26,
1535 <https://doi.org/10.1038/s43247-023-01190-w>, 2024.

1536 Vanderkelen, I. and Thiery, W.: GCOS EHI 1960-2020 Inland Water Heat Content,
1537 https://doi.org/10.26050/WGCC/GCOS_EHI_1960-2020_IWHC, 2022.

1538 Vimont, I. J., B. D. Hall, G. Dutton, S. A. Montzka, J. Mühle, M. Crotwell, K. Petersen, S. Clingan, and D. Nance, [in
1539 “State of the Climate in 2022”]. *Bull. Amer. Meteor. Soc.*, 104, 9, S76–S78, [https://doi.org/10.1175/BAMS-D-23-](https://doi.org/10.1175/BAMS-D-23-0090.1)
1540 [0090.1](https://doi.org/10.1175/BAMS-D-23-0090.1), 2022.

1541 Vollmer, M. K., Young, D., Trudinger, C. M., Mühle, J., Henne, S., Rigby, M., Park, S., Li, S., Guillevic, M.,
1542 Mitrevski, B., Harth, C. M., Miller, B. R., Reimann, S., Yao, B., Steele, L. P., Wyss, S. A., Lunder, C. R., Arduini, J.,
1543 McCulloch, A., Wu, S., Rhee, T. S., Wang, R. H. J., Salameh, P. K., Hermansen, O., Hill, M., Langenfelds, R. L., Ivy,
1544 D., O’Doherty, S., Krummel, P. B., Maione, M., Etheridge, D. M., Zhou, L., Fraser, P. J., Prinn, R. G., Weiss, R. F.,
1545 and Simmonds, P. G.: Atmospheric histories and emissions of chlorofluorocarbons CFC-13 (CClF₃), ΣCFC-114
1546 (C₂Cl₂F₄), and CFC-115 (C₂ClF₅), *Atmos. Chem. Phys.*, 18, 979–1002, <https://doi.org/10.5194/acp-18-979-2018>,
1547 2018.

1548 Watson-Parris, D., Christensen, M. W., Laurenson, A., Clewley, D., Gryspeerdt, E., and Stier, P.: Shipping regulations
1549 lead to large reduction in cloud perturbations, *Proc. Natl. Acad. Sci. U.S.A.*, 119, e2206885119,
1550 <https://doi.org/10.1073/pnas.2206885119>, 2022.

1551 Western, L. M., Vollmer, M. K., Krummel, P. B., Adcock, K. E., Fraser, P. J., Harth, C. M., Langenfelds, R. L.,
1552 Montzka, S. A., Mühle, J., O’Doherty, S., Oram, D. E., Reimann, S., Rigby, M., Vimont, I., Weiss, R. F., Young, D.,
1553 and Laube, J. C.: Global increase of ozone-depleting chlorofluorocarbons from 2010 to 2020, *Nat. Geosci.*, 16, 309–
1554 313, <https://doi.org/10.1038/s41561-023-01147-w>, 2023.

1555 van der Werf, G. R., Randerson, J. T., Giglio, L., van Leeuwen, T. T., Chen, Y., Rogers, B. M., Mu, M., van Marle,
1556 M. J. E., Morton, D. C., Collatz, G. J., Yokelson, R. J., and Kasibhatla, P. S.: Global fire emissions estimates during
1557 1997–2016, *Earth System Science Data*, 9, 697–720, <https://doi.org/10.5194/essd-9-697-2017>, 2017.

1558 Wild, M., Gilgen, H., Roesch, A., Ohmura, A., Long, C. N., Dutton, E. G., Forgan, B., Kallis, A., Russak, V., and
1559 Tsvetkov, A.: From Dimming to Brightening: Decadal Changes in Solar Radiation at Earth’s Surface, *Science*, 308,
1560 847–850, <https://doi.org/10.1126/science.1103215>, 2005.

1561 Zhang, Z., Poulter, B., Feldman, A.F., Ying, Q., Ciais, P., Peng, S. and Xin, L.: Recent intensification of wetland
1562 methane feedback, *Nat. Clim. Chang.* 13, 430–433, <https://doi.org/10.1038/s41558-023-01629-0>, 2023.
1563